SYNTHESIS OF ISOSTERE CAPSAICIN DERIVATIVES AND THEIR BIOLOGICAL ACTIVITIES

SUWICHAN MAJAKORN

A Thesis Submitted to the Graduate School of Naresuan University
in Partial Fulfillment of the Requirements
for the Master Degree in Chemistry
July 2017

Copyright 2017 by Naresuan University

Thesis entitled "Synthesis of Isostere Capsaicin Derivatives and Their Biological Activities"

by Mr. Suwichan Majakorn

has been approved by the Graduate School as partial fulfillment of the requirements for the Master of Science Degree in Chemistry of Naresuan University

Oral Defense Committee

..... Chair

(Pattama Pittayakhajonwut, Ph.D.)

..... Advisor

(Uthai Wichai, Ph.D.)

..... Co – Advisor

(Wikorn Punyain, Ph.D.)

..... Internal Examiner

(Assistant Professor Boonjira Rutnakornpituk, Ph.D.)

Approved

.....

(Panu Putthawong, Ph.D.)

Associate Dean for Administration and Planning

for Dean of the Graduate School

27 JUL 2017

ACKNOWLEDGEMENT

First of all, I would like to thank my advisor Dr.Uthai Wichai for his patience, guidance and support for the completion of my research. Sincerely thanks to Dr.Wikorn Punyain for the computational calculation and his advice. The authors acknowledge National e-Science Infrastructure Consortium for providing computing resources that how contributed to the research results reported within the thesis. I also would like to thank the committees for comments and suggestions.

I would like to thank all of the staffs at Department of Chemistry, Faculty of Science, Naresuan University. Unforgettable, all of the members in Uthai's Research Group (URG) for their kindness and friendship.

I also would like to thank Center for Innovation in Chemistry: Postgraduate Education and Research Program in Chemistry (PERCH-CIC) for research budgets.

Finally, I would like to thank my parents for their love, support and encourage for entirely my education.

Suwichan Majakorn

Title	SYNTHESIS OF ISOSTERE CAPSAICIN DERIVATIVES AND THEIR BIOLOGICAL ACTIVITIES
Author	Suwichan Majakorn
Advisor	Uthai Wichai, Ph.D.
Co - Advisor	Wikorn Punyain, Ph.D.
Academic Paper	Thesis M.S. in Chemistry, Naresuan University, 2016
Keywords	capsaicin derivatives, alzheimer's disease, acetylcholinesterase inhibitor, anti-inflammatory

ABSTRACT

Capsaicin is great interest due to its markedly application including culinary and medicine. Capsaicin is acts specifically on Transient Receptor Potential receptor Variant type 1 (TRPV1) and showed activity such as anti-inflammatory and anti –pain sensory. Here study, a new analogue of capsaicin is synthesized to enhance π-π stacking properties. The capsaicin derivative is divided into four steps including formylation reaction to benzaldehyde derivatives, a conversion to amine salt derivatives, coupling with fatty acid by using EDC.HCl/HOBt and purified by HPLC to pure products in final step. The completely synthesis was obtained in low yields. For anti-inflammatory assay, 3-trifluoromethyl capsaicin (**21**) clearly showed the interaction with TRPV1 via π-π stacking that indicated -OCF3 substituent on aromatic ring enhances the anti-inflammatory by inhibiting secretion of TNFα on LPS-stimulated PBMC.

Furthermore, the aromatic region of capsaicin (vanillin moiety) showed inhibitory against Alzheimer's disease that caused of the permanent damage of brain cells and affected memory. In the brain of AD patients, acetylcholine is easily broken down by acetylcholinesterase to acetic acid and choline. To improve the AChE inhibition, vanillylbenzaldehyde derivatives **2-7** were prepared by a simple one-pot reaction via Duff reaction. Then, vanillylamine hydrochloride salts **14-19** were prepared by catalytic hydrogenation via oximes.

LIST OF CONTENTS

Chapter		Page
I	**INTRODUCTION**	1
	Rationale for the study	1
	Significance of the study	5
	Scope of the study	5
II	**LITERATURE REVIEWS**	7
	Capsaicin	7
	Clinical uses of capsaicin	8
	Capsaicin with mode of action	9
	Capsaicin with anti-inflammatory property	10
	Alzheimer's Disease	12
	Acetylcholinesterase (AChE)	15
	Quantitative Structure Activity Relationships (QSAR)	18
III	**RESEARCH METHODOLOGY**	21
	Research study overview	21
	General Procedure	24
	Experiments	26

LIST OF CONTENTS (CONT.)

Chapter		Page
IV	**RESULTS AND DISCUSSION**	35
	Synthesis of Synthesis of 3-trifluoromethoxy capsaicin (21) ...	35
	Determination of anti-inflammation activity onto immunology system via human TNF-α immunoassay of 3-trifluoromethoxy capsaicin (21)	42
	Synthesis of vanillylamine hydrochloride derivatives (15-19)...	46
	Investigation of Acetylcholinesterase inhibitory activity	51
V	**CONCLUSION**	54
REFERENCES		55
APPENDIX		61
BIOGRAPHY		107

LIST OF TABLES

Table		Page
1	EC_{50} values compared with capsaicin derivatives.....	11
2	Absorption of screening assay of TNF-α production after applied 5.00 μM capsaicin and isostere capsaicin (21).....	45
3	AChE inhibitory and IC_{50} of compounds 14-15 and compounds 18-19.....	51
4	Log P, dipole moment and Hammett constant of compound 14-15 and compound 18-19.....	52
5	Cell viability of isostere capsaicin (21) in 1% of PEG after 24 hours.....	99
6	Absorption of TNF-α standard at 1,000, 500, 250, 125, 62.5, 31.2, 15.6 and 0 pg/mL.....	100
7	Absorption of screening assay of TNF-α production after dose 5.00 μM of capsaicin and isostere capsaicin (21) using LPS-stimulated (n=1).....	101

LIST OF FIGURES

Figures		Page
1	Structures of capsaicin (1) and their analogues (2-5).....	1
2	Three region of Capsaicin: A region-Aromatic ring, B region Amide bond and C region-Hydrophobic side chain.....	2
3	Anti-inflammatory and immunomodulatory effects of TRPV1....	3
4	Breakdown of acetylcholine to choline and acetic acid	4
5	The structure of isomeric vanilloid derivatives MBALD and vanillin.....	4
6	The new design of capsaicin derivative and vanillin derivatives...	6
7	Structures of capsaicin and dihydrocapsaicin.....	8
8	The position of 3 and 4 at the A region of capsaicin.....	9
9	Interaction between capsaicin and TRPV 1 Receptor.....	9
10	TRPV1 and the six transmembrane domains.....	10
11	Capsaicin interacting with transmembrane helices TM3 and TM4 of TRPV1.....	12
12	Healthy brain and severe Alzheimer's disease.....	13
13	The disintegration of microtubules in brain cells.....	14
14	Breakdown mechanism of acetylcholine to choline and acetic acid.....	14
15	Acetylcholinesterase inhibitors (AChEIs) drugs: Galanthamine, Donepezil, Tacrine and Rivastigmine.....	15
16	AChE inhibition activity between galanthamine (IC_{50}=1165 nM) and galanthamine derivative (IC_{50}=5.2 nM) bearing long chain methylene subunit which interact at peripheral anionic site of AChE via π-π stacking at Tyr 341.....	16
17	The structure of isomeric vanilloid derivatives MBALD and vanillin.....	16
18	Schematic of the binding sites at esteratic site.....	17

LIST OF FIGURES (CONT.)

Figures		Page
19	Separation of PBMC from human blood.....	30
20	Preparing of TNF-α standards procedure.....	32
21	AChE inhibitory activity procedures.....	34
22	Mechanism of 3-trifluoromethyl vanillin (2) via Duff reaction...	36
23	^{1}H-NMR spectrum of 3-trifluoromethoxy-4-hydroxybenzaldehyde (2) ($CDCl_3$-d_1).....	37
24	Mass spectrum of 3-trifluoromethoxy-4-hydroxybenzaldehyde (2).....	37
25	IR spectrum of 3-trifluoromethoxy-4-hydroxybenzaldehyde (2).....	38
26	^{1}H-NMR spectrum of 4-hydroxy-3-(trifluoromethoxy) vanillylamine hydrochloride (14) (D_2O-d_2).....	38
27	IR spectrum of 3-trifluoromethoxy-4-hydroxybenzylamine hydrochloride (14).....	39
28	Mechanism of coupling reaction by using HOBt and EDC.HCl...	40
29	^{1}H-NMR spectrum of 21 ($CDCl_3$-d_1).....	41
30	Mass spectrum of Isostere Capsaicin (21).....	41
31	Cell viability of PBMC from hemacytometer grid via microscope; a) clear cytoplasm for viable cell and b) blue cytoplasm for nonviable cell.....	43
32	Percentage of Cell viability of PBMC using trypan blue technique after dose of 3-trifluoromethoxy capsaicin (21) at 1, 5, 50, 100 and 200 μM for 24 h.....	44
33	The screening inhibition of TNF-α production after applied 5 μM capsaicin and capsaicin derivative (21) using LPS-stimulated.....	45

LIST OF FIGURES (CONT.)

Figure		Page
34	IR spectrum of 3-fluoro-4-hydroxybenzylamine hydrochloride (15).....	47
35	^{1}H-NMR spectrum of 3-fluoro-4-hydroxybenzylamine hydrochloride (15) (D_2O-d_2).....	48
36	IR spectrum of 4-hydroxybenzylamine hydrochloride (18).....	49
37	^{1}H-NMR spectrum of 4-hydroxybenzylamine hydrochloride (18) (D_2O-d_2).....	49
38	^{1}H-NMR spectrum of 4-hydroxy-3-methoxybezylamine hydrochloride (19) (D_2O-d_2).....	50
39	IR spectrum of 4-hydroxy-3-methoxybezylamine hydrochloride (19).....	50
40	^{1}H-NMR spectrum of 3-trifluoromethoxy-4-hydroxybenzaldehyde (2) ($CDCl_3$-d_1).....	62
41	^{13}C-NMR spectrum of 3-trifluoromethoxy-4-hydroxybenzaldehyde (2) ($CDCl_3$-d_1).....	63
42	IR spectrum of 3-trifluoromethoxy-4-hydroxybenzaldehyde (2)...	64
43	Mass spectrum of 3-trifluoromethoxy-4-hydroxybenzaldehyde (2).....	65
44	^{1}H-NMR spectrum of 3-fluoro-4-hydroxybenzaldehyde (3) ($CDCl_3$-d_1).....	66
45	^{13}C-NMR spectrum of 3-fluoro-4-hydroxybenzaldehyde (3) ($CDCl_3$-d_1)	67
46	IR spectrum of 3-fluoro-4-hydroxybenzaldehyde (3).....	68
47	Mass spectrum of 3-fluoro-4-hydroxybenzaldehyde (3).....	69
48	^{1}H-NMR spectrum of 3-chloro-4-hydroxybenzaldehyde (4) ($CDCl_3$-d_1).....	70

LIST OF FIGURES (CONT.)

Figures		Page
49	^{13}C-NMR spectrum of 3-chloro-4-hydroxybenzaldehyde (4) ($CDCl_3$-d_1).....	71
50	IR spectrum of 3-chloro-4-hydroxybenzaldehyde (4).....	72
51	Mass spectrum of 3-chloro-4-hydroxybenzaldehyde (4).....	73
52	^{1}H-NMR spectrum of 3-bromo-4-hydroxybenzyaldehyde (5) ($CDCl_3$-d_1).....	74
53	^{13}C-NMR spectrum of 3-bromo-4-hydroxybenzyaldehyde (5) ($CDCl_3$-d_1).....	75
54	IR spectrum of 3-bromo-4-hydroxybenzyaldehyde (5).....	76
55	Mass spectrum of 3-bromo-4-hydroxybenzyaldehyde (5).....	77
56	^{1}H-NMR spectrum of 3-trifluoromethoxy-4-hydroxybenzylamine hydrochloride (14) (D_2O-d_2).....	78
57	^{13}C-NMR spectrum of 3-trifluoromethoxy-4-hydroxybenzylamine hydrochloride (14) (D_2O-d_2).....	79
58	IR spectrum of 3-trifluoromethoxy-4-hydroxybenzylamine hydrochloride (14).....	80
59	Mass spectrum of 3-trifluoromethoxy-4-hydroxybenzylamine hydrochloride (14)	81
60	^{1}H-NMR spectrum of 3-fluoro-4-hydroxybenzylamine hydrochloride (15) (D_2O-d_2).....	82
61	^{13}C-NMR spectrum of 3-fluoro-4-hydroxybenzylamine hydrochloride (15) (D_2O-d_2).....	83
62	IR spectrum of 3-fluoro-4-hydroxybenzylamine hydrochloride (15).....	84
63	Mass spectrum of 3-fluoro-4-hydroxybenzylamine hydrochloride (15).....	85

LIST OF FIGURES (CONT.)

Figures		Page
64	^{1}H-NMR spectrum of 4-hydroxybenzylamine hydrochloride (18) (D_2O-d_2).....	86
65	^{13}C-NMR spectrum of 4-hydroxybenzylamine hydrochloride (18) (D_2O-d_2).....	87
66	IR spectrum of 4-hydroxybenzylamine hydrochloride (18).....	88
67	Mass spectrum of 4-hydroxybenzylamine hydrochloride (18).....	89
68	^{1}H-NMR spectrum of 4-hydroxy-3-methoxybezylamine hydrochloride (19) (D_2O-d_2).....	90
69	^{13}C-NMR spectrum of 4-hydroxy-3-methoxybezylamine hydrochloride (19) (D_2O-d_2).....	91
70	IR spectrum of 4-hydroxy-3-methoxybezylamine hydrochloride (19).....	92
71	Mass spectrum of 4-hydroxy-3-methoxybezylamine hydrochloride (19).....	93
72	^{1}H-NMR spectrum of Isostere Capsaicin (21) before purified by HPLC ($CDCl_3$-d_1).....	94
73	^{1}H-NMR spectrum of Isostere Capsaicin (21) after purified by HPLC ($CDCl_3$-d_1).....	95
74	^{13}C-NMR spectrum of Isostere Capsaicin (21) ($CDCl_3$-d_1).....	96
75	IR spectrum of Isostere Capsaicin (21).....	97
76	Mass spectrum of Isostere Capsaicin (21).....	98
77	Calibration curve of TNF-α production at 1,000, 500, 250, 125, 62.5, 31.2, 15.6 and 0 pg/mL.....	100
78	3D structure of 3-fluoro-4-hydroxybenzaldehyde (3).....	102
79	3D structure of 4-hydroxybenzaldehyde (6).....	102
80	3D structure of 3-trifluoromethoxy-4-hydroxybenzaldehyde (2)..	103
81	3D structure of 3-methoxy-4-hydroxybenzaldehyde (7).....	103

LIST OF FIGURES (CONT.)

Figure		Page
82	3D structure of capsaicin.....	104
83	3D structure of isostere capsaicin (21).....	104
84	3D structure of interaction of capsaicin and capsaicin *via* H-bond	105
85	3D structure of interaction of isostere capsaicin and isostere capsaicin *via* π-π stacking.....	105
86	3D structure of interaction of capsaicin and isostere capsaicin *via* π-π stacking.....	106

LIST OF SCHEMES

Scheme		Page
1	Synthesis of 3-trifluoromethoxy vanillin (2) and 3-trifluoromethoxy vanillinamine hydrochloride (14).....	21
2	Synthesis of 3-trifluoromethoxy capsaicin (21).....	22
3	Synthesis of vanillylamine hydrochloride derivatives (15-19).....	22
4	Preparation of (*E*)-8-methyl-6-nonenic acid (20).....	23
5	Synthesis of 3-trifluoromethoxy vanillin (2) and 3-trifluoromethoxy vanillinamine hydrochloride (14).....	26
6	Synthesis of 3-trifluoromethoxy capsaicin (21).....	27
7	Synthesis of vanillylamine hydrochloride derivatives (15-19).....	28
8	Summary of synthesis of 3-trifluoromethoxy vanillin (2).....	35
9	Summary of synthesis of 3-trifluoromethoxy capsaicin (21).....	39
10	Summary of the synthesis of vanillylamine hydrochloride derivatives (15-19).....	46

ABBREVIATIONS

δ	=	chemical shift
μM	=	micromolar
μmole	=	micromole
μL	=	microliter
$CDCl_3$	=	deuterated chloroform
d	=	doublet
DMF	=	*N,N'*-dimethylformamide
EC_{50}	=	50% Effective Concentration
AChE	=	Acetylcholinesterase
AChEI	=	Acetylcholinesterase inhibitor
AD	=	Alzheimer's disease
FT-IR	=	Fourier transform infrared spectroscopy
g	=	gram
h	=	hour
HPLC	=	high performance liquid chromatography
HOBt	=	1-Hydroxybenzotriazole
IC_{50}	=	half maximal inhibitory concentration
J	=	coupling constant
m	=	meta
MeOH	=	methanol
mL	=	milliliter(s)
mg	=	milligram(s)
mmol	=	millimole
m/z	=	mass-to-charge ratio
mM	=	millimolar
MS	=	Mass Spectrometry
NMR	=	Nuclear Magnetic Resonance
TFA	=	Trifluoroacetic acid
TLC	=	Thin Layer Chromatography
TRPV1	=	The Transient Receptor Potential Vanilloid 1

ABBREVIATIONS (CONT.)

AA	=	Acetic acid
Ch	=	Choline
PAS	=	The peripheral anionic binding site
ACh	=	Acetylcholine
SAR	=	The structure–activity relationship
TM	=	Transmembrane
TNFα	=	Tumor necrosis factor alpha
MBALD	=	2-hydroxy-4-methoxybenzaldehyde
Tyr 341	=	Tyrosine 341
QSAR	=	Quantitative Structure Activity Relationships
P	=	partition coefficient
Log P	=	hydrophobicity or lipophilicity
σ	=	The Hammett substitution constant
PSA	=	Molecular Polar Surface Area
LPS	=	Lipopolysaccharide
PBMC	=	Peripheral Blood Mononuclear Cell

CHAPTER I

INTRODUCTION

Rationale for the study

Capsaicin was first isolated in 1876 by Tresh et al. [1] and its structure was elucidated in 1919 by Nelson and Dawson [2], caused the spicy flavor of chili pepper fruit. Capsaicin is an irritant substance for mammals, including humans, and produces a burning sensation in any tissues which it comes into contact. Pure capsaicin is a hydrophobic, colorless, and crystalline to waxy. Capsaicin and dihydrocapsaicin are the main capsaicinoids founded in chili pepper followed by nordihydrocapsaicin, homodihydrocapsaicin and homocapsaicin (**Figure 1**).

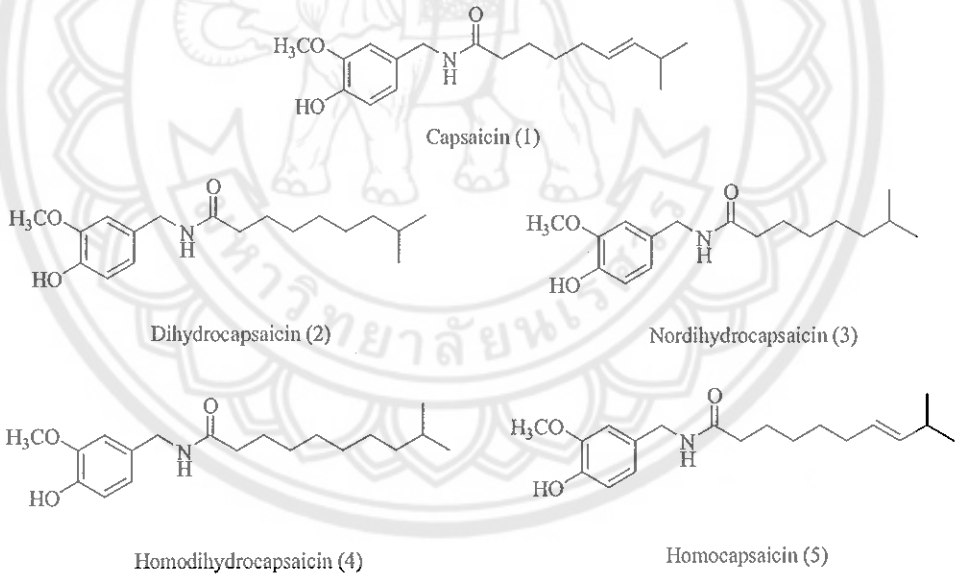

Figure 1 Structures of capsaicin (1) and their analogues (2-5)

Previously reported in 1993, capsaicin was divided into three main regions in the structure which are an aromatic region which known as vanilloid, the amide linker and the aliphatic region or lipophilic hydrocarbon long chain (**Figure 2**) [2].

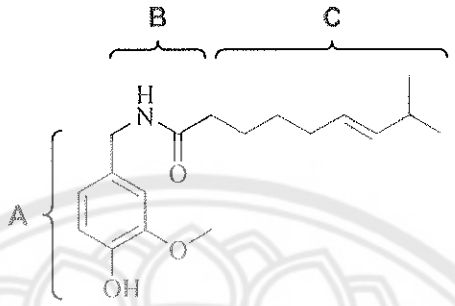

Figure 2 Three regions of Capsaicin: A region-Aromatic ring, B region-Amide linker and C region-Hydrophobic side chain

In addition, capsaicin and analogues have been synthesized and evaluated for the biological activities. Several works showed that capsaicinoids, capsaicin in particular, had a wide range of biological activities such as antioxidant, anti-carcinogenic, and anti-inflammatory.

The anti-inflammatory mechanism of capsaicin was proposed that Transient Receptor Potential action channel (subfamily V) type 1 agonists (or TRPV1 agonists) modulated cytokine production *via* neuropeptide that released from afferent C fibers in neuron system and showed anti-inflammatory effects (**Figure 3**) [3, 4, 5].

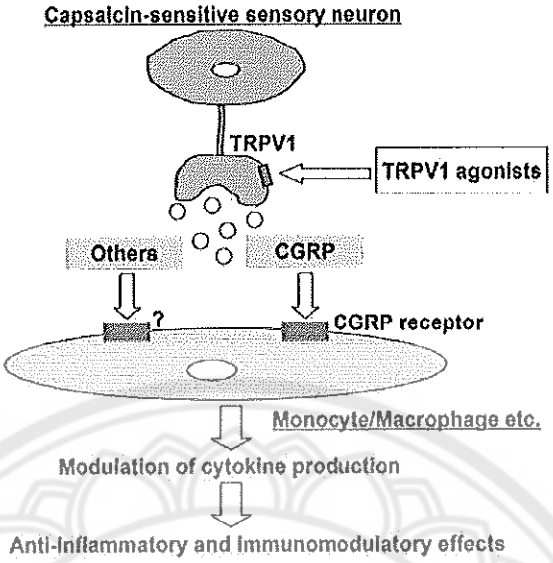

Figure 3 Anti-inflammatory and immunomodulatory effects of TRPV1

However, the potential applications of these molecules are limited by the irritation caused by their pungency and burning sensation [6].

Additionally, previously studied have been reported that vanilloid derivative of capsaicin showed an activity against acetylcholinesterase (AChE) which is one of the key enzyme for treatment of Alzheimer's disease (AD), one of neurodegenerative disease. It is one of the most common types of dementia in elderly population with age over 65 years old. AD affects individuals by limiting their abilities in daily life e.g. memory loss, difficulty in thinking, communication and problem solving [7].

One of the generally accepted hypotheses for AD was the change of concentration acetylcholine (ACh), a neurotransmitter in the brain [8]. Usually, the level of acetylcholine, regulated by AChE, was hydrolyzed ACh to acetic acid (AA) and choline (Ch) (**Figure 4**).

The active site of AChE includes two subsites; anionic and esteric site that interacting with the quaternary ammonium ion of ACh and hydrolysis into AA and Ch. Moreover, the peripheral anionic binding site (PAS) is shown another binding site with ACh and aromatic residues that line the active site gorge interact with the positive charged quaternary ammonium ion of ACh by cation-π interactions [9].

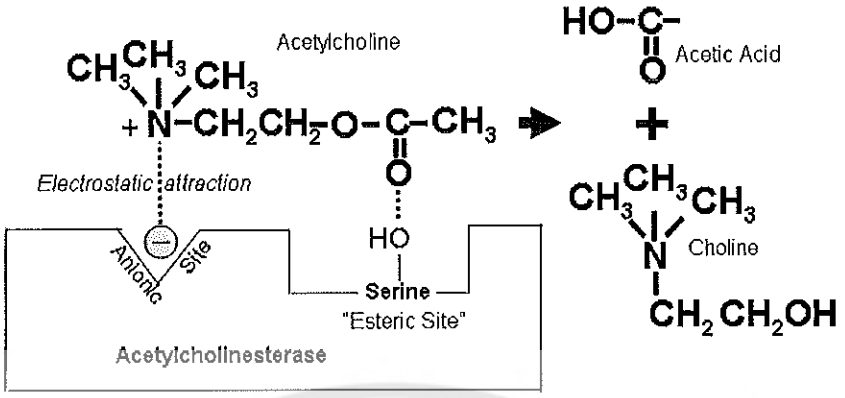

Figure 4 Breakdown mechanism of acetylcholine to choline and acetic acid

Acetylcholinesterase inhibitors (AChEIs) are one of the choices in treatment for reducing the hydrolysis process. From the previous work, two isomeric vanilloid derivatives from the edible plants, 2-hydroxy-4-methoxybenzaldehyde (MBALD) and 4-hydroxy-3-methoxybenzaldehyde (Vanilla) (**Figure 5**), were identified as AChEI and possessed the moderate AChEIs with IC_{50} of 0.67 and 8.36 μM, respectively [10].

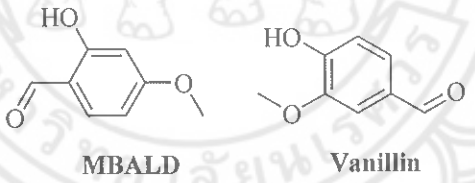

Figure 5 The structures of isomeric vanilloid derivatives (MBALD and Vanillin)

Currently, the great numbers of compounds which contain fluorine atom are synthesized in pharmaceutical research for using in medicinal applications [11]. In 1955, the first aryl trifluoromethoxy were prepared by using substituted anisoles. Nowadays, trifluoromethoxy group is playing a key role in several pharmaceutical and agrochemical researches. The presence of fluorine atoms in molecules, with a small size, minimal steric and the most highly electronegative element in the Periodic Table (4.00 Pauling scale), can enhance their biological activity and including with the binding affinity with a target protein [12].

In this research, the new novel analogue of capsaicin, 3-trifluoromethoxy capsaicin derivative is synthesized to enhance the interaction of π-π stacking by changing methoxy to trifluoromethoxy with minimum disturbing on steric hindrance but different in hydrophobicity and dipole moment. By the specific design, the biological activity is also observed from the result of either contribution of π-π stacking or changing hydrophobicity due to different dipole moment. Moreover, similar idea in changing dipole moment is also designed for new analogues of vanillin and the activity against AChE will be investigated.

Significance of the study

Biological activities such as inflammatory activity, anti-pain activity and anti-Alzheimer of capsaicin are generally related to the binding to receptor or enzyme. The specific part of capsaicin that contributes to the interaction was aromatic residue with the receptor or an enzyme *via* π-π interaction. The better binding to the receptor resulted in the better biological activity. Therefore, if manipulation of π-π interaction resulted in the binding improvement at the receptor, it would be one of the alternative approaches for improvement of biological activity.

Furthermore, to prove the concept of AChEI that mentioned above, the new derivatives of vanillin will be designed to enhance π-π stacking interaction by manipulation the dipole moment by changing to the amine salts for increasing the solubility that used as new candidate AD treatment in the future.

Scope of the study

To synthesize vanillinamine hydrochloride derivatives and capsaicin derivative evaluate anti-inflammation activity by using human TNF-α immunoassay of synthesized compounds and to investigate on AChE inhibitory activity of vanillylamine hydrochloride derivatives (**Figure 6**).

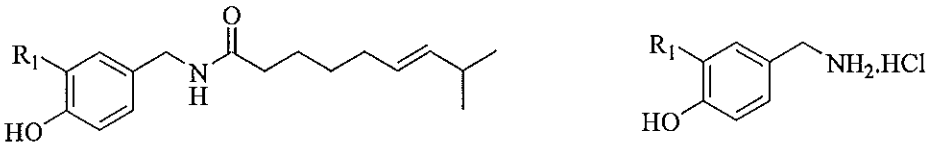

capsaicin derivative **vanillin derivatives**

Figure 6 The new design of capsaicin derivative and vanillin derivatives

CHAPTER II

LITERATURE REVIEWS

Capsaicin

Chili peppers are the fruits of plants from the genus Capsicum. There are several species, which are *Capsicum annuum*, *C. frutescens* and *C. chinense*. These peppers are extensively used in many parts of the world for their valued and characteristic sensory properties: color, heat, pungency and aroma [13].

The heat of chili peppers was measured in Scoville heat units (SHU), which is a measure of the dilution of an amount of chili extract added to sugar syrup before its heat becomes undetectable to a panel of tasters; the more it has to be diluted to be undetectable, the more powerful the variety and therefore the higher the rating.

The method for quantitative analysis of SHU rating was measured by a method that using high-performance liquid chromatography (HPLC) to directly measure the capsaicinoid content of a chili pepper variety.

Capsaicinoids are the compounds responsible for the pungency of their products. Pungency, an important attribute of peppers, is due to the presence of chemicals from the characteristic capsaicinoids group. The two major capsaicinoids in chili peppers are capsaicin (8-methyl-*N*-vanillyl-*trans*-6-nonenamide) and dihydrocapsaicin, followed by nordihydrocapsaicin, homodihydrocapsaicin and homocapsaicin, both constituting about 90%, with ~71% of capsaicin of the total capsaicinoids in most of the pungent varieties [14].

Capsaicin ($C_{18}H_{27}NO_3$), was first isolated in 1876 [1] and resolved in 1919 by Nelson and Dawson [2]. Pure capsaicin is a hydrophobic, colorless, odorless, and crystalline-to-waxy solid at room temperature.

The capsaicin compound is known to drain the neurotransmitter of painful from the sensory nerve terminals, which provides a rationale for its use as various experimental tools for studying pain mechanisms and also for pharmacotherapy to treat some peripheral painful states, such as rheumatoid arthritis, post-herpetic neuralgia, post-mastectomy pain syndrome and diabetic neuropathy.

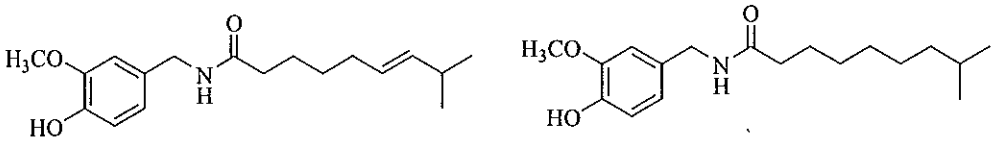

capsaicin dihydrocapsaicin

Figure 7 Structures of capsaicin and dihydrocapsaicin

Clinical uses of capsaicin [15]

Pain relief

Capsaicin helps in reducing inflammatory heat and noxious chemical hyperalgesia and pain from rheumatoid arthritis or fibromyalgia. Capsaicin is also the key ingredient in Adlea, a drug which is in Phase 2 as a long-acting analgesic to treat post-surgical and osteoarthritis pain.

Cancer prevention

Anticancer activity of capsaicin has been reported. In the cultured cells, capsaicin was able to block breast cancer cell migration and kill prostate cancer cells, and dihydrocapsaicin was reported to induce the autophagy in HCT116 human colon cancer cells.

Weight reduction

Capsaicin enhances energy and reduces body fat in animal experiments as well as clinical studies. Molecular mechanisms responsible for the effect of capsaicin showed that thermogenesis and lipid metabolism related proteins were depended on capsaicin treatment. The result also suggested an important role of capsaicin in regulating energy metabolism.

In addition, capsaicin has attracted much research interests because of its biological effects on pain, inflammation, anti-Alzheimer and anti-cancer. It effects through a specific receptor, which belongs to the transient receptor potential (TRP) of store-operated Ca^{2+} channels.

Capsaicin with mode of action

The structure–activity relationship (SAR) studies of capsaicin can be divided into three regions: A (aromatic part), B (amide bond) and C (hydrophobic side chain) (**Figure 2**) [16]. For agonist activity, substituents at position 3 and 4 in the aromatic ring is necessary, and the 4-OH of phenol group in capsaicin analogue is particular importance, H-bond donor/acceptor properties of the phenol group are important for the agonist [15].

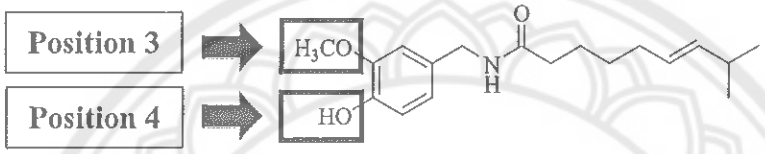

Figure 8 The position 3 and 4 at the A region of capsaicin

Moreover, the electron-poor vanillyl group in the capsaicin molecule is attached to and binds with the electron-rich area on the receptor, causing the heat-activated TRPV1 channel to open below the standard minimum temperature of 43°C and producing the sensation of heat. The painful feeling results in the release of endorphins, as well as blocks the production of Substance P, a neurotransmitter for pain and heat, preventing nerve intercommunication and leading to a reduction in pain and inflammation [17].

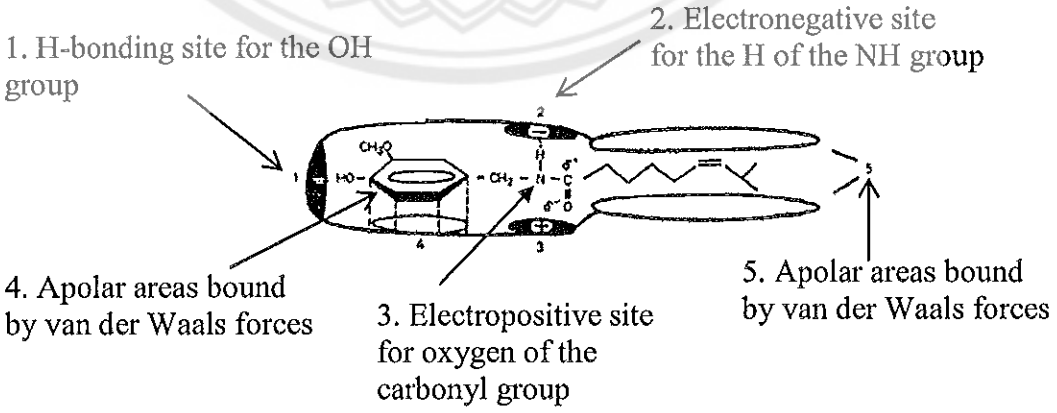

Figure 9 Interaction between capsaicin and TRPV 1 Receptor [17]

The "capsaicin receptor" has been named the Transient receptor potential vanilloid 1 receptor (TRPV1). Although most attention has been directed to sensory neurons as the site of action of capsaicin action, evidence is accumulated that capsaicin also acts specifically in various brain regions.

The TRPV1 receptor is the first discovered mammalian member of the TRP superfamily. The members of this superfamily contain six transmembrane helices (TM1–TM6) with a pore domain between helices 5 and 6, and the N- and C-terminal on the cytosolic side of cell membrane and contain 839 amino acids [18].

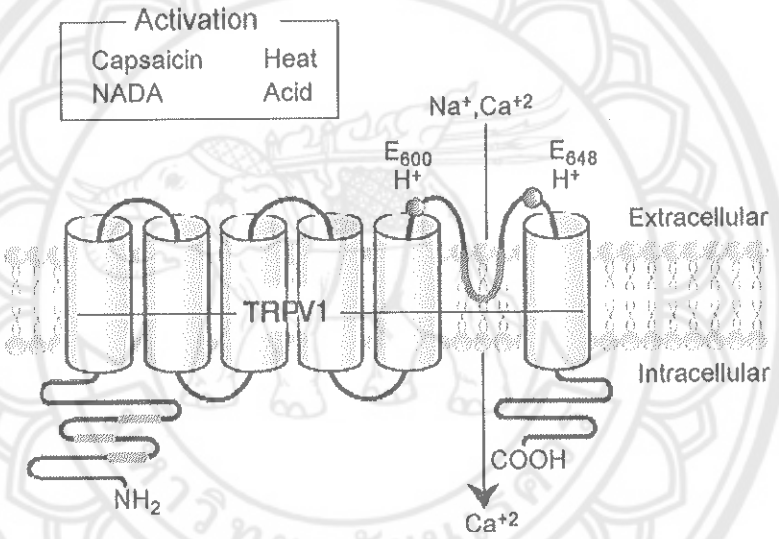

Figure 10 TRPV1 and the six transmembrane domains

Capsaicin with anti-inflammatory property

Capsaicin has also been shown an anti-inflammatory property. Previous researches represented that capsaicin can inhibits the production of pro-inflammatory mediators such as prostaglandin (PG), nitric oxide and TNFα by TRPV1 agonist deactivation in macrophages.

From the previous study in 2005, the first demonstration of capsaicin that abolishes the production of TNFα by acting as an agonist for TRPV1 receptor in LPS-stimulated macrophages was successful [19]. Capsaicin may be employed as a naturally occurring binding for TRPV1 receptor, which can be useful treatment against

inflammation. Accordingly, the modified molecule of capsaicin has been interest due to it is the best drug that provides the most effective response on the primary neuron system.

However, various researches pay attention to synthesize and explore capsaicin and their derivatives to decrease effect of burning sensation by pungency. Moreover, the investigation of enhancement the life time of inflammatory authority for success of inhibition or suppression of inflammatory mediator [20].

In 1993, Christopher S.J. Walpole et al. [16] studied the effects of Capsaicin and synthesized their derivatives to test the ability to reduce pain and irritation when capsaicin on the body.

In their study, the functional groups on the aromatic ring were changed and then compounds were tested and compared with capsaicin (**Table 1**).

Table 1 EC_{50} values compared with capsaicin derivatives

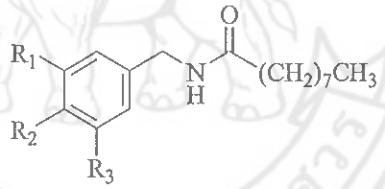

Compound	R_1	R_2	R_3	EC_{50}(μM)
1	H	H	H	>100
2	H	OH	OCH_3	0.55
3	H	OCH_3	OCH_3	6.41
4	H	OH	OH	0.63
5	H	NO_2	OCH_3	7.91

The results showed that when the substitute functional on the aromatic for R_2, hydroxyl make an EC_{50} increased compared with capsaicin due to lost hydrogen bonding in R_2.

In 2004, Narender R. Gavva et al. proposed the structural model of capsaicin interacting with transmembrane helices TM3 and TM4 of TRPV1 indicated interactions of vanillyl moiety with Thr 550 via hydrogen bonding and Trp 549 via π-π stacking interaction that show in **Figure 11** [21].

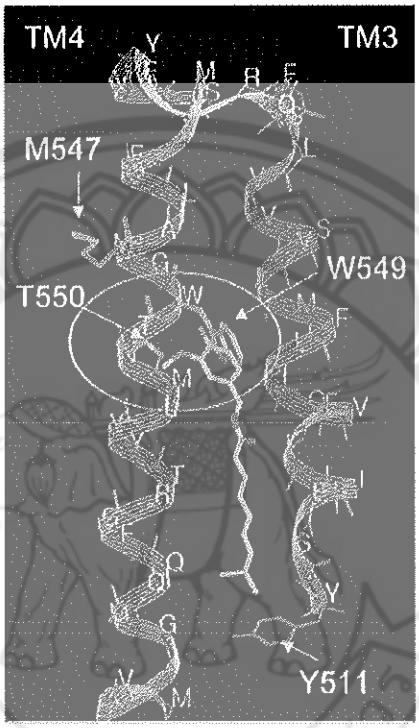

Figure 11 Capsaicin interacting with transmembrane helices TM3 and TM4 of TRPV1

Alzheimer's disease

Alzheimer's disease (AD) is a neurodegenerative disease that is one of the most common types of dementia in elderly population with age over 65 years old. AD affects individuals by limiting their abilities in daily life e.g. memory loss, difficulty in thinking, communication and problem solving [8].

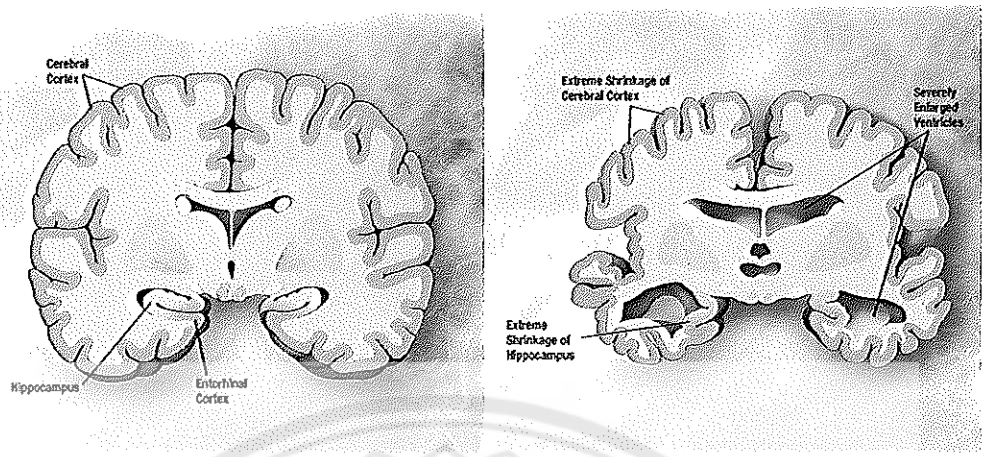

Figure 12 Healthy brain and severe Alzheimer's disease

Several hypotheses of pathogenesis for AD have been considered to explain the cause of the disease such as amyloid hypothesis, genetics and tau hypothesis [22, 23, 24].

There are mainly 3 assumptions that explain the causes of Alzheimer's disease. In 1991, an amyloid hypothesis was hypothesized that the accumulation of amyloid beta (A_β) was one of the major causes of Alzheimer's disease [25, 26]. The amyloid beta precursor gene (APP) is found on chromosome 21 and people with trisomy 21, the triplication of chromosome 21 is also known as Down Syndrome (DS), normally showing symptoms of AD at the age of 40 years [27, 28]. In addition, the APOE4 gene, which is a genetic risk factor for AD and leading to excess amyloid buildup in the brain, that indicated the accumulation of A_β results in the launching of AD [29].

For the next hypothesis, the tau hypothesis was proposed that tau protein abnormalities initiate the disease [26]. It begins with hyperphosphorylated tau pairs with another normal thread and form neurofibrillary tangles (NFTs) inside nerve cell that result in degradable of microtubule and destroying the transport system of the substance in the neuron [30].

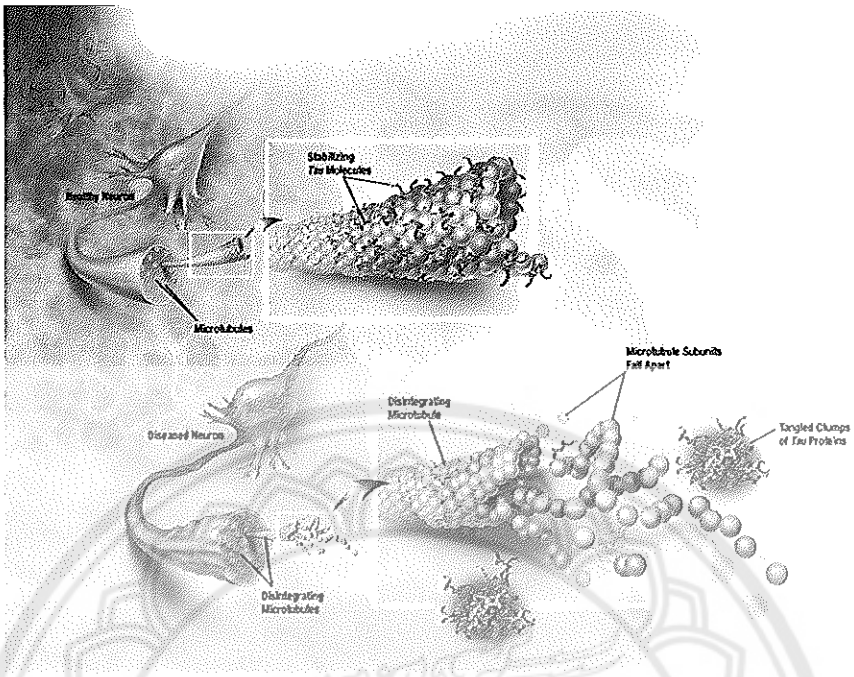

Figure 13 The disintegration of microtubules in brain cells.

However, one of the significant and generally accepted hypotheses was the concentration of acetylcholine, a neurotransmitter in the brain, has been changed [9].

Usually, the level of acetylcholine was regulated by acetylcholinesterase (AChE) which hydrolyzes acetylcholine (ACh) to acetic acid (AA) and choline (Ch). Acetylcholineesterase inhibitor (AChEI) is one of the choices of treatment to reduce the hydrolysis process.

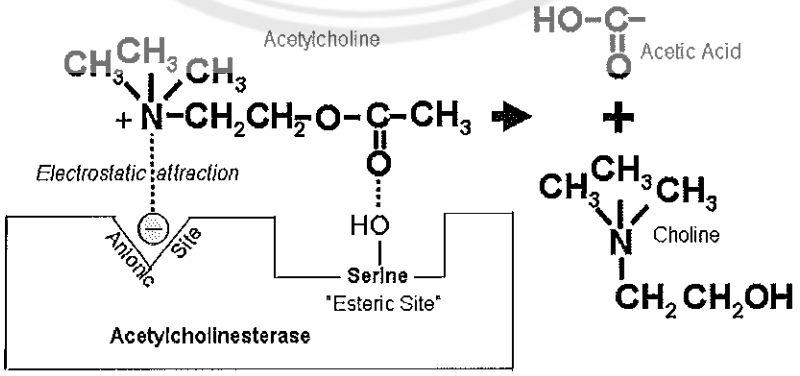

Figure 14 Breakdown mechanism of acetylcholine to choline and acetic acid

Acetylcholinesterase (AChE)

Acetylcholinesterase or AChE, a serine hydrolase, mainly found at neuromuscular junctions and cholinergic brain synapses. Its biological role is termination of impulse transmission at cholinergic synapses by hydrolysis of the neurotransmitter Acetylcholine or ACh to acetate and choline.

AChE has a remarkably high specific catalytic activity especially for a serine hydrolase - each molecule of AChE degrades about 25,000 molecules of ACh per second [31].

Presently, several drugs were discovered and synthesized by various research groups such as Rivastigmine, Tacrine, Galanthamine and Dopenzil (**Figure 15**), have been employed for treatment of AD [10, 32, 33, 34].

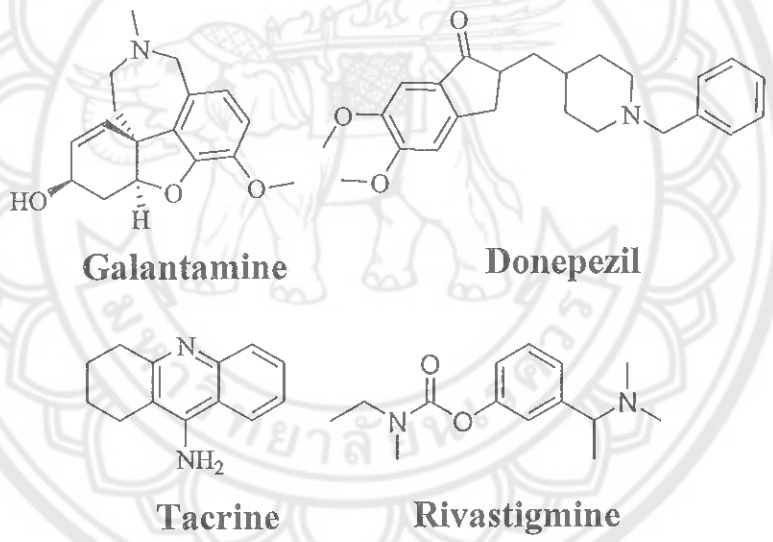

Figure 15 Acetylcholinesterase inhibitors (AChEIs) drugs: Galanthamine, Donepezil, Tacrine and Rivastigmine

The evidence of PAS contributed to the enhancement on AChEI was demonstrated in galanthamine derivative bearing long chain methylene unit with aromatic residue at the terminal position (**Figure 15**). It demonstrated strongly interacts with Tyr 341 at PAS via π-π stacking resulting the drug tightly locked at the eastratic subunit and partially blocked the traffic of ACh from entering to the esteratic unit [35].

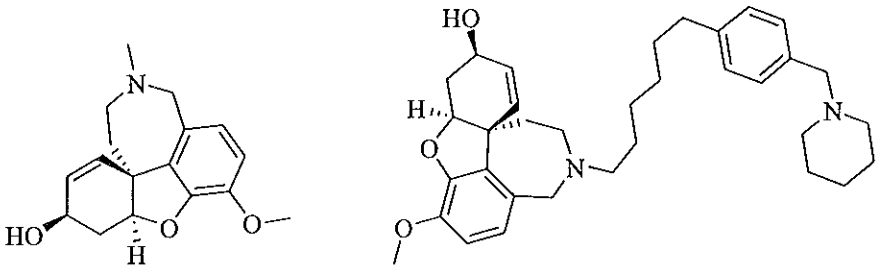

Galanthamine
IC_{50} = 1165 nM

Galanthamine derivative
IC_{50} = 5.2 nM

Figure 16 AChE inhibition activity between galanthamine (IC_{50}=1165 nM) and galanthamine derivative (IC_{50}=5.2 nM) bearing long chain methylene subunit which interact at peripheral anionic site of AChE via π-π stacking at Tyr 341 [35]

However, some serious side effects of these drugs were still observed such as vomiting, diarrhea, anorexia and headache have been observed and reported [22].

In 2013, Kundu and co-workers was the first group that investigated the two isomeric vanilloid derivatives from the edible plants as promising AChEIs. 2-hydroxy-4-methoxybenzaldehyde (MBALD) was extracted from roots of *Hemidesmus indicus*, source for making an aroma refreshment beverage in India and 4-hydroxy-3-methoxybenzaldehyde or vanilla (**Figure 17**), widely use as food additive, was extracted from *Vanilla planifolia*. Both compounds possessed the moderate AChEIs with IC_{50} of 0.047 mM and 0.037 mM, respectively [10].

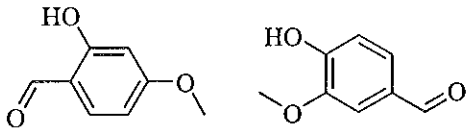

MBALD **Vanillin**

Figure 17 The structure of isomeric vanilloid derivatives MBALD and Vanillin

Interestingly, it was the first reported that vanillin showed anti-AChE. Generally, mode of action of anti-AChE was proposed with three approaches; I) binding at the esteratic subsite composed of serine 220, histidine 440 and glutamine 327, (**Figure 18**) [36]. II) aromatic residues that line the active site gorge interact with the positive charged quaternary ammonium ion of ACh by cation-π interactions [9] and III) blocking the peripheral anionic site (PAS) by interacted with aromatic residue of the PAS via π-π stacking. This has been observed in the study of galanthamine derivatives bearing the different length of linker attaching to the terminal phenyl reside. It was found that anti-AChE activity directly related with the length of the linker in order to promote the perfect π-π stacking between phenyl ring and Tyr 341 [35]. Possibly, vanillin might play the similar role by interaction with aromatic resides at PAS in order to possess AChEIs.

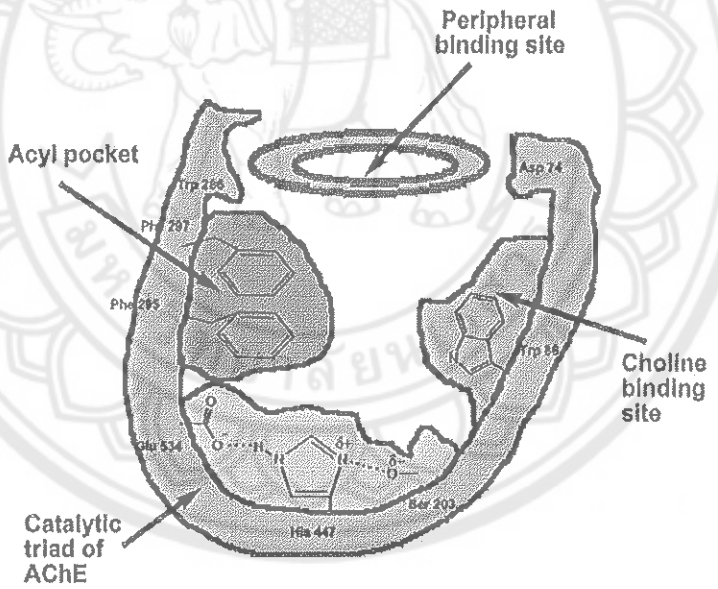

Figure 18 Schematic of the binding sites at esteratic site [31]

Quantitative Structure Activity Relationships (QSAR)

Quantitative Structure Activity Relationships (QSAR) has been applied for development of relationships between physical properties of chemical substances and their biological activities to obtain a dependable mathematical and statistical model [37]. In addition, this study is useful to optimize and improve their biological activities including with prediction the biological activities of untested and sometimes yet unavailable compounds.

Biological activity can be the result of covalent bond formation or fission, both homolytic and heterolytic, which give rise to either free radicals or ions, respectively; or it can involve one or more types of intermolecular interactions, such as electrostatic (ionic), dipolar, charge transfer, hydrogen bonding, hydrophobic, and van der Waals interactions; the last is composed of a combination of permanent, induced, and instantaneous dipole-dipole interactions. Each of these forms of intermolecular interactions will now be discussed in some detail.

Parameters used in QSAR

1. Hydrophobicity

Meyer and Overton made their discovery on the correlation between oil/water partition coefficients and the narcotic potencies of small organic molecules. Many years later, Hansch established a model to measure the lipophilicity in term of partition coefficient. Drug travels to the site of action that means solubility in 1-octanol that simulates the lipid membrane then it goes to via cytoplasm that is simulated by Aqueous buffer "water". Hansch proposed the lipophilicity measurement in term of partition coefficient "**P**" [37].

$$\mathbf{P = [C]octanol / [C]water}$$

Hydrophobic compounds will have a high P value, whereas hydrophilic compounds will have a low P value. The hydrophobic character of a drug can be measured experimentally by testing the drug's relative distribution coefficient.

Varying substituents on the lead compound will produce a series of analogues having different hydrophobicities and therefore different P values. Various substituents make to hydrophobicity. This contribution is known as the substituent

hydrophobicity constant (Log P). This constant is a measure of how hydrophobic a substituent is, relative to hydrogen. A positive value indicates that the substituent is more hydrophobic than hydrogen. A negative value indicates that the substituent is less hydrophobic.

$$\textbf{Log P = Log \{[C]octanol / [C]water\}}$$

The value of Log P at the maximum (Log P^0) represents the optimum partition coefficient for biological activity. Beyond that point, an increase in Log P results in a decrease in biological activity.

2. Hammett's constant

This is one of the electronic factors. The electronic effects of various substituents will clearly have an effect on a drug's ionization or polarity. This in turn may have an effect on how easily a drug can pass through cell membranes or how strongly it can bind to a receptor. It is therefore useful to have some measure of the electronic effect a substituent can have on a molecule. As far as substituents on an aromatic ring are concerned, the measure used is known as the Hammett substitution constant (σ).

This leads to definition of the Hammett substitution constant [37]. It is a measure of the size of the electronic effect i.e. whether an electron withdrawing or electron donating for a given substituent and represents a measure of electronic charge distribution in the benzene nucleus.

2.1 Positive σ: if σ is positive, the substituent is electron attracting, which means it takes out the electrons from the ring.

2.2 Negative σ: if σ is negative, the substituent is electron donating, which means it gives out its own electron to the species.

3. Steric effect

Determination of steric properties is more difficult than either hydrophobic or electronic properties. The bulky size and shape of novel drugs played how easy to interact with the binding site. Compounds with the bulky moiety may show hinder and shielding interaction between drug and its binding site; however, it can increase the activity depending on the active site [38].

4. Dipole Moment

This quantity is the resultant dipole of a molecule brought about from contributions of individual bond dipoles. As calculated from electronic structure determinations.

The dipole moment is obtained from considerations of individual partial atomic charges brought about by electronic distributions within the molecule. The dipole moment of simple linear diatomic molecules is defined as the product of charge separation and interatomic distance [37];

$$m = q \times d$$

q = charge and d = distance. The units of dipole moments are debyes (D.) and 1 debye = 3.33×10^{-30} coulomb.meter.

The magnitude of the dipole moment is a description of the degree of polarity of the molecule and, as such, is an important quantity in intermolecular interactions, including those associated with hydrogen-bond formation and other related dipole-dipole and ion-dipole interactions.

5. Molecular polar surface area

Several new parameters have been introduced for absorption prediction, including molecular size and shape descriptors, hydrogen-bonding capabilities, and surface properties. Molecular polar surface area (PSA) is a descriptor that was shown to correlate well with passive molecular transport through membranes [39].

Polar surface area is defined as a sum of surfaces of polar atoms or high electronegativity value (fluorines, oxygens and nitrogens) in a molecule. This parameter has been shown to correlate very well with the human intestinal absorption, Caco-2 monolayers permeability, and blood-brain barrier penetration.

CHAPTER III

RESEARCH METHODOLOGY

Research study overview

Investigation of vanillinamine hydrochloride derivatives (**14-19**) and 3-trifluoromethoxy capsaicin (**21**) were divided into three parts: 1. synthesis of vanillinamine hydrochloride derivatives (**14-19**) and 3-trifluoromethoxy capsaicin (**21**), 2. evaluation for anti-inflammation activity by using human TNF-α immunoassay of 3-trifluoromethoxy capsaicin (**21**) and capsaicin 3. investigation on AChE inhibitory activity of vanillylamine hydrochloride derivatives (**14-19**).

1. Synthesis of vanillinamine hydrochloride derivatives (14-19) and 3-trifluoromethoxy capsaicin (21)

Synthesis of vanillinamine hydrochloride derivatives (**14-19**) and 3-trifluoromethoxy capsaicin (**21**) was divided into four parts: 1.1 synthesis of 3-trifluoromethoxy vanillin (**2**), 1.2 synthesis of vanillinamine hydrochloride derivatives (**14-19**), 1.3 synthesis of 3-trifluoromethoxy capsaicin (**21**) and 1.4 Preparation of (E)-8methyl-6-nonenic acid (**20**).

1.1 Synthesis of 3-trifluoromethoxy vanillin and (2) and 3-trifluoromethoxy vanillinamine hydrochloride (14)

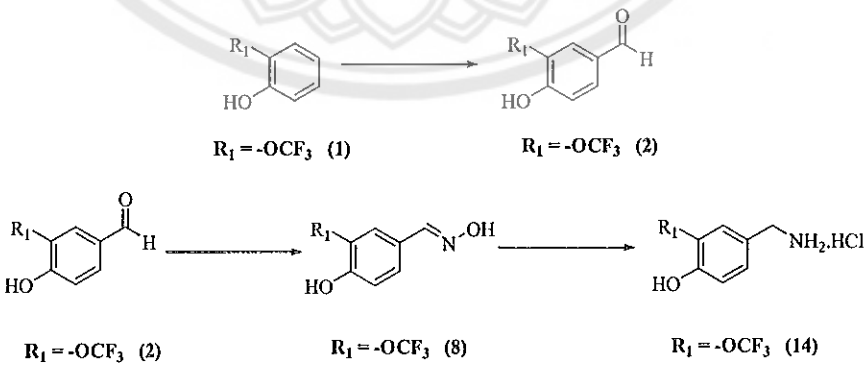

Scheme 1 Synthesis of 3-trifluoromethoxy vanillin and (2) and 3-trifluoromethoxy vanillinamine hydrochloride (14)

1.2 Synthesis of 3-trifluoromethoxy capsaicin (21)

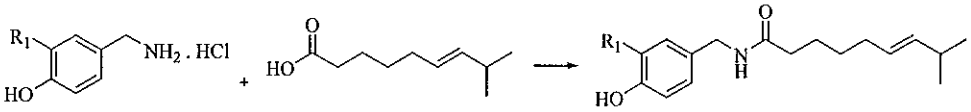

R_1 = -OCF_3 (14) (20) R_1 = -OCF_3 (21)

Scheme 2 Synthesis of 3-trifluoromethoxy capsaicin (21)

1.3 Synthesis of vanillylamine hydrochloride derivatives (15-19)

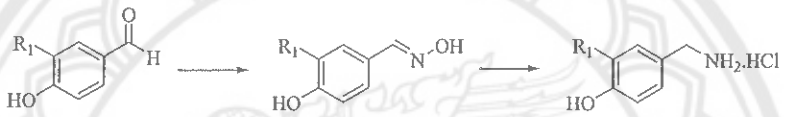

R_1 = -F	(3)	R_1 = -F	(9)	R_1 = -F	(15)
-Cl	(4)	-Cl	(10)	-Cl	(16)
-Br	(5)	-Br	(11)	-Br	(17)
-H	(6)	-H	(12)	-H	(18)
-OCH_3	(7)	-OCH_3	(13)	-OCH_3	(19)

Scheme 3 Synthesis of vanillylamine hydrochloride derivatives (15-19)

1.4 Preparation of (*E*)-8-methyl-6-nonenic acid (20)

(*E*)-8-methyl-6-nonenic acid can be prepared by ethanolysis of capsaicinoids. This reaction gave the mixture products of saturated and unsaturated fatty acid and fatty ester (**Scheme 4**). The mixture products can be further purified by HPLC technique to give purre *(E)*-8-methyl-6-nonenic acid (20).

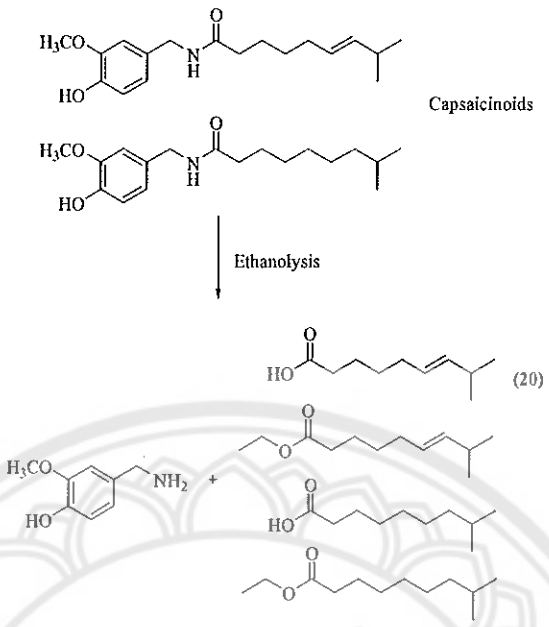

Scheme 4 Preparation of (*E*)-8-methyl-6-nonenic acid (20)

2. Determination of anti-inflammation activity via human TNF-α immunoassay

This procedure was achieved via immunology system of PBMC that separated into two parts: I) effect of 3-trifluoromethoxy capsaicin (**21**) on cell viability and II) effect of 3-trifluoromethoxy capsaicin (**21**) in human TNF-α assay using LPS stimulation on PMBC.

3. Investigation for AChE inhibitory activity of vanillinamine hydrochloride derivatives (14-19)

Determination of AChE inhibition was based on Ellman's method [40]. This method measured the color intensity after acetylthiocholine iodide (ACTI) was hydrolyzed by AChE into thiocholine and actetic acid allowing thiocholine reacted with 5,5'-dithiobis-2-nitrobenzoic acid (DTNB) to generate yellow color.

General Procedure

1. Apparatus

All of the reactions were checked by thin layer chromatography (TLC) (Merck D.C. silica gel 60 F254 0.2 mm-precoated aluminum plates). Column chromatography Visualization of TLC plates was accomplished by UV light at 254 nm. Evaporator was performed on Buchi Rotavapor R-114 with either a water aspirator model B-480 or a Refco Vacubrand pump. All the glassware were oven dried and all chemicals weight on the Mettler Toledo model ML104/01.

^{1}H-NMR at 400 MHz and ^{13}C-NMR at 100 MHz spectra were recorded on the Bruker NMR spectrometer model Avance 400. Chemical shirt (δ) were reported in part per million (ppm) relative to either tetramethylsilane (TMS) or the residual of protonated solvent signal as a reference. IR spectra were obtained from Perkin-Elmer FT-IR spectrophotometer Model 1600 series at range 4000-400 cm^{-1} of wave number. Mass spectra were measured in positive ion mode with an Agilent 6540 Q-TOF mass spectrometer.

3-trifluoromethoxy capsaicin (**21**) was purified by reverse phase HPLC with fraction collector on an Agilent 1260 series controller system equipped with gradient pump and Agilent 1260 series photodiode array detector. Avertisep^{TM} C_{18} HPLC column 5 µm particle size 10x150 mm. Peak monitors and data processes were operated on the base Empower software. The fractions were automatically collected and assisted by real-time HPLC chromatogram monitor.

Acetylcholinesterase inhibition assay was performed by the microplate spectrophotometer model Synergy H1 Hybrid Reader (Bio-Tek) and calculation of lipophilicity (miLogP) and molecular volume were performed via Molinspiration program [41].

The dipole moment calculations were done by using Density Functional Theory (DFT) at B3LYP/6-31+G(d,p) level of theory in gas phase. The calculations were performed by using Gaussian09 program package [42].

2. Materials and Method

The reagents used for the synthesis of vanillinamine hydrochloride derivatives (**14-19**) and 3-trifluoromethoxy capsaicin (**21**) were an analytical reagent (AR) grade. All commercially chemicals were purchased from Aldrich Co., Fluka Co., Ltd, Merck Co., Ltd, Chempep Co., Ltd and Lab Scan Co., Ltd, Thai can biotech Co., Ltd. and were used without purification unless otherwise stated.

IUPAC name 2-(trifluoromethoxy) phenol was purchased from Aldrich Co., Ltd., 99% trifluoroacetic acid (TFA), ≥99% hexametylenetetramine HMTA), 99.9% sodium acetate trihydrate ($NaOAc.3H_2O$), 99% hydroxylamine hydrochloride, 10% palladium on carbon, 37% hydrochloric acid, 98% 1-hydroxybenzotriazole (HOBt), *N*-(3-dimethylaminopropyl)-*N'*-ethylcarbodiimide hydrochloride (EDC.HCl), 99.5% triethylamine (TEA), 98% formic acid, *N,N*-Dlimethylformamide (DMF) were dried with molecular sieve 3 Å under N_2 atmosphere, ≥98% vanillin were purchased from Acros Co Ltd. and Aldrich Co., Ltd. The commercial grade solvents for column chromatography were distilled prior use. Chloroform-d ($CDCl_3$) and deuterium oxide (D_2O) for NMR characterization were purchased from Aldrich Co., Ltd.

For the assay agents of anti-inflammatory procedure, lipopolysaccharides from *Escherichia coli* was purchased from Aldrich Co., Ltd. Typan blue, RPMI 1640 without L-glutamine, fetal bovine serum (FBS) were purchased from Thermo Fisher Scientific Co., Ltd. Lymphoprep, penicillin streptomycin (pen strep) and phosphate buffer saline (PBS) were purchased from Biotech and Scientific Co., Ltd. The human TNF-α Elisa kit was purchased from Advanced Medical Science Co., Ltd.

Acetylthiocholine iodide (ACTI), 5,5'-dithiobis-2-nitrobenzoic acid (DTNB) and acetylcholinesterase from electric eel (type VI-S; lyophilized powder) were purchased from Aldrich Co., Ltd. 50 mM Tris-HCl pH 8.0 (buffer I) was used as a buffer for microplate assay. Moreover, the enzyme was diluted in 0.1% BSA in buffer. DTNB was dissolved in buffer I and ATCI was dissolved in deionized water.

Experiment

1. Synthesis of 3-trifluoromethoxy vanillin and (2) and 3-trifluoromethoxy vanillinamine hydrochloride (14)

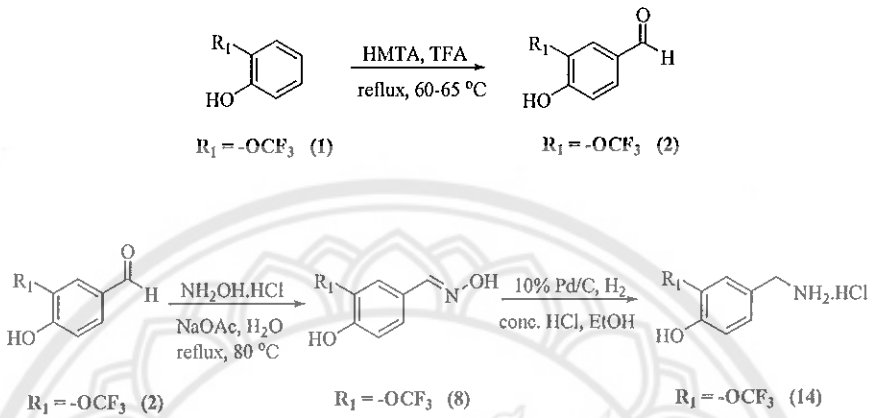

Scheme 5 Synthesis of 3-trifluoromethoxy vanillin and (2) and 3-trifluoromethoxy vanillinamine hydrochloride (14)

Compound 2 was prepared by mixing 2-(trifluoromethoxy)phenol **(1)** (1.0 eq.) with HMTA (1.2 eq.) and dissolved in trifluoroacetic acid overnight at 60-65 °C to give 44% yield of crude crystalline compound. The desired product was further purified by flash column chromatography using 1%MeOH:CH_2Cl_2 as an eluent.

(**2**) Yellow crystal; 44% yield; column chromatography with 1%MeOH:CH_2Cl_2; R_f = 0.46 (1%MeOH in CH_2Cl_2)

^{1}H-NMR (400 MHz, $CDCl_3$) δ: 9.86 (1H, s, CHO), 7.77 (2H, m, ArH), 7.19 (1H , d, *J*=8.4 Hz, ArH); ^{13}C NMR (100 MHz, $CDCl_3$) δ: 190.0, 153.5, 130.8, 130.1, 122.3, 122.0, 119.4, 118.0; FT-IR (KBr) cm^{-1}: 3,338 (OH stretching), 2,854 (C-H stretching of CHO), 1,678 (C=O stretching of CHO); HRMS Calcd. for $C_8H_5F_3O_3$: m/z 206.0190, found m/z 207.0322 $(M+H)^+$.

Compound **14** was synthesized by reduction reaction of oxime (**3**). Mixing vanillin derivative (**3**) (1.0 eq.) with hydroxylammonium chloride (1.2 eq.) and sodium carbonate trihydrate (1.2 eq.) and then was heated at 80 °C for 3 hours to give oxime derivative (**8**).

Next, oxime derivative (**8**) was reduced by hydrogenation by using 10% palladium on carbon (1.2 eq.) in ethanolic hydrochloride solution as solvent to give crude product of **14**. Crude product of **14** was filtered through celite and then purified by crystallization from ethyl acetate and ethanol as co-solvent to give pure product of **14**.

(**14**) white crystal; 31% yield; R_f = 0.19 (1%MeOH in EtOAc)

^{1}H-NMR (400 MHz, D_2O) δ: 7.45 (1H, s, *J*=1.8 Hz, ArH), 7.33 (1H, dd, ArH), 7.12 (1H, d, *J*=8.4 Hz, ArH), 4.13 (2H, s, CH_2); ^{13}C NMR (100 MHz, D_2O) δ: 148.8, 129.3, 125.1, 123.7, 118.3, 117.4, 115.4, 42.32; FT-IR (KBr) cm^{-1}: 3,120 (N-H stretching), 1,604 (N-H bending); HRMS Calcd. for $C_8H_8F_3NO_2$: m/z 207.0507, found 208.0635 m/z $(M+H)^+$.

2. Synthesis of 3-trifluoromethoxy capsaicin (21)

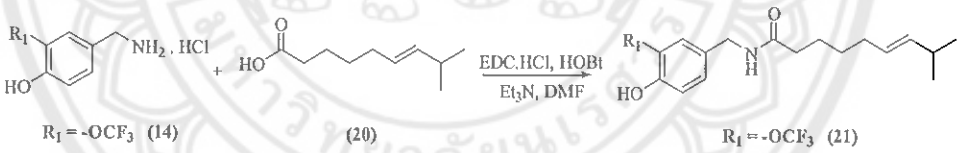

Scheme 6 Synthesis of 3-trifluoromethoxy capsaicin (21)

The synthesis of **21** was synthesized by the coupling reaction between (E)-8-methyl-6-nonenoic acid (**20**) and **14**. The mixture of **20** (1.00 eq.) was activated with HOBt (1.50 eq.) and EDC.HCl (1.50 eq.) at 0 ◦C for 30 minutes and stirred continuous at ambient temperature for 30 minutes. Before coupling, **14** (1.00 eq.) was activated with trietylamine (2.50 eq.) for 30 minutes in anhydrous DMF as a solvent. After that, the **20** and **14** were coupling at room temperature for 24 hours. Then, the reaction mixture were diluted with brine and extracted into EtOAc (3x20 mL). The organic layers were washed successfully with 10% citric acid solution (3x20 mL) and 0.5 M $NaHCO_3$ solution (3x20 mL) and dried over Na_2SO_4. The organic layers were

concentrated under vacuum and were purified by column chromatography. The crude product of **21** was purified by column chromatography (30% EtOAc/hexane as a mobile phase). Finally, crude product of **21** was further purified to give pure compound by HPLC technique using C18-column with acetonitrile:water containing 0.1 % formic acid (1 : 1.2) as a mobile phase and flow rate at 3.5 mL/min.

Compound **21** oil product; 16% yield; column chromatography with 30%EtOAC:Hexane; R_f = 0.28 (30%EtOAC in Hexane)

^{1}H NMR (400 MHz, $CDCl_3$-d_1) δ 7.10 (2H, m, ArH), 6.96 (1H, m, Ar), 5.74 (1H, s, NH), 5.33 (2H, m, CH=CH), 4.37 (2H, d, J = 5.8 Hz, CH_2), 2.21 (3H, m, CH_2,CH), 1.99 (2H, m, CH_2), 1.64 (2H, m CH_2), 1.38 (2H, p, J = 7.6 Hz, CH_2), 0.95 (6H, d, J = 6.8 Hz, CH_3, CH_3); ^{13}C-NMR (100 MHz, $CDCl_3$) δ: 173.23, 147.47, 138.29, 131.31, 127.64, 126.56, 121.08, 119.54, 117.73, 42.83, 36.78, 33.32, 31.11, 29.37, 25.35, 22.78; FT-IR (KBr) cm^{-1}: 3,279 (N-H stretching), 1,623 (N-H bending); HRMS: Calcd. For $C_{18}H_{24}F_3NO_3$: m/z 359.17, found 360.1832 m/z $(M+H)^+$

3. Synthesis of vanillylamine hydrochloride derivatives (15-19)

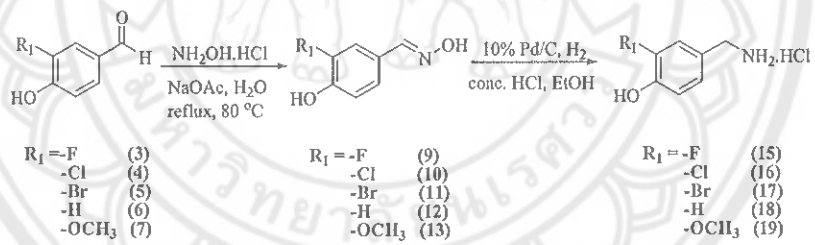

Scheme 7 Synthesis of vanillylamine hydrochloride derivatives (15-19)

Synthesis of vanillylamine hydrochloride derivatives (**15-19**) were synthesized by reduction reaction of oxime **9-13**. Mixing vanillin derivatives (**3-7**) (1.0 eq.) with hydroxylammonium chloride (1.2 eq.) and sodium carbonate trihydrate (1.2 eq.) and then was heated at 80 °C for 3 hours to give oxime derivatives (**9-13**).

Next, oxime derivatives (**9-13**) were reduced by hydrogenation by using 10% palladium on carbon (1.2 eq.) in ethanolic hydrochloride solution as solvent to give crude products of **15** and **18-19**. Unfortunately, 3-chloro and 3-bromo-4-hydroxybenzylamine hydrochloride (**16- 17**) were not successfully synthesized. Crude

products of **15** and **18-19** were filtered through celite and then purified by crystallization from ethyl acetate and ethanol as co-solvent to give pure products of **15** and **18-19**.

(**15**) white crystal; 34% yield; R_f = 0.24 (25% MeOH in EtOAc)

^{1}H-MMR (400 MHz, D_2O) δ: 7.22 (1H, dd, *J*=11.9, 2.0 Hz, ArH), 7.11 (1H, dd, *J*=8.4, 2.1 Hz, ArH), 7.03 (1H, t, *J*=7.9 Hz, ArH), 4.12 (2H, s, CH_2); ^{13}C-NMR (100 MHz, D_2O) δ: 152.39, 150.00, 125.75, 125.22, 118.27, 117.05, 42.42; FT-IR (KBr) cm^{-1}: 3,179 (N-H stretching), 1,626 (N-H bending); HRMS: Calcd. For C_7H_8FNO: m/z 141.0590, found 142.0663 m/z $(M+H)^+$.

(**18**) light yellow solid; 73% yield; R_f = 0.28 (20% MeOH in EtOAc)

^{1}H-MMR (400 MHz, D_2O) δ: 7.32 (2H, d, *J*=8.0 Hz, ArH), 6.92 (2H, d, *J*=8.0 Hz, ArH), 4.08 (2H, s, CH_2); ^{13}C-NMR 100 MHz, D_2O) δ: 156.26, 130.79, 124.59, 115.95, 42.72; FT-IR (KBr) cm^{-1}: 3,369 (N-H stretching), 1,613 (N-H

(**19**) white crystal; 32% yield; R_f = 0.22 (1%MeOH in EtOAc)

^{1}H NMR (400 MHz, MeOD-d_4) δ: 7.04 (1H, d, Ar, *J*=2.0 Hz), 6.91 (1H, dd, J_1=8.1 Hz, J_2=2.0 Hz, ArH), 6.85 (1H, d, *J*=8.1 Hz, ArH), 4.11 (2H, s, CH_2), 3.88 (3H, s, OCH_3); FT-IR (KBr) cm^{-1}: 3,428 (N-H stretching), 1,614 (N-H bending); HRMS Calcd. for $C_8H_{11}NO_2$: m/z 153.08, found 154.0829 m/z $(M+H)^+$.

4. Determination of anti-inflammation activity onto immunology system via human TNF-α immunoassay of 3-trifluoromethoxy capsaicin (21)

4.1 Effect of 3-trifluoromethoxy capsaicin (21) on cell viability

A viability assay was the procedure to determine the death cells or living cells. This assay was performed by suspended and mixed the cells with dye and then visually examined to determine the cell viability. For the viable cells, it showed a clear cytoplasm while the death cells showed a blue stain on cytoplasm.

1. Separation of peripheral blood mononuclear cell (PBMC)

25 mL of Human blood was diluted with phosphate buffer saline (25 mL) in sterilized centrifuge tube and mixed to homogeneous solution (solution A) and slowly added 30 mL of solution A on top of lymphoprep (15 mL) without spreading of blood. After that, it was centrifuged in swing-out rotor at 800 x g for 25 min with no break at approximately 20°C. After centrifugation, a PBMC band at the middle of centrifuge tube was kept out from the solution (**Figure 19**). The PBMC was washed in

phosphate buffer saline (35 mL) for two times and centrifuged at 600 x g for 10 minutes with break at approximately 5˚C in swing-out rotor to give the desired PBMC. They were incubated in RPMI culture medium containing 10 % FBS and 1% penicillin streptomycin in 5% CO_2 at 37 ˚C for cell viability test.

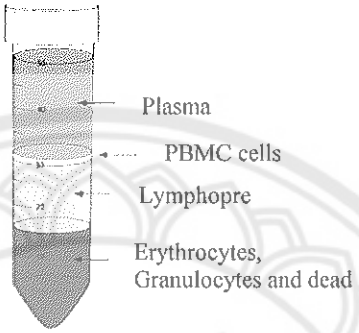

Figure 19 Separation of PBMC from human blood

2. Cell viability of 3-trifluoromethoxy capsaicin (21) using trypan blue exclusion test

PBMC in RPMI solution was added into 96-well plate at a concentration of $1x10^5$cell/well and volume in each well was 100 μL. The concentrations at 1, 5, 50, 100 and 200 μM in RPMI containing 1 %PEG (100 μL) was added to each well plate and were incubated for 24 hours. After that, PBMC cell suspension was simply mixed with trypan blue and then visually examined *via* microscope. A viable cell was a clear cytoplasm whereas a non-viable cell was a blue cytoplasm.

4.2 Effect of 3-trifluoromethoxy capsaicin (21) on human TNF-α production by LPS-stimulated PBMC

The concentration of TNF-α in culture supernatants was assessed by enzyme-linked immune sorbent assay (ELISA). The assays were conducted utilizing the OptEIATM Human TNF-α immunoassay kit (Advanced Medical Science Co., Ltd) according to the manufactories instruction. The sample was thawed, diluted properly in assay diluents and assayed for TNF-α concentration. The absorbance of each well was read at 450 nm on a microplate reader (PerkinElmer Life Sciences, Downers

Grove, IL, USA). TNF-α was measured from standard curve using Plate Reader version 3.0 programs (PerkinElmer Life Sciences, Downers Grove, IL, USA).

1. Sample preparation

PBMC in RPMI solution was added into the 96-well plate at$1x10^5$ cells/well in 100 µL. Then, a mixture of 10 µM of 3-trifluoromethoxy capsaicin (**21**) in RPMI (50 µL) and 50 nM of LPS in RPMI (50 µL) was added in each well plate. After that, the cell suspension was incubated for 16 hours. Thereafter, cell culture supernatant samples were kept at -20 ˚C until being assayed for TNF-α testing.

Sample preparation step

1.1 Buffer Diluent preparation

5X Assay Diluent A was diluted to concentration at 1X with PBS (pH 7.4).

1.2 Coating Antibody preparation

The buffer was diluted of 5X Coating Buffer A to 1X with deionized water. Then, pre-titrated Capture Antibody was diluted with 1X coating Buffer A to concentration in 1:200.

1.3 Reagent preparation

First, all reagents were brought to room temperature and, before assay procedure; all of reagent were freshly prepared as below.

1.4 Wash Buffer

The buffer was prepared from 0.05% Tween-20 in PBS.

1.5 Human TNF-α Standard

The lyophilized Human TNF-α Standard are under vacuum pressure. Reconstitute lyophilized standard with 1,000 µL of 1X Assay Diluent A. Allow the reconstituted standard to sit for 15 minutes at room temperature, then briefly vortex to making dilutions.

1.6 Sample

For assay, standard reagent and samples are analyzed without dilutions.

1.7 Detection Antibody preparation

The pre-titrated Biotinylated Detection Antibody was diluted in 1X Assay Dilution A to ratio at 1:200.

1.8 Avidin-HRP preparation

The Avidin-HRP was diluted in 1X Assay Diluent A at ratio as 1:1000.

1.9 Substrate Solution preparation

The TMB Substrate Solution is a mixture of equal volumes of Substrate Solution A and Substrate Solution B. Mix the two components immediately prior to use. The mixed solution should be clear and colorless.

1.10 Stop Solution

The solution was used acid solution for example 2N of sulfuric acid which used in this assay.

2. Calibration curve of TNF-α standards

Human TNF-α standard was diluted with 1X Assay Buffer A and prepared 500 µL of the 1,000 pg/mL to top standard. Perform six two-fold serial dilutions of the 1,000 pg/mL in separate tubes using Assay Buffer A as the diluent. Consequently, the human TNF-α standard concentration in the tubes were 1,000, 500, 250, 125, 62.5, 31.3 and 15.6 pg/mL; respectively. Assay Buffer A operated as the zero standard (0 pg/mL) (**Figure 20**).

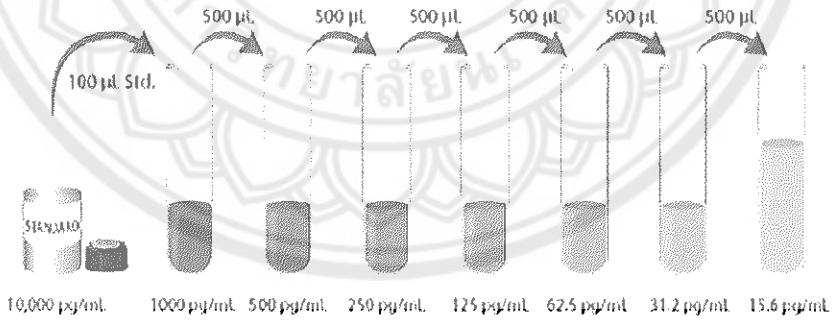

Figure 20 Preparing of TNF-α standards procedure

3. Human TNF-α assay procedure

One day prior to running the ELISA, Capture Antibody was diluted and was added 100 µL to all wells of a 96-well plate provide in this set. Plates were sealed and incubated overnight (16-18 h) between 2 ˚C and 8 ˚C. Brought the all

reagents and samples to room temperature before used, it was recommended that all standards, samples, and controls be assayed in duplicate.

First, the plate was washed 4 times with 300 µL of Wash Buffer per well and blot any residual buffer by firmly tapping the plate upside down on absorbent paper. To block non-specific binding and reduced background, plates were added 200 µL of 1X Assay Diluent A per well. Plates were sealed and incubated at RT for 1 h with shaking on a plated shaker (500 rpm) and washed plate 4 times with wash buffer. Next, added 100 µL of Assay Buffer A to each well and added 100 µL of standard dilutions or samples to the wells. Sealed the plate with a Plate Sealer and incubate at room temperature for 2 h and shaking at 500 rpm.

After that, discarded the contents in the plate and wash the plate 4 times with Wash Buffer. Add 100 µL of diluted Detection Antibody solution to each well, covered plate and incubate at room temperature for an hour and shaking. Discard the contents, and then wash the plate 4 times with Wash Buffer. Added 100 µL of diluted Avidin-HRP solution to each well, sealed the plate and incubate at room temperature for 30 minutes and shaking.

Discard and wash the plate 5 times with Wash Buffer. For final wash, soak wells in Wash Buffer for a minute this will help minimize background. Add 100 µL of freshly mixed TMB substrate solution to each well and incubate for 15 minutes in the dark. Wells containing TNF-α will turn into blue color with an intensity depend on its concentration. Finally, 100 µL of Stop Solution was added to stop the reaction. The color of solution will change from blue to yellow and read absorbance at 450 nm within 30 minutes using microplate reader instrument.

4. Investigation for AChE inhibitory activity of vanillinamine hydrochloride derivatives (14-19)

Determination of AChE inhibition was based on Ellman's method. All of vanillinamine hydrochloride derivatives **14-15** and **18-19** were dissolved in buffer I for screening AChE inhibition at 10 mM concentration in 96-well plate. Mixing 25 µL of sample, 50 µL of buffer I with 0.0005 unit/mL AChE and incubated in 96 well-plate for 2 min at room temperature and then 25 µL of 1.5 mM ATCI substrate and 125 µL of 3.0 mM DTNB were added and measured with microplate spectrophotometer model Synergy H1 Hybrid Reader (Bio-Tek) at 405 nm for every

20 second for 2.0 minutes. The percent inhibition was calculated by the comparison of velocity of the reaction between inhibitor buffer and buffer with free inhibitor (**Figure 21**). The calculation of the inhibition at 50% enzymatic activity (IC_{50}) was used by the GraphPad Prism software.

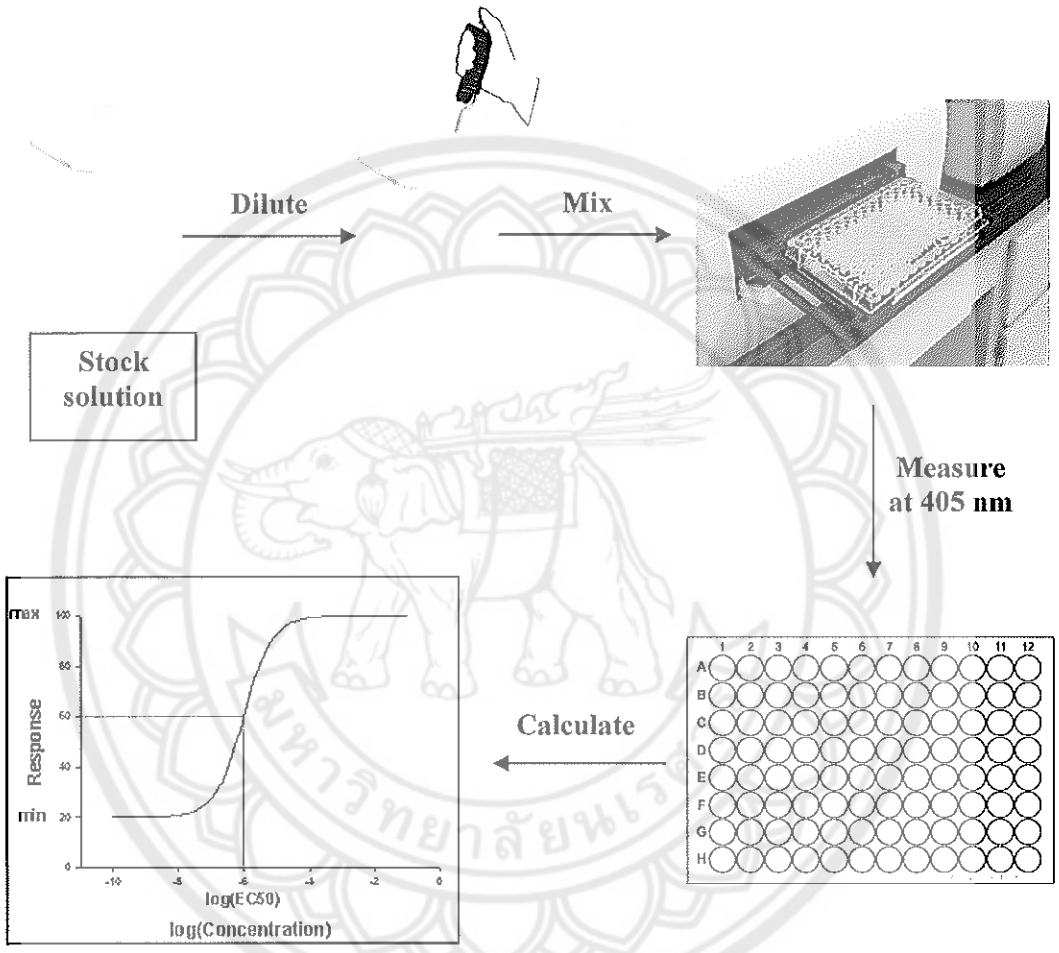

Figure 21 AChE inhibitory activity procedures

CHAPTER IV

RESULTS AND DISCUSSION

Synthesis of Synthesis of 3-trifluoromethoxy capsaicin (21)

1. Synthesis of 3-trifluoromethoxy vanillin (2)

The synthesis of compound **2** (**Scheme 8**) was successfully prepared *via* Duff reaction (**Figure 22**) by using hexamethylenetetramine (HMTA) [43] in 44% yield and the presence of the aldehyde group (CHO) was spectroscopically presented at 9.86 ppm (**Figure 23**). For HRMS of compound **21**, Calcd. For $C_{18}H_{24}F_3NO_3$: m/z 206.02, found 207.0322 m/z $(M+H)^+$ (**Figure 24**). Also, the IR peak at 2,854 cm^{-1} (C-H stretching of CHO), 1,678 cm^{-1} (C=O stretching of CHO) reconfirmed the existence of aldehyde group on aromatic residue (**Figure 25**).

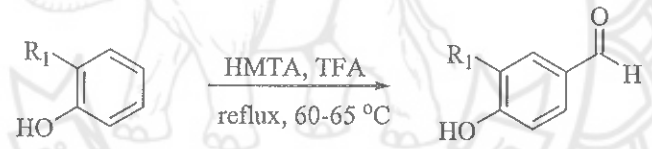

$R_1 = -OCF_3$ (1) $R_1 = OCF_3$ (2)

Scheme 8 Summary of the synthesis of 3-trifluoromethoxy vanillin (2)

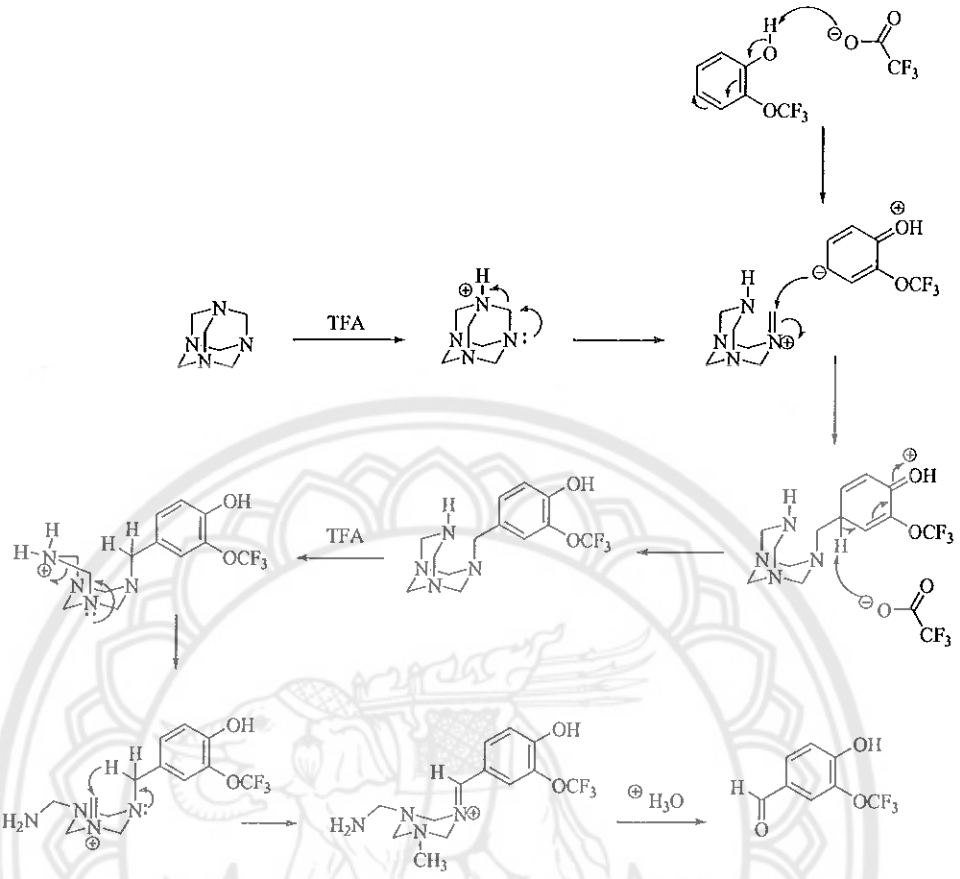

Figure 22 Mechanism of 3-trifluoromethoxy vanillin (2) *via* Duff reaction

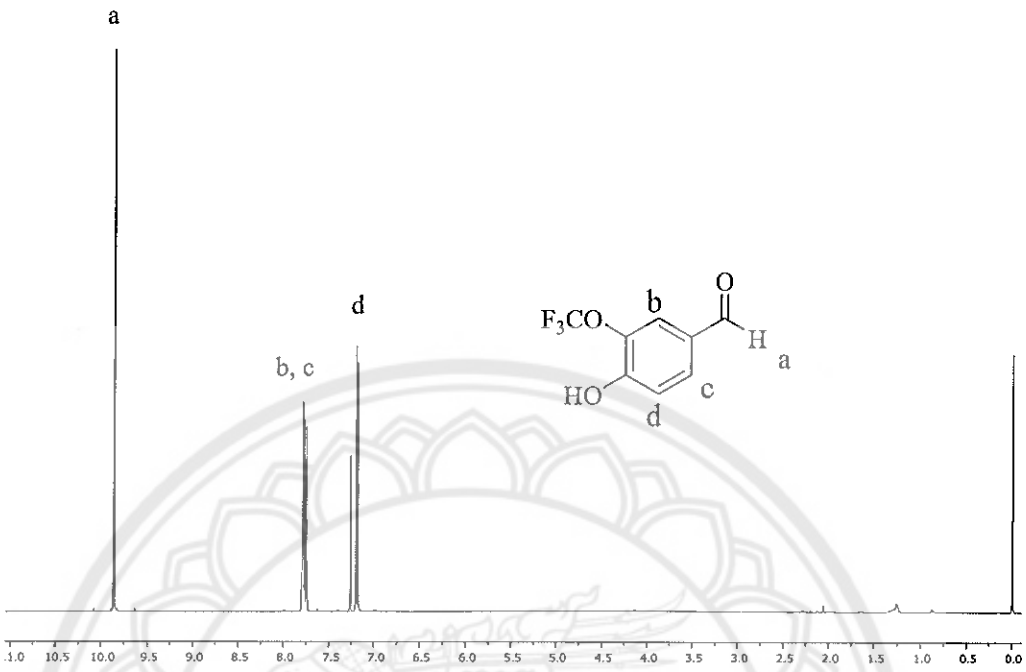

Figure 23 ^{1}H-NMR spectrum of 3-trifluoromethoxy-4-hydroxybenzaldehyde (2) ($CDCl_3$-d_1)

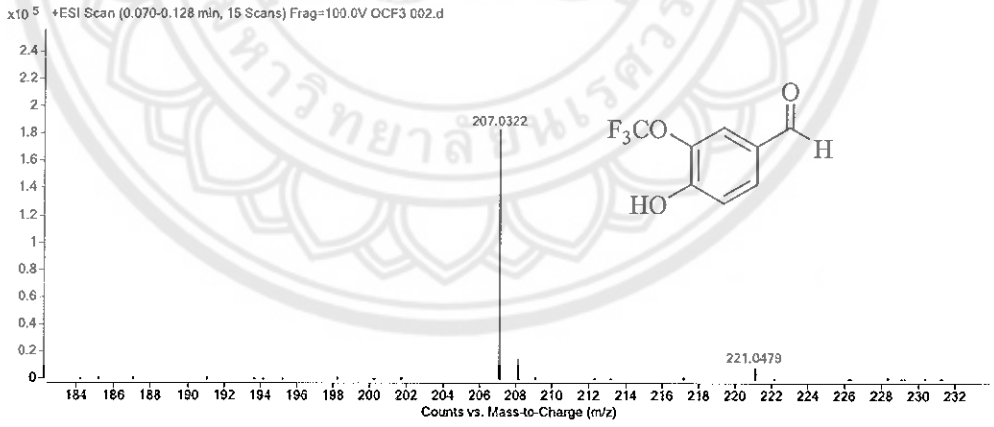

Figure 24 Mass spectrum of 3-trifluoromethoxy-4-hydroxybenzaldehyde (2)

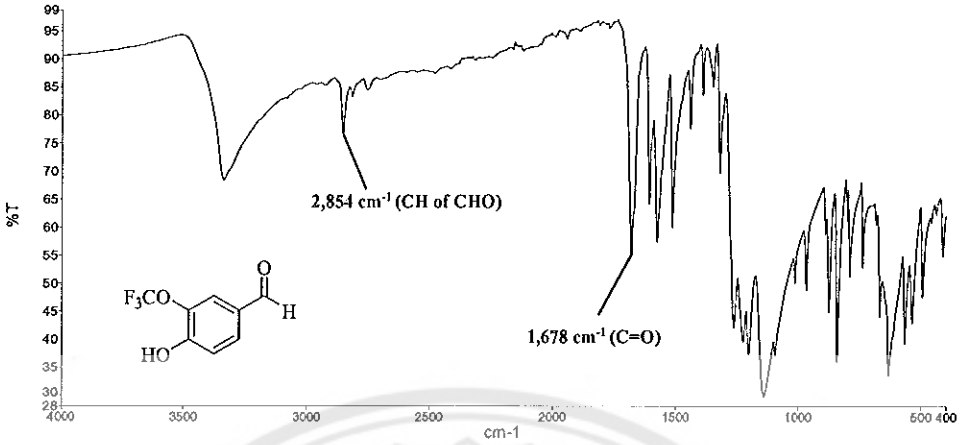

Figure 25 IR spectrum of 3-trifluoromethoxy-4-hydroxybenzaldehyde (2)

2. 3-trifluoromethoxy-4-hydroxybenzylamine hydrochloride (14)

The product of **14** was prepared via oxime (**Scheme 8**). Compound **14** was obtained in 31% yield as white crystals. The structure was confirmed by ^{1}H-NMR spectroscopy, showing the singlet pattern of methylene proton at 4.13 ppm (**Figure 26**). IR spectroscopy showed the absence of C=O stretching of aldehyde while the N-H stretching and N-H bending were observed at 3,120 and 1,604 cm^{-1} respectively (**Figure 27**).

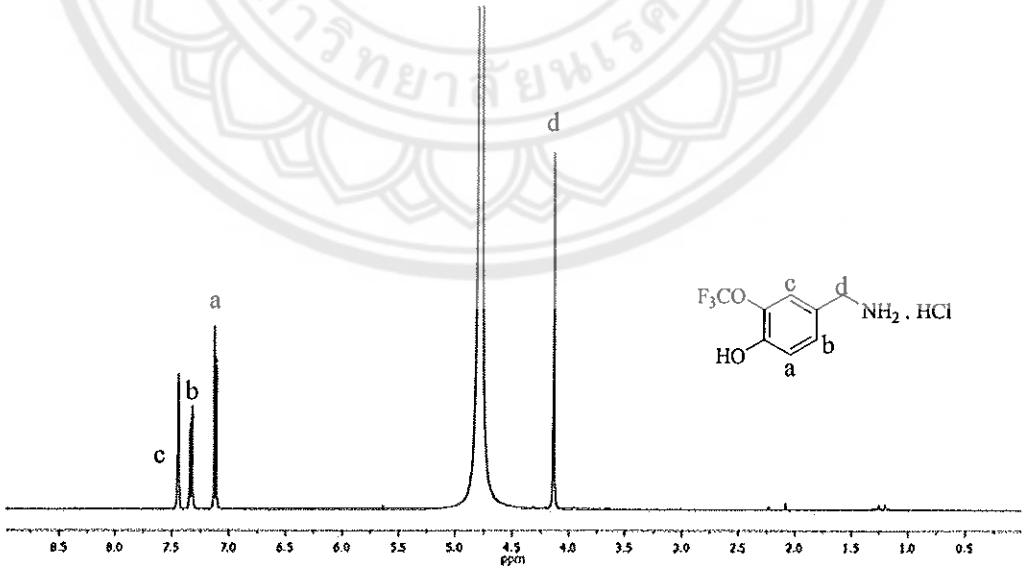

Figure 26 ^{1}H-NMR spectrum of 4-hydroxy-3-(trifluoromethoxy) vanillylamine hydrochloride (14) (D_2O-d_2)

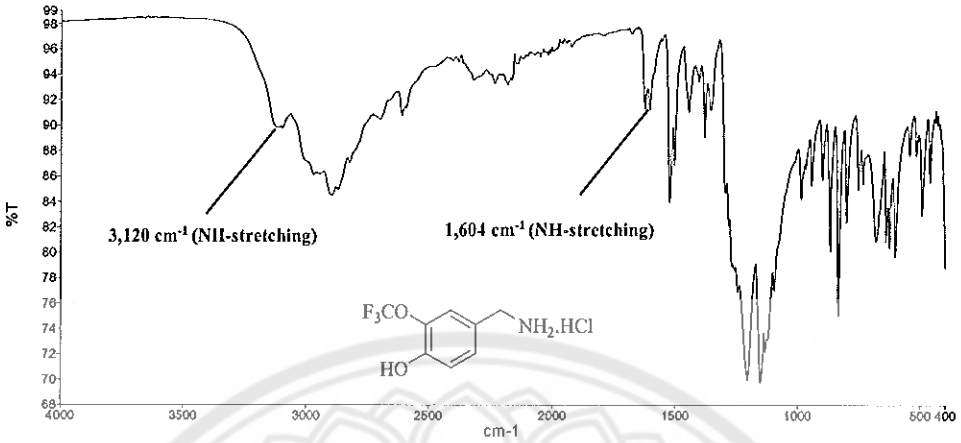

Figure 27 IR spectrum of 3-trifluoromethoxy-4-hydroxybenzylamine hydrochloride (14)

3. Synthesis of 3-trifluoromethoxy capsaicin (21)

The synthesis of **21** was prepared through the coupling reaction between aromatic amine hydrochloride derivative (**14**) and (*E*)-8-methyl-6-noneoic acid **(20)** (**Scheme 9**). This experimental was successfully by using HOBt and EDC.HCl to activate fatty acid and reaction was shown in **figure 28**.

Scheme 9 Summary of synthesis of 3-trifluoromethoxy capsaicin (21)

Compound **21** was purified by column chromatography using 30% EtOAc in hexane as a mobile phase and the product was given in moderate yield. The final pure compound of **21** was further purified *via* HPLC technique using C18-column with acetonitrile : water : formic acid (1:1:0.1) as a mobile phase.

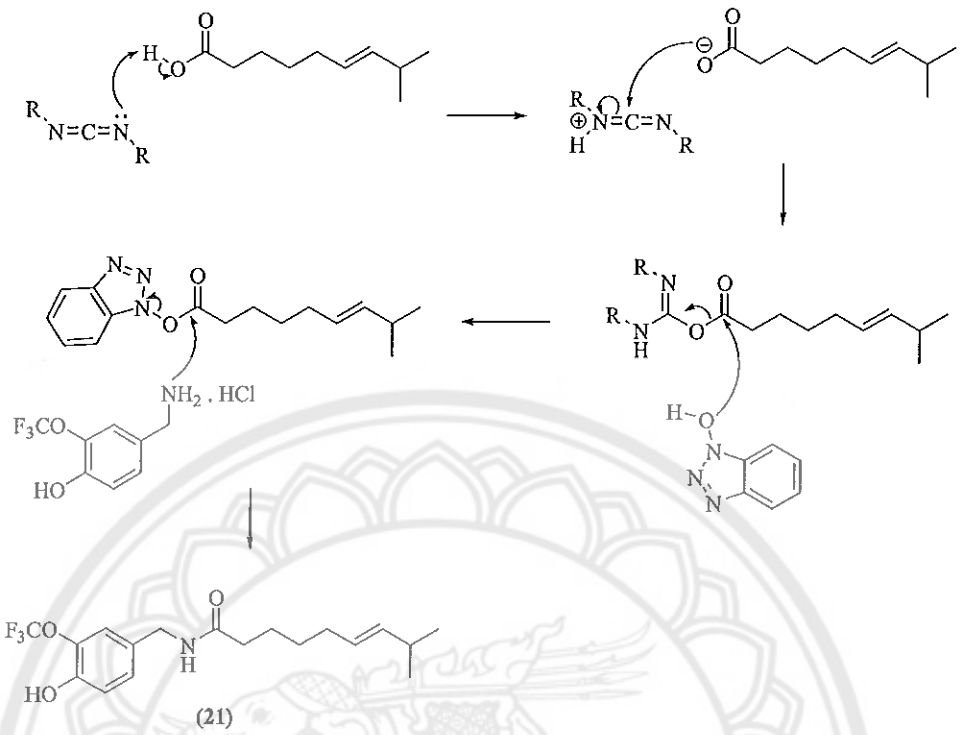

Figure 28 Mechanism of coupling reaction by using HOBt and EDC.HCl

The structure of **21** was confirmed the structure by the ^{1}H NMR by showing the key signal of NH of amide bond at 5.74 ppm, hydrocarbon chain pattern of fatty acid part in the range of 4.40-0.92 ppm and 7.14-6.94 ppm for monosubstituent of aromatic moiety (**Figure 29**). The identification of compound **21** was further confirmed by the HRMS for the molecular weight of new capsaicin analogue. For HRMS of compound **21**, Calcd. For $C_{18}H_{24}F_3NO_3$: m/z 359.17, found 360.1832 m/z $(M+H)^+$ (**Figure 30**).

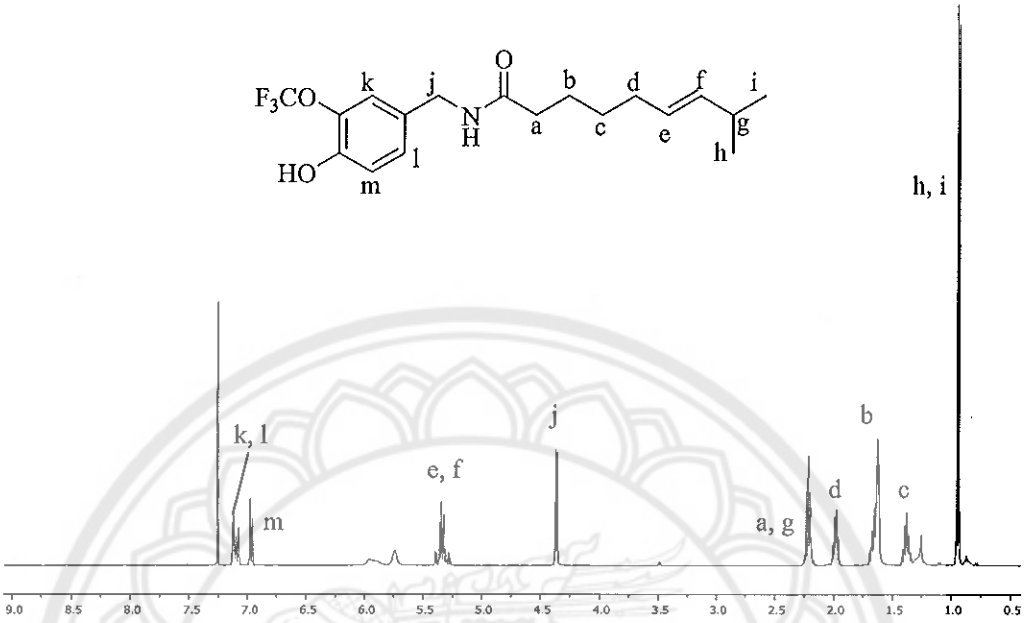

Figure 29 ^{1}H-NMR spectrum of 21 ($CDCl_3$-d_1)

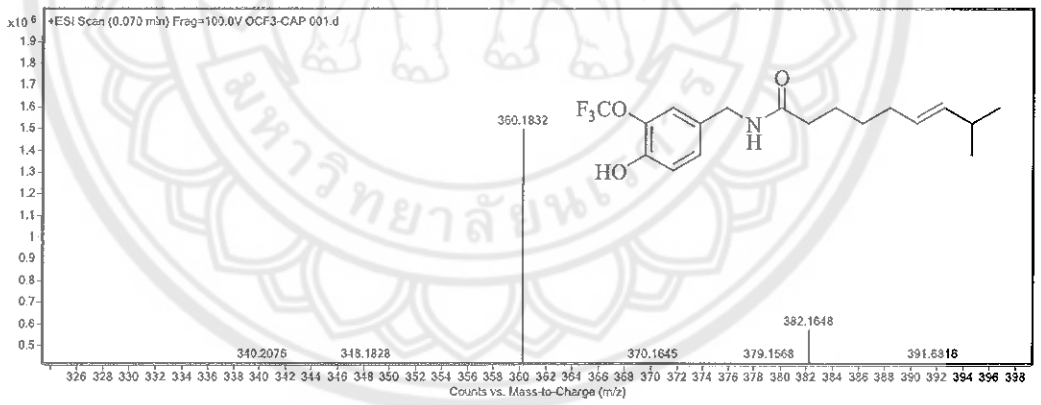

Figure 30 Mass spectrum of Isostere Capsaicin (21)

Determination of anti-inflammation activity onto immunology system via human TNF-α immunoassay of 3-trifluoromethoxy capsaicin (21)

The anti-inflammation assay was employed to evaluate the structure relationship of the new capsaicin analogue (**21**) and TRPV1 activity on the immune system using PBMC. This assay was used to describe the relationship of the structure of **21** with TRPV1 activity

The procedure was divided into two parts by determining the effect of 3-trifluoromethoxy capsaicin on cell viability via trypan blue technique and by determining the effect of 3-trifluoromethoxy capsaicin on human TNF-α production by using LPS-stimulated PBMC.

1. Effect of 3-trifluoromethoxy capsaicin (21) on cell viability *by using* trypan blue technique

The anti-inflammation assay was used to describe the structure relationship of compound **21** with TRPV1 activity on the immune system by using human PBMC. This model applied LPS to the human PBMC in order to stimulate the inflammation resulting in the secretion of TNF-α. As surface of human PBMC cover with TRPV1, the added drugs that bind well with TRPV1 should modulate the inflammation effect and the amount of TNF-α would decrease. The better binding with TRPV1 should show the great reduction amount of TNF-α.

The effect of compound **21** on cell viability was firstly investigated in order to define the appropriate concentration for anti-inflammatory assay. Previously, it was noted that capsaicin is a toxic substances at high dose concentration resulting in destruction of tissue and killing normal cells [44]. From this information, this study must obtain the concentration in order to ensure that the PBMC were still alive during investigation of TNF-α production because the death of PBMC would cause the reduction of TNFα production. Consequently, it interfere inhibition effect of TNF-α production from compound **21**.

In this work, five concentrations, which are 1, 5, 10, 50, 100 and 200 μM, of compound **21** were investigated before the anti-inflammatory test. Each concentration was treated in PBMC cells and incubated at 37°C under 5% CO_2 for 24 hour. At maturity, PBMC cells were counted for viable cells *via* hemacytometer grid to calculate percentage of cell viability compared with control (untreated cell). Finally, PBMC cell suspension was simply mixed with trypan blue solution and then visually examined to determine whether cells either take up or exclude dye. For general standard protocol for a viable cell, a clear cytoplasm would be observed, whereas a non-viable cell would show a blue color in its cytoplasm.

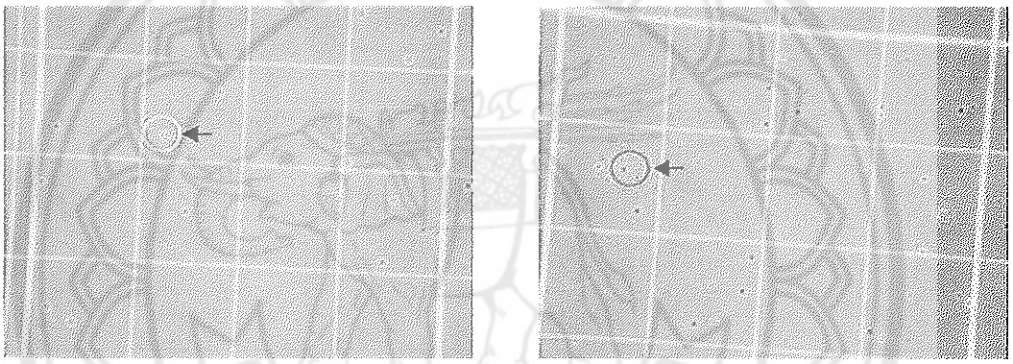

a) Clear cytoplasm b) Blue cytoplasm

Figure 31 Cell viability of PBMC from hemacytometer grid via microscope; a) clear cytoplasm for viable cell and b) blue cytoplasm for nonviable cell

The concentrations of the new capsaicin analogue (**21**) at 1, 5, 50 and 100 μM was less toxic and cell viability was more than 95 percentages at 24 hours. However, cell viability at 200 μM showed significant toxicity (**Figure 32**). From this result, the concentration at below 100 μM of 3-trifluoromethoxy capsaicin (**21**) was safe and suitable for the anti-inflammatory investigation.

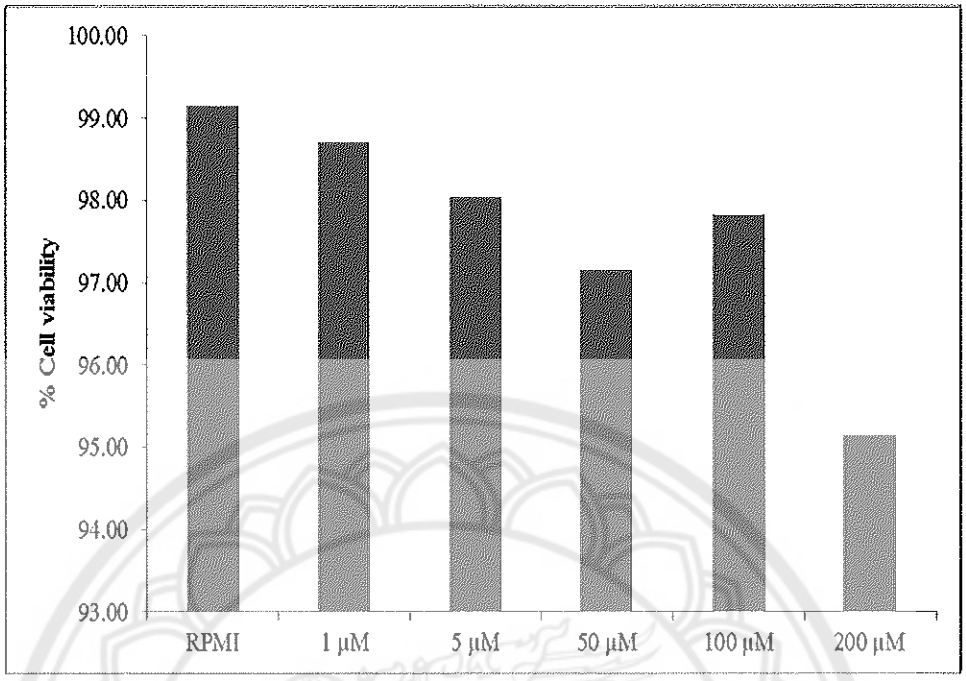

Figure 32 Percentage of Cell viability of PBMC using trypan blue technique after dose of 3-trifluoromethoxy capsaicin (21) at 1, 5, 50, 100 and 200 µM for 24 h

2. Effect of 3-trifluoromethoxy capsaicin on human TNF-α production by LPS-stimulated PBMC

To demonstrate the hypothesis on π-π stacking interaction via TNF-α production by LPS-stimulated PBMC to anti-inflammatory effect, the protons of methoxy group of capsaicin was chosen to replace with fluorine atoms to observe π-π stacking effect without interfering steric effect. The capsaicin was used as a positive control to compare with compound **21**.

In this investigation, increasing binding interaction of capsaicin analogue (**21**) on aromatic moiety with TRPV1 receptor using concept of changing electron donating group (-OCH_3) to electron withdrawing group (-OCF_3) by replacing H-atom to F-atom should increase biological activity by increasing dipole moment as well as improving stacking interaction [45]. Moreover, the small size of F-atom can replace an H-atom in organic molecule with slightly disturbing of total volume [46].

This experiment focused on concentration of TNF-α in cell culture supernatants that evaluated by enzyme-linked immune sorbent assay (ELISA) kit. From the previous studied, sample at 5 μM was chosen to observe the inhibition of TNF-α production. A result was shown in table 2, TNF-α production at 5 μM of compound **21** showed the inhibition better than capsaicin itself and decreased the amount of TNF-α to 362.64 pg/ml (**Appendix C**), lower than capsaicin.

Table 2 Absorption of screening assay of TNF-α production after applied 5.00 μM capsaicin and isostere capsaicin (21)

Sample	Absorption	%RSD	% inhibition of TNF-α production
PBMC	0.283 ± 0.006	1.999	-
PBMC+LPS	2.250 ± 0.093	4.118	0.00
PBMC+LPS+capsaicin	1.592 ± 0.184	11.548	33.41
PBMC+LPS+21	1.113 ± 0.137	12.325	57.75

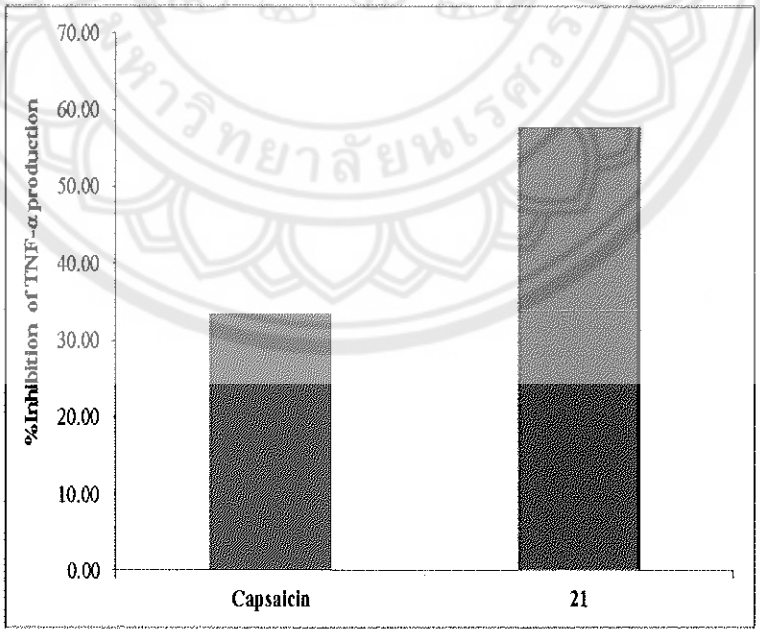

Figure 33 The screening inhibition of TNF-α production after applied 5 μM capsaicin and capsaicin derivative (21) using LPS-stimulated

Although, 3-trifluoromethoxy capsaicin (**21**) can exhibited anti-inflammatory greater than capsaicin due to F-atom on the aromatic residue has a high electronagativity which increasing dipole moment of compound **21** higher than capsaicin at 3.4148 and 2.0971 debye, respectively [42]. In addition, the volume of capsain and compound **21** were calculated by Density Functional Theory (DFT) using Gaussian09 [42] that showed at 257.334 and 270.661 cm^3/mol, respectively.

Moreover, the hydrophobicity was one of the reasons that needed to be considered. With the calculation by using Molininspiration program [41], it was found that the miLogP of capsaicin = 3.10 and miLogP of compound **21** = 4.01 than the higher milogP of compound **21** which showed the higher value of inhibition than capsaicin. There was more information need to be obtained and the docking information of compound **21** should be further explored to give the plausible reason for the special behavior of trifluoromethoxy capsaicin derivative **21**.

Synthesis of vanillylamine hydrochloride derivatives (15-19)

The vanillylamine hydrochloride derivatives (**15-19**) were synthesized by reduction reaction *via* oxime (**9-13**) (**Scheme 10**). Compounds of **9-13** were prepared by heating the vanillylbenzaldehyde analogues (**3-7**) with hydroxylamine hydrochloride (NH_2OH). Then, the crude products of **9-13** were reduced by hydrogen in a presence of palladium catalyst to generate vanillylamine hydrochloride derivatives (**15-19**). This reaction occurred *via* one-pot reaction and was purified by re-crystallization from ethyl acetate/ethanol.

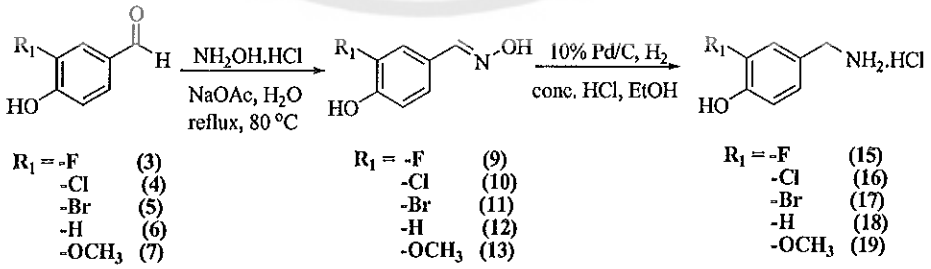

Scheme 10 Summary of the synthesis of vanillylamine hydrochloride derivatives (15-19)

1. 3-fluoro-4-hydroxybenzylamine hydrochloride (15)

Compound **15** (34% yield) was confirmed by IR spectroscopy and showed the disappearance of C=O stretching of aldehyde, while the NH-stretching and NH-bending of amine were detected at 3,179 and 1,626 cm^{-1} respectively (**Figure 34**). The structure was confirmed by ^{1}H-NMR spectroscopy (**Figure 35**). The proton NMR showed the methylene proton at 4.12 ppm as singlet.

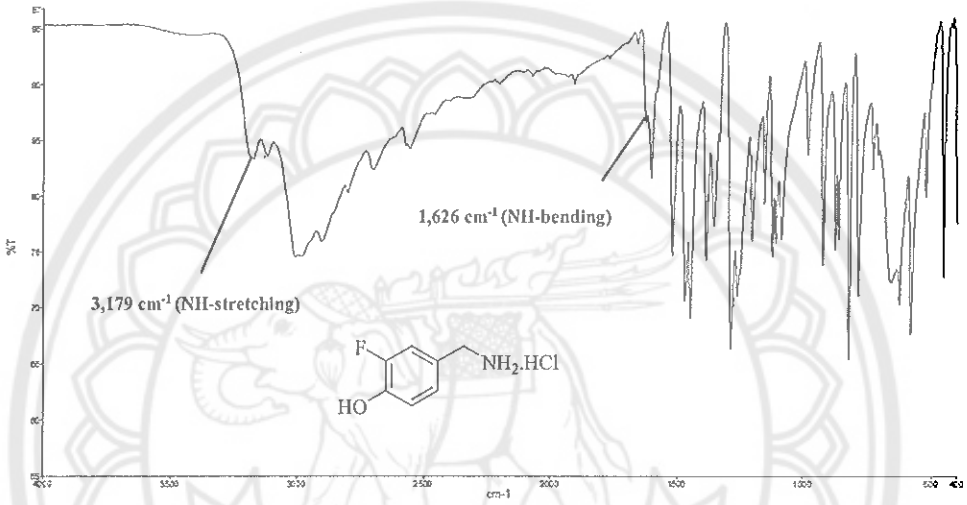

Figure 34 IR spectrum of 3-fluoro-4-hydroxybenzylamine hydrochloride (15)

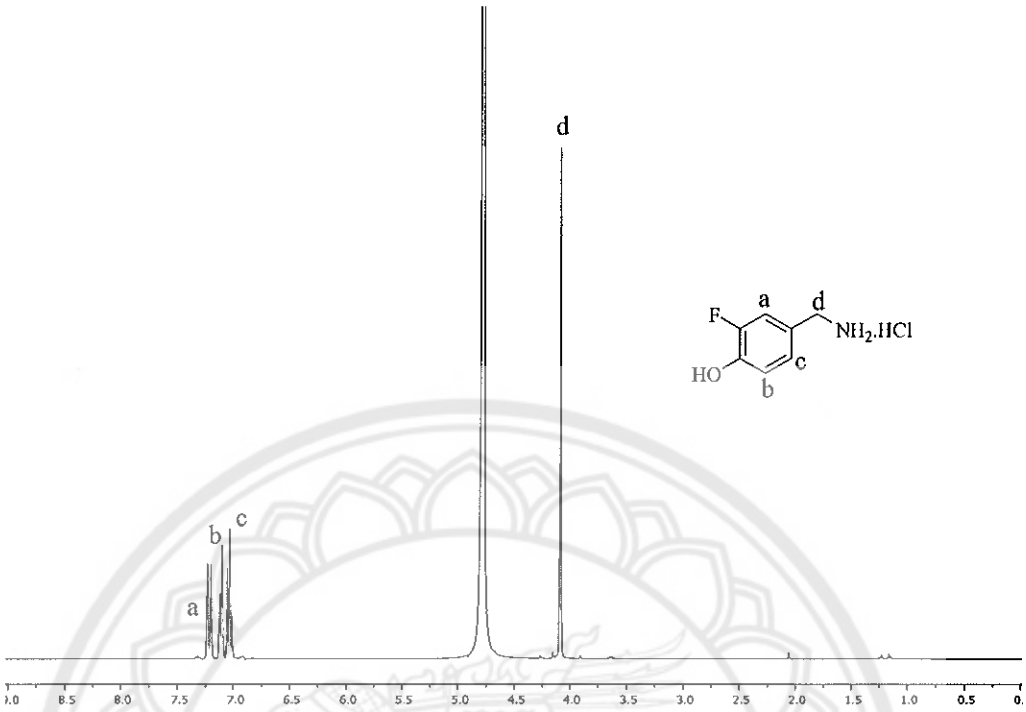

Figure 35 ^{1}**H-NMR spectrum of 3-fluoro-4-hydroxybenzylamine hydrochloride (15) (D_2O-d_2)**

2. 4-hydroxybenzylamine hydrochloride (18)

The product of **18** was obtained as a light yellow solid (73% yield). The structure was confirmed by IR technique showing ν_{max} 3,369 cm^{-1} of NH stretching and NH-bending at ν_{max} 1,613 cm^{-1} (**Figure 36**). The ^{1}H-NMR spectroscopy of **18** showed the methylene proton (CH_2) attached to amine at 4.08 ppm (**Figure 37**).

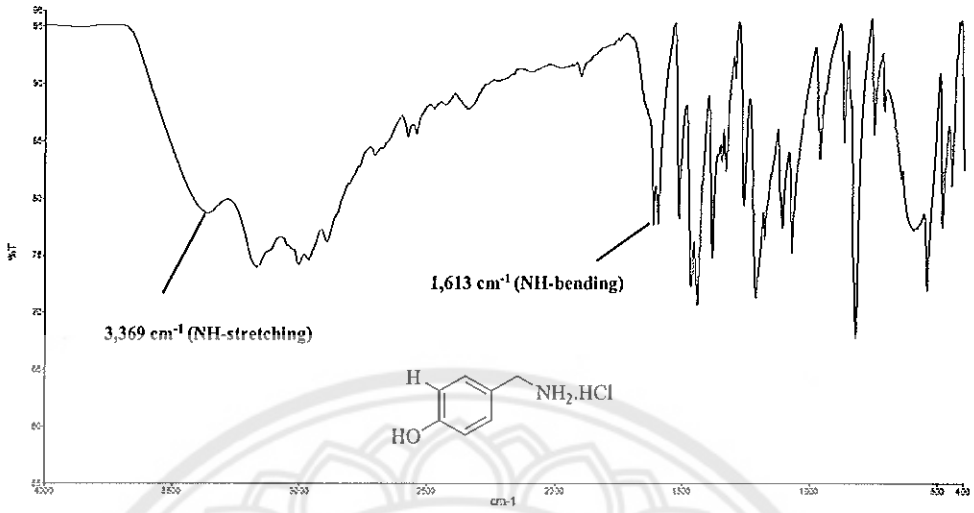

Figure 36 IR spectrum of 4-hydroxybenzylamine hydrochloride (18)

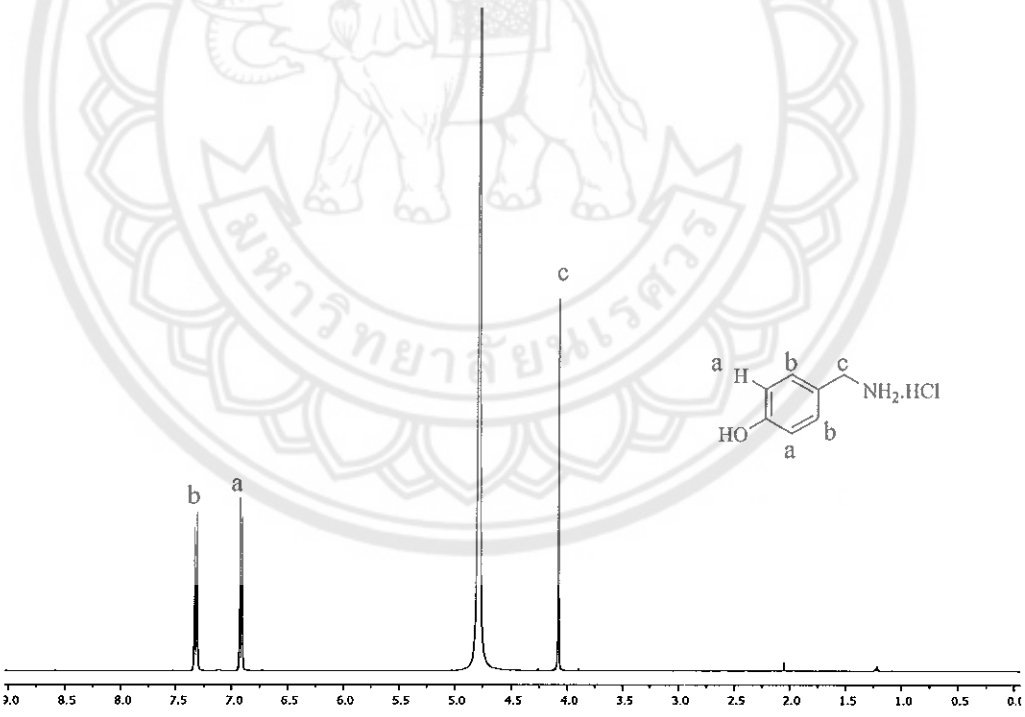

Figure 37 ^{1}H-NMR spectrum of 4-hydroxybenzylamine hydrochloride (18) (D_2O-d_2)

3. 4-hydroxy-3-methoxybezylamine hydrochloride (19)

The white crystal product of **19** (32% yield) was confirmed by the ^{1}H-NMR spectroscopy showing the peaks of two methylene protons and a methoxy group at 4.11 and 3.88 ppm, respectively (**Figure 38**). The NH stretching and NH bending of compound **19** were shown at ν_{max} 3,428 and 1,614 cm^{-1}, respectively (**Figure 39**).

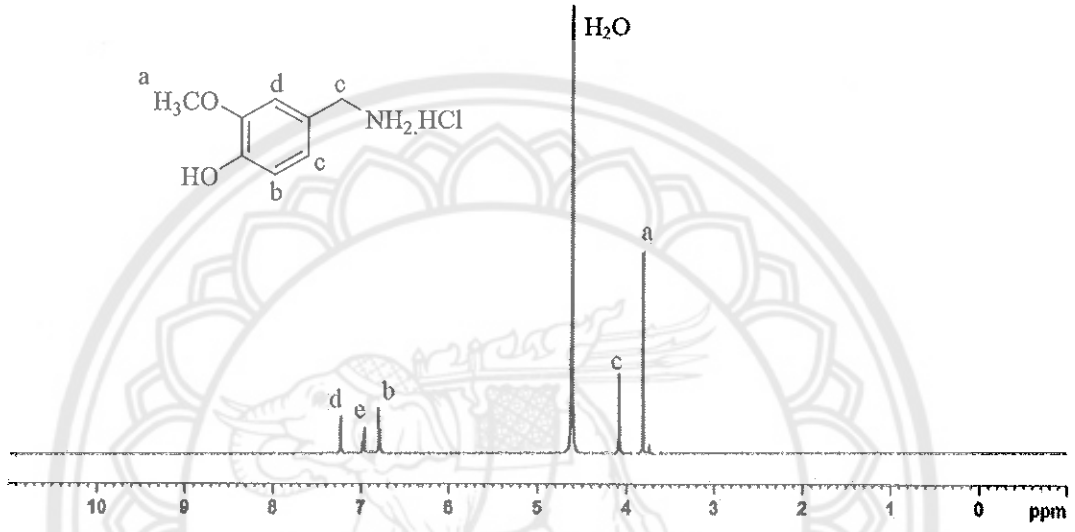

Figure 38 ^{1}H-NMR spectrum of 4-hydroxy-3-methoxybezylamine hydrochloride (19) (D_2O-d_2)

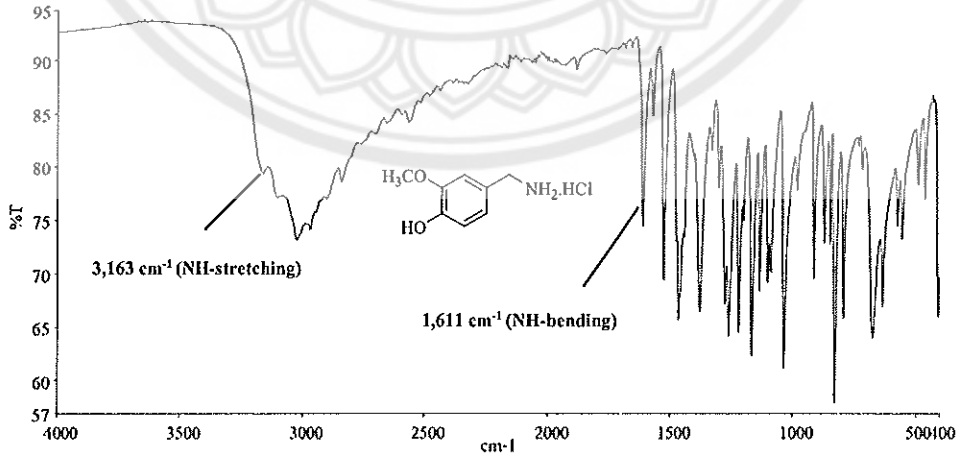

Figure 39 IR spectrum of 4-hydroxy-3-methoxybezylamine hydrochloride (19)

4. 3-chloro and 3-bromo- methoxybezylamine hydrochloride (16-17)

To prepare compounds **16** and **17**, both were used the same reaction as these for compounds **14-15** and compounds **18-19**, by using hydrogen with 10% Pd on charcoal *via* oximes (**10-11**). However, both compounds were not successful. From the previous study of Ramanathan and Jimenez [47], they used chlro and bromo substituents serve as blocking group on aromatic moiety before removed them by catalytic hydrogenation under neutral conditions and this is may be one of the reasons to explains that **16** and **17** were not prepared under this condition.

Investigation of Acetylcholinesterase inhibitory activity

The series of vanillylamine derivatives (**14-15** and **18-19**) were observed for AChE inhibition. The result was shown in **table 3**.

Table 3 AChE inhibitory and IC_{50} of compounds 14-15 and compounds 18-19

Compound	% Inhibition (10 mM)	IC_{50} (mM)
14	85.29 ± 0.44	2.85 ± 0.44
15	83.69 ± 0.05	1.27 ± 0.04
18	66.67 ± 0.59	2.62 ± 0.23
19	95.73 ± 0.07	0.14 ± 0.01

1. 4-hydroxybenzylamine hydrochloride (18) and 3-fluoro-4-hydroxybenzylamine hydrochloride (15) as AChEIs

At 10 mM concentration, amine salt **15** showed inhibition against AChE better than **18** (83.69% and 66.67 respectively) due to the lower hydrophobicity of compound **15** than that of compound **18**. Compound **15** was replaced with F (EN = 4.0) resulting in an improved interaction of AChE through aromatic π-π stacking. Compound **18** exhibited IC_{50} at 2.62 ± 0.23 mM while compound **15** showed IC_{50} = 1.27 ± 0.04 mM.

Table 4 Log P, dipole moment and Hammett constant of compound 14-15 and compound 18-19

Compounds	Log P	Dipole moment (Debye)	Hammett constant
14	1.98	3.2760	0.38
15	1.60	3.0547	0.34
18	1.25	2.6076	0.00
19	1.07	2.7533	0.12

The calculation of dipole moment by using Density Functional Theory (DFT) at B3LYP/6-31+G(d,p) level of theory in gas phase, the fluorinated compound **15** showed higher than compound **18** approximately 0.44 Debye. The other factors showed the slightly difference in AChE inhibition such as the effective steric volume (F and H substituent were 0.27 and 0.00, respectively), the molecular steric volume of free salts of compounds **15** and **18** (125.08 and 120.15 $Å^3$, respectively) and Hammett constant of F and H substituent were 0.34 and 0.00, respectively. Consideration of Log P, the higher hydrophobicity of compound than those in compound **18** that indicated the π-π stacking of compound **15** with aromatic residues at PAS showed better binding at PAS subsite resulting in better binding at PAS subsite to produce better AChE inhibition.

2. 4-hydroxy-3-methoxybezylamine hydrochloride (19) and 3-trifluoromethoxy-4-hydroxybenzylamine hydrochloride (14) as AChEIs

At the same concentration at 10 mM, it was found that compound **14** showed lower AChE inhibition than compound **19** because of the higher hydrophobicity in table 4 (logP of compounds **14** and **19** were 1.98 and 1.07, respectively [27]). Compound **19** exhibited IC_{50} of 0.14 ± 0.01 mM, while compound **14** showed IC_{50} of 2.85 ± 0.44 mM.

From the calculation, the dipole moment of **14** was obviously higher than **19** approximately by 0.50 Debye by using Density Functional Theory (DFT) at B3LYP/6-31+G(d,p) level of theory in gas phase. Therefore, the π-π stacking of **14** with aromatic residues at PAS should be more effective than those in **19**; consequently

resulting in better binding at PAS subsite to produce better AChE inhibition. Unexpectedly, **19** inhibited AChE almost 20-fold better than **14**.

Possibly, other factors might have the drastic difference in AChE inhibition such as the effective steric volume (CF_3 and CH_3 substituent were 0.90 and 0.52, respectively) and the molecular steric volume of free salts of **14** and **19** (160.43 and 145.70 $Å^3$, respectively). More of vanillin derivatives with different steric volume were designed for further investigation on this concept.

CHAPTER V

CONCLUSION

Synthesis of the new capsaicin derivative (**21**) was divided into four steps including formylation reaction to benzaldehyde derivatives, conversion to amine salt derivatives via oixme, coupling reaction and purification by HPLC. The coupling reaction between 3-trifluoromethoxy-4-hydroxybenzylamine hydrochloride derivative with fatty acid of (*E*)-8-methyl-6-nonenoic acid by using HOBt and EDC.HCl as the coupling agent. After that, the crude product was successfully purified by HPLC technique to obtain the product in 16.18% yield.

For anti-inflammatory assay, capsaicin and compound **21** suppressed the production of pro-inflammatory cytokine TNF-α by LPS-stimulated cell culture supernatant with 5 μM for 16 hours. Interestingly, the new capsaicin analogue (**21**) showed the better suppression of TNF-α production than capsaicin. However, the further study need to be investigated and the docking information of compound **21** should be further explored to give the plausible reason for the special behavior of tetrafluoroaromatic capsaicin derivative **21**.

For the investigation of AChEIs, the preparations of vanillylamine hydrochloride derivatives (**14-15** and **18-19**) were successfully prepared. However, compounds with 3-chloro and 3-bromo substituents (**16-17**) were not successfully prepared because of chloro and bromo-substituent on the aromatic residue were removed during the reaction were going under condition of hydrogen (conc. HCl) with 10%Pd/C and H_2 gas.

The biological activity result of compound **14-15** and **18-19** against AChE, fluorinated vanillylamine hydrochloride (**15**) showed the better activity than that of compound **18** due to the less hydrophobicity of compound **15**. Otherwise, 4-hydroxy-3-methoxybezylamine hydrochloride (**19**) showed 95.73 %inhibition against AChE at 10 mM, while vanillylamine hydrochloride (**14**) had 85.29 %inhibition at the same concentration.

REFERENCE

REFERENCE

[1] Macho, A., Lucena, C., Sancho, R., Daddario, N., Minassi, A., Munoz, E., & Appendino, G. (2003). Non-pungent capsaicinoids from sweet pepper synthesis and evaluation of the chemopreventive and anticancer potential. *Eur J Nutr, 42*(1), 2-9.

[2] Reyes-Escogido, M., Gonzalez-Mondragon, E. G., & Vazquez-Tzompantzi, E. (2011). Chemical and Pharmacological Aspects of Capsaicin. *Molecules, 16*(2), 1253-1270.

[3] Krause, D. L., & Müller, N. (2010). Neuroinflammation, Microglia and Implications for Anti-Inflammatory Treatment in Alzheimer's disease. *International Journal of Alzheimer's Disease, 2010*, 1-9.

[4] Ma, W., & Quirion, R. (2007). Inflammatory mediators modulating the transient receptor potential vanilloid 1 receptor: therapeutic targets to treat inflammatory and neuropathic pain. *Expert Opinion on Therapeutic Targets, 11*(3), 307-320.

[5] Clark, N., Keeble, J., Fernandes, E. S., Starr, A., Liang, L., Sugden, D., ... Brain, S. D. (2007). The transient receptor potential vanilloid 1 (TRPV1) receptor protects against the onset of sepsis after endotoxin. *The FASEB Journal, 21*(13), 3747-3755.

[6] Huang, X. F., Xue, J. Y., Jiang, A. Q., & Zhu, H. L. (2013). Capsaicin and Its Analogues: Structure-Activity Relationship Study. *Current Medicinal Chemistry, 20*(21), 2661-2672.

[7] Francis, P. T., Palmer, A. M., Snape, M., & Wilcock, G. K. (1999). The cholinergic hypothesis of Alzheimer's disease: a review of progress. *Journal of Neurology, Neurosurgery & Psychiatry, 66*(2), 137-147.

[8] Tabet, N. (2006). Acetylcholinesterase inhibitors for Alzheimer's disease: anti-inflammatories in acetylcholine clothing! *Age and Ageing, 35*(4), 336-338.

[9] Dvir, H., Silman, I., Harel, M., Rosenberry, T. L., & Sussman, J. L. (2010). Acetylcholinesterase: From 3D Structure to Function. *Chemico-biological interactions, 187*(1-3), 10-22.

[10] Kundu, A., & Mitra, A. (2013). Flavoring extracts of Hemidesmus indicus roots and Vanilla planifolia pods exhibit in vitro acetylcholinesterase inhibitory activities. *Plant foods for human nutrition, 68*(3), 247-253.

[11] Leroux, F. R., Manteau, B., Vors, J.-P., & Pazenok, S. (2008). Trifluoromethyl ethers – synthesis and properties of an unusual substituent. Beilstein Journal of Organic Chemistry, *4*(13), 1-15.

[12] Shah, P., & Westwell, A. D. (2007). The role of fluorine in medicinal chemistry. *Journal of Enzyme Inhibition and Medicinal Chemistry, 22*(5), 527-540.

[13] Othman, Z. A. A., Ahmed, Y. B. H., Habila, M. A., & Ghafar, A. A. (2011). Determination of Capsaicin and Dihydrocapsaicin in Capsicum Fruit Samples using High Performance Liquid Chromatography. *Molecules, 16*(10), 8919-8929.

[14] Kawabata, F., Inoue, N., Yazawa, S., Kawada, T., Inoue, K., & Fushiki, T. (2006). Effects of CH-19 Sweet, a Non-Pungent Cultivar of Red Pepper, in Decreasing the Body Weight and Suppressing Body Fat Accumulation by Sympathetic Nerve Activation in Humans. *Bioscience, Biotechnology, and Biochemistry, 70*(12), 2824-2835.

[15] Arora, R., Gill, N. S., Chauhan, G., & Rana, A. C. (2011). An overview about versatile molecule capsaicin. *Int J Pharm Sci Drug Res, 3*, 280-86.

[16] Walpole, C. S. J., Wrigglesworth, R., Bevan, S., Campbell, E. A., Dray, A., James, I. F., ... Winter, J. (1993). Analogs of capsaicin with agonist activity as novel analgesic agents; structure-activity studies. 1. The aromatic "A-region". *Journal of Medicinal Chemistry, 36*(16), 2362-2372.

[17] Bevan, S., & Szolcsányi, J. (1990). Sensory neuron-specific actions of capsaicin: mechanisms and applications. *Trends in Pharmacological Sciences, 11*(8), 331-333.

[18] Kym, P. R., Kort, M. E., & Hutchins, C. W. (2009). Analgesic potential of TRPV1 antagonists. *Biochem Pharmacol, 78*(3), 211-216.

[19] Park, J.-Y., Kawada, T., Han, I.-S., Kim, B.-S., Goto, T., Takahashi, N., ... Yu, R. (2004). Capsaicin inhibits the production of tumor necrosis factor α by LPS-stimulated murine macrophages, RAW 264.7: a PPARγ ligand-like action as a novel mechanism. *FEBS Letters, 572*(1-3), 266-270.

[20] Szallasi, A., & Blumberg, P. M. (1999). Vanilloid (capsaicin) receptors and mechanisms. *Pharmacological reviews, 51*(2), 159-212.

[21] Gavva, N. R., Klionsky, L., Qu, Y., Shi, L., Tamir, R., Edenson, S., ... Treanor, J. J. (2004). Molecular determinants of vanilloid sensitivity in TRPV1. *J Biol Chem, 279*(19), 20283-20295.

[22] Wilson, R. S., Barral, S., Lee, J. H., Leurgans, S. E., Foroud, T. M., Sweet, R. A., ... Bennett, D. A. (2011). Heritability of Different Forms of Memory in the Late Onset Alzheimer's Disease Family Study. *Journal of Alzheimer's disease : JAD, 23*(2), 249-255.

[23] Hardy, J., & Allsop, D. (1991). Amyloid deposition as the central event in the aetiology of Alzheimer's disease. *Trends in Pharmacological Sciences, 12*, 383-388.

[24] Mudher, A., & Lovestone, S. (2002). Alzheimer's disease – do tauists and baptists finally shake hands? *Trends in Neurosciences, 25*(1), 22-26.

[25] Hardy, J., & Allsop, D. (1991). Amyloid deposition as the central event in the aetiology of Alzheimer's disease. *Trends in pharmacological sciences*, *12*, 383-388.

[26] Mudher, A., & Lovestone, S. (2002). Alzheimer's disease–do tauists and baptists finally shake hands?. *Trends in neurosciences*, *25*(1), 22-26.

[27] Nistor, M., Don, M., Parekh, M., Sarsoza, F., Goodus, M., Lopez, G. E., ... & Hill, M. (2007). Alpha-and beta-secretase activity as a function of age and beta-amyloid in Down syndrome and normal brain. *Neurobiology of aging*, *28*(10), 1493-1506.

[28] Lott, I. T., & Head, E. (2005). Alzheimer disease and Down syndrome: factors in pathogenesis. *Neurobiology of aging*, *26*(3), 383-389.

[29] Polvikoski, T., Sulkava, R., Haltia, M., Kainulainen, K., Vuorio, A., Verkkoniemi, A., ... & Kontula, K. (1995). Apolipoprotein E, dementia, and cortical deposition of β-amyloid protein. *New England Journal of Medicine*, *333*(19), 1242-1248.

[30] Iqbal, K., Alonso, A. D. C., Chen, S., Chohan, M. O., El-Akkad, E., Gong, C. X., ... & Tanimukai, H. (2005). Tau pathology in Alzheimer disease and other tauopathies. Biochimica et Biophysica Acta (BBA)-Molecular Basis of Disease, 1739(2), 198-210.

[31] Čolović, M. B., Krstić, D. Z., Lazarević-Pašti, T. D., Bondžić, A. M., & Vasić, V. M. (2013). Acetylcholinesterase Inhibitors: Pharmacology and Toxicology. *Current Neuropharmacology, 11*(3), 315-335.

[32] Bar-On, P., Millard, C. B., Harel, M., Dvir, H., Enz, A., Sussman, J. L., & Silman, I. (2002). Kinetic and Structural Studies on the Interaction of Cholinesterases with the Anti-Alzheimer Drug Rivastigmine. *Biochemistry, 41*(11), 3555-3564.

[33] Jin, H., Nguyen, T., & Mei-Lin, G. (2014) Acetylcholinesterase and Butyrylcholinesterase Inhibitory Properties of Functionalized Tetrahydroacridines and Related Analogs. *Med chem, 4*, 688-696.

[34] Atanasova, M., Yordanov, N., Dimitrov, I., Berkov, S., & Doytchinova, I. (2015). Molecular Docking Study on Galantamine Derivatives as Cholinesterase Inhibitors. *Molecular Informatics, 34*(6-7), 394-403.

[35] Jia, P., Sheng, R., Zhang, J., Fang, L., He, Q., Yang, B., & Hu, Y. (2009). Design, synthesis and evaluation of galanthamine derivatives as acetylcholinesterase inhibitors. *European Journal of Medicinal Chemistry, 44*(2), 772-784.

[36] Sussman, J., Harel, M., Frolow, F., Oefner, C., Goldman, A., Toker, L., & Silman, I. (1991). Atomic structure of acetylcholinesterase from Torpedo californica: a prototypic acetylcholine-binding protein. *Science, 253*(5022), 872-879.

[37] Jhanwar, B., Sharma, V., Singla, R. K., & Shrivastava, B. (2011). QSAR-Hansch analysis and related approaches in drug design. *Pharmacology online, 1*, 306-44.

[38] Taft, R. W., in Newman, M. S. Ed., (1956). *Steric Effects in Organic Chemistry*. New York: John Wiley & Sons.

[39] Ertl, P., Rohde, B., & Selzer, P. (2000). Fast Calculation of Molecular Polar Surface Area as a Sum of Fragment-Based Contributions and Its Application to the Prediction of Drug Transport Properties. *Journal of Medicinal Chemistry, 43*(20), 3714-3717. doi: 10.1021/jm000942e

[40] Ellman, G. L., Courtney, K. D., Andres, V., & Featherstone, R. M. (1961). A new and rapid colorimetric determination of acetylcholinesterase activity. *Biochem Pharmacol, 7*(2), 88-95. doi: http://dx.doi.org/10.1016/0006-2952(61)90145-9

[41] Molinspiration Cheminformatics. (1986). *Molinspiration*. Retrieved Jan 8, 2017, from http://www.molinspiration.com/cgi-bin/properties

[42] Frisch M. J., Trucks G. W., Schlegel H. B., Scuseria G. E., Robb M. A., Cheeseman J. R., ... Fox D. J. (2009). *Gaussian 09*. Wallingford, CT, USA: Gaussian.

[43] Smith, W. E. (1972). Formylation of aromatic compounds with hexamethylenetetramine and trifluoroacetic acid. *The Journal of Organic Chemistry, 37*(24), 3972-3973.

[44] Wichai, U. and Woski, S. (2003). *Synthesis and investigation of PNA:DNA complexes containing novel aromatic residues*. America: University of Alabama.

[45] Caterina, M. J., Schumacher, M. A., Tominaga, M., & Rosen, T. A. (1997). The capsaicin receptor: a heat-activated ion channel in the pain pathway. *Nature, 389*(6653), 816-824.

[46] Hunter, L. (2010). The C–F bond as a conformational tool in organic and biological chemistry. *Beilstein Journal of Organic Chemistry, 6*(38), 1-14

[47] Ramanathan, A., & Jimenez, L. S. (2010). Reductive dehalogenation of aryl bromides and chlorides and their use as aryl blocking groups. *Synthesis, 2010*(02), 217-220.

APPENDIX

APPENDIX A ^{1}H and ^{13}C-NMR spectra, FT-IR spectra and Mass spectra

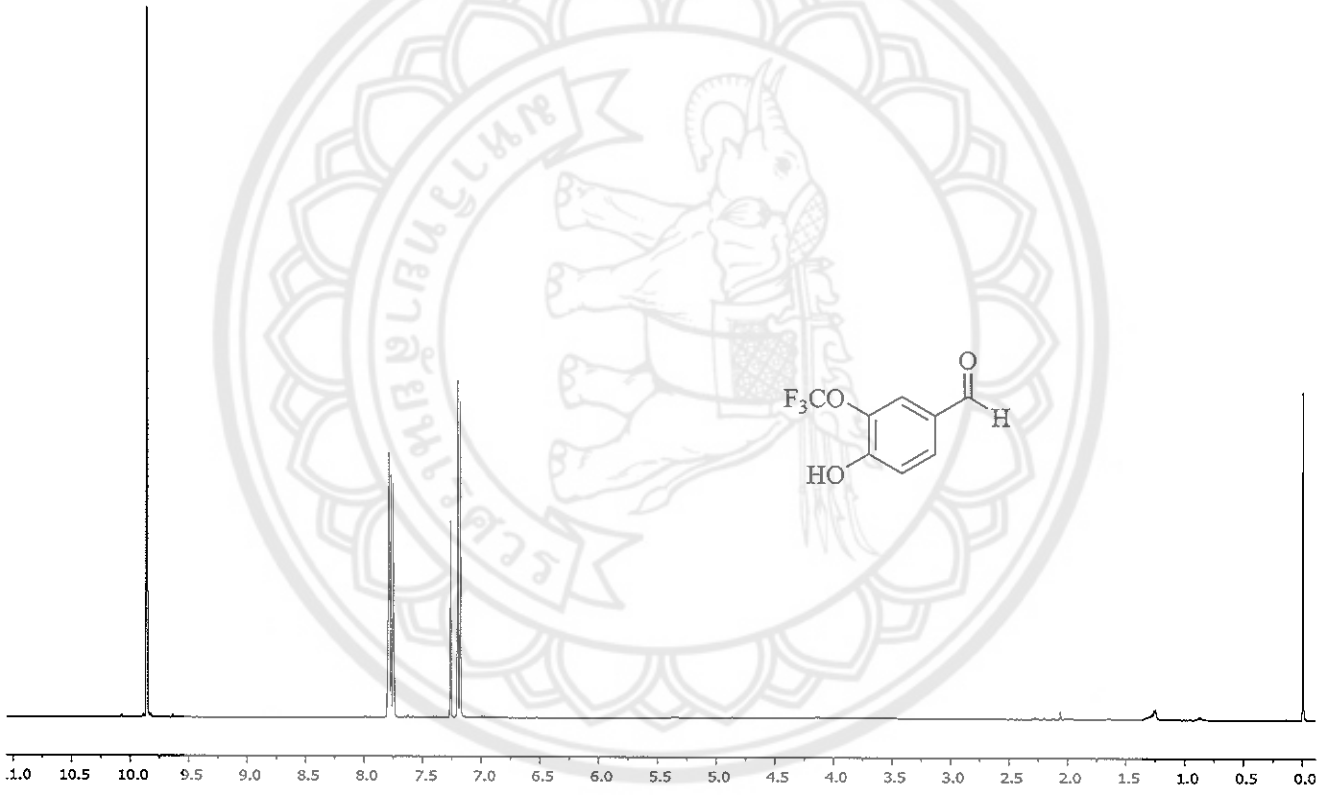

Figure 40 ^{1}H-NMR spectrum of 3-trifluoromethoxy-4-hydroxybenzaldehyde (2) ($CDCl_3$-d_1)

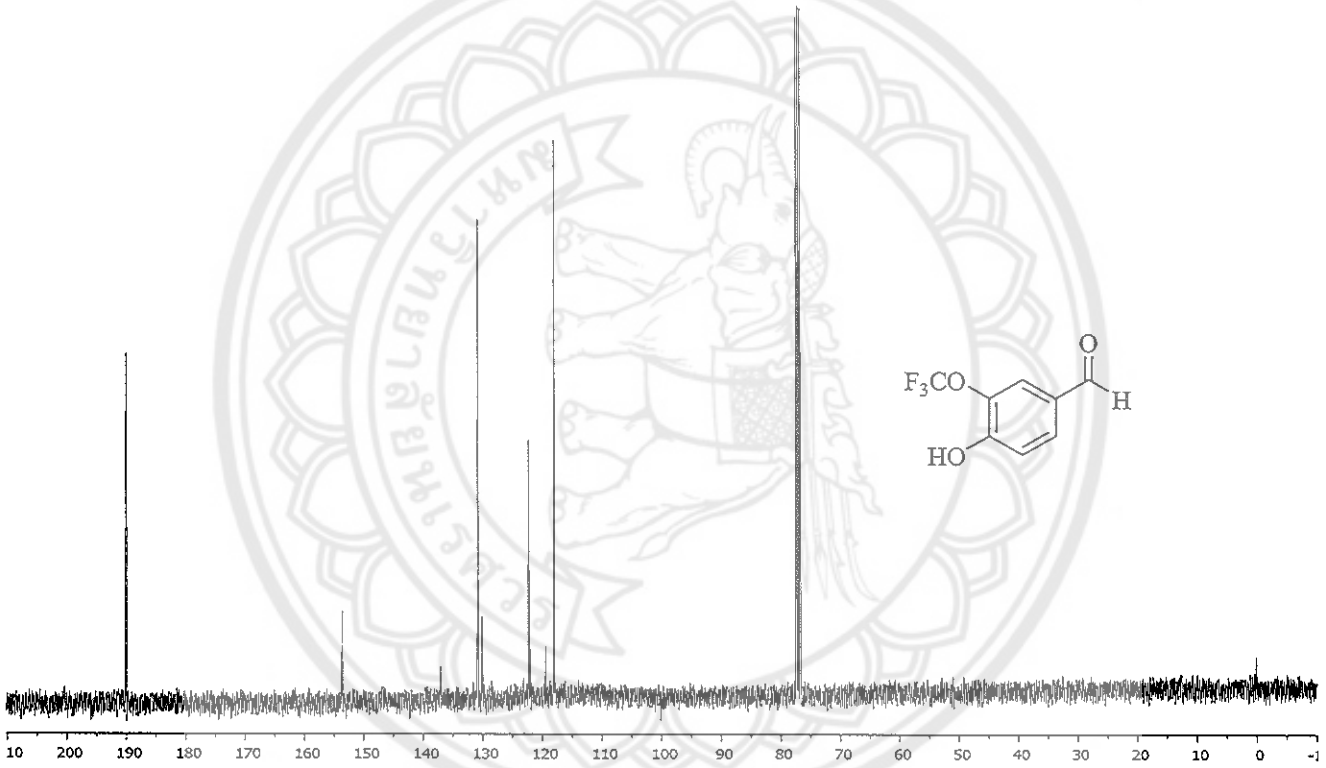

Figure 41 ^{13}C-NMR spectrum of 3-trifluoromethoxy-4-hydroxybenzaldehyde (2) **($CDCl_3$-d_1)**

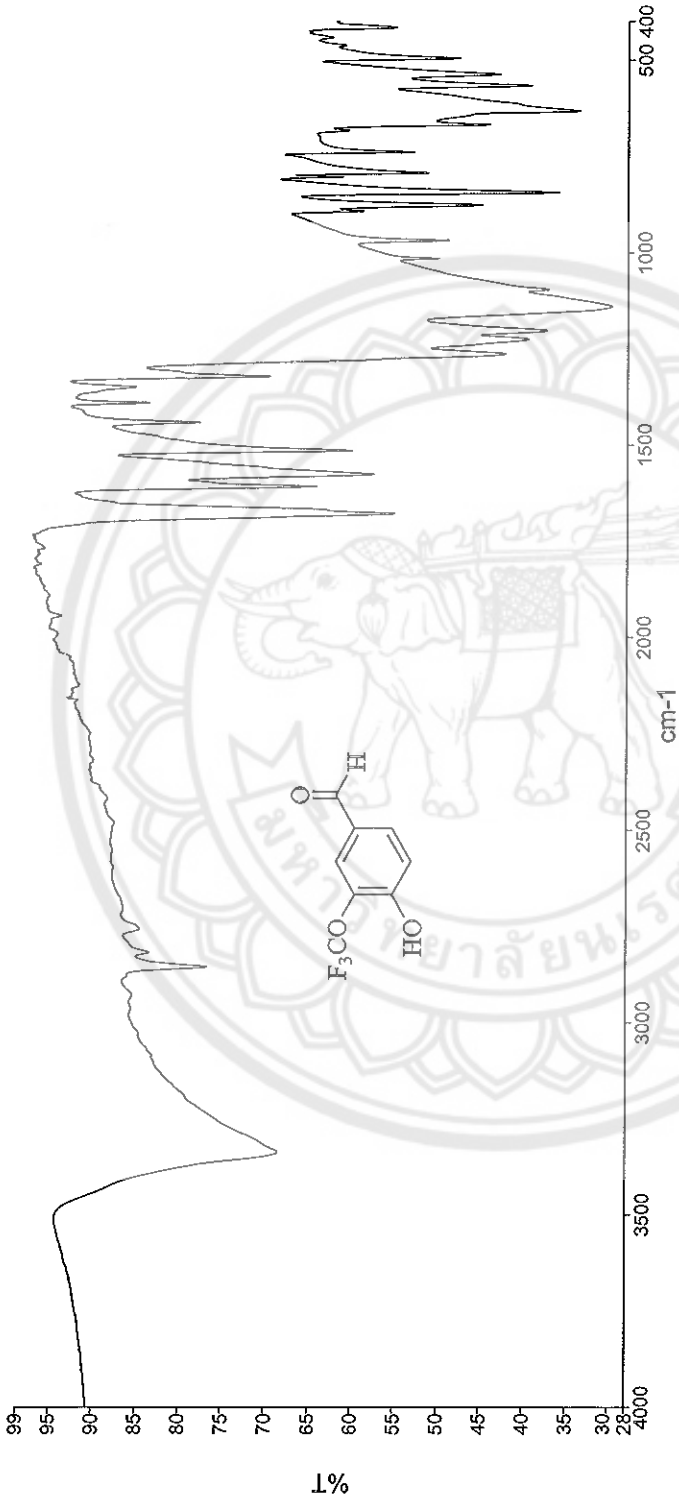

Figure 42 IR spectrum of 3-trifluoromethoxy-4-hydroxybenzaldehyde (2)

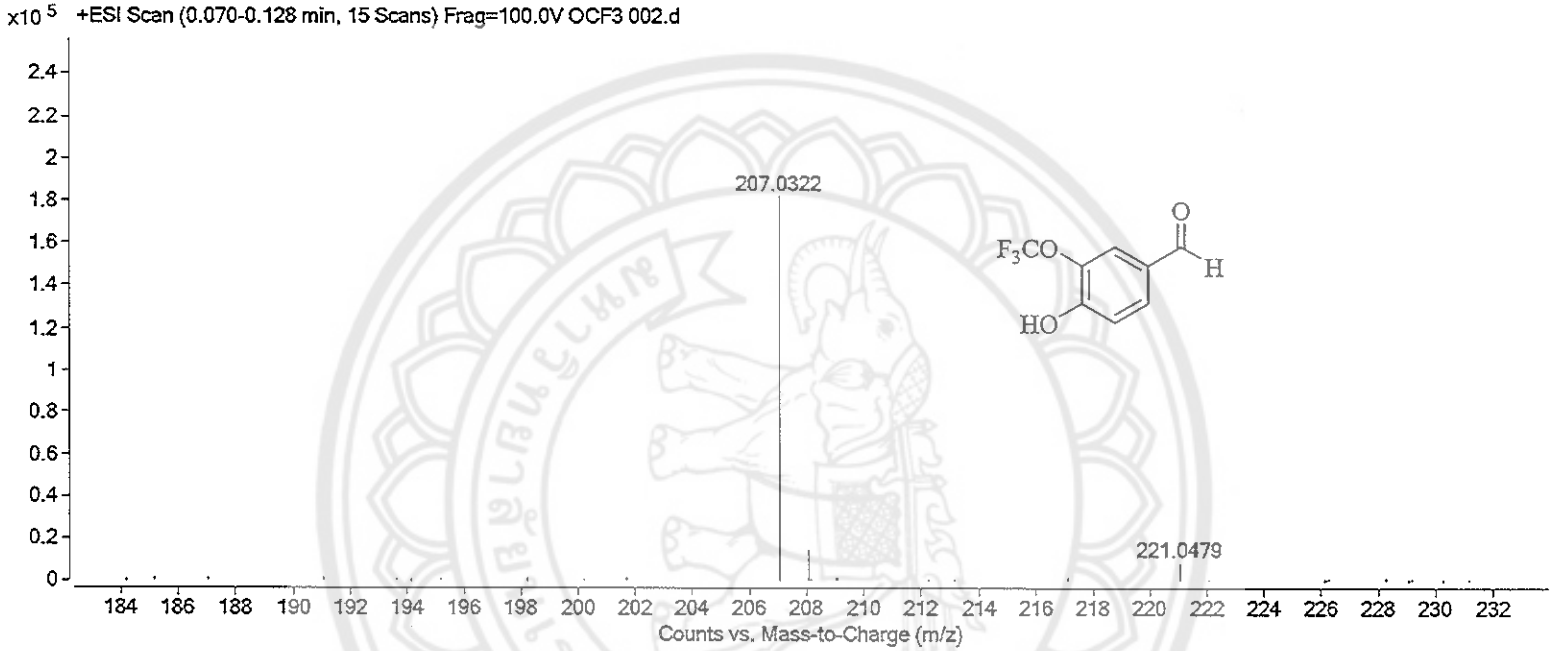

Figure 43 Mass spectrum of 3-trifluoromethoxy-4-hydroxybenzaldehyde (2)

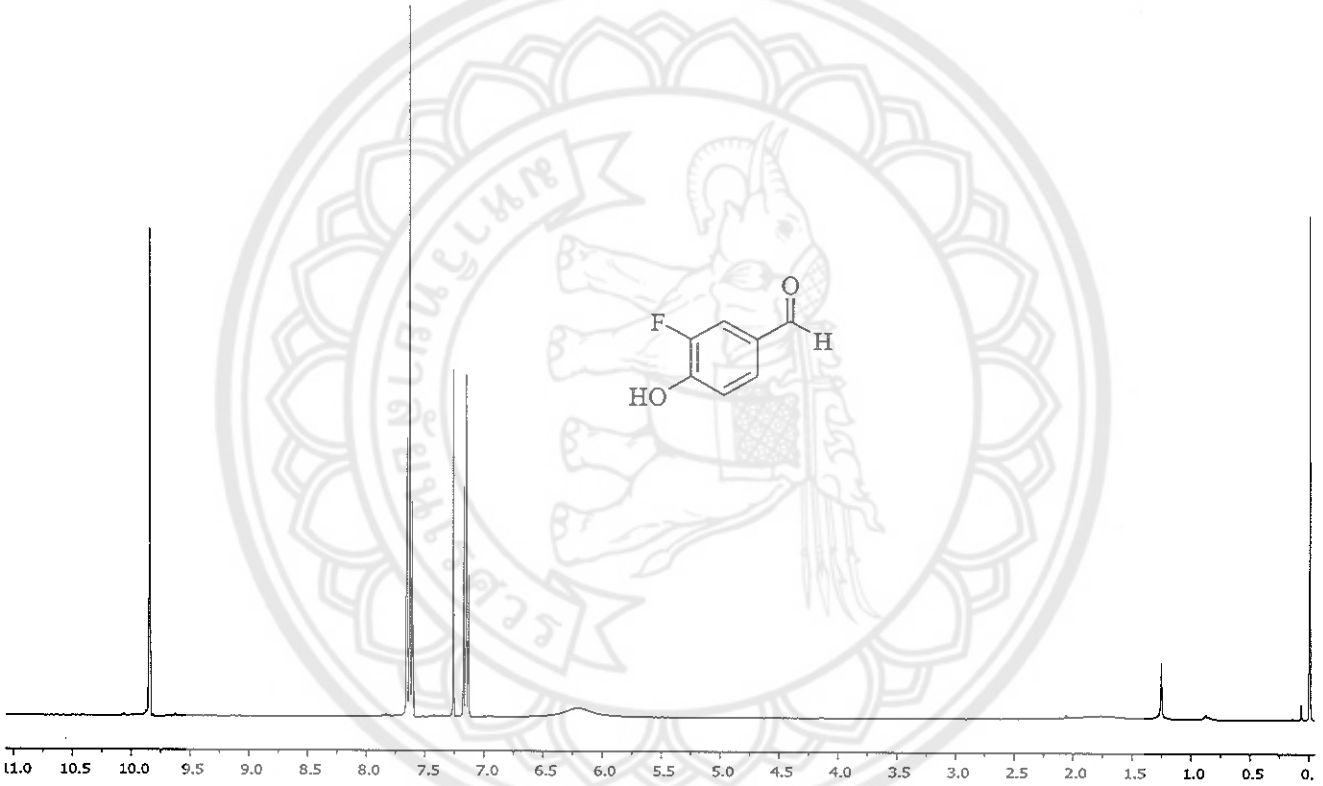

Figure 44 ^{1}H-NMR spectrum of 3-fluoro-4-hydroxybenzaldehyde (3) ($CDCl_3$-d_1)

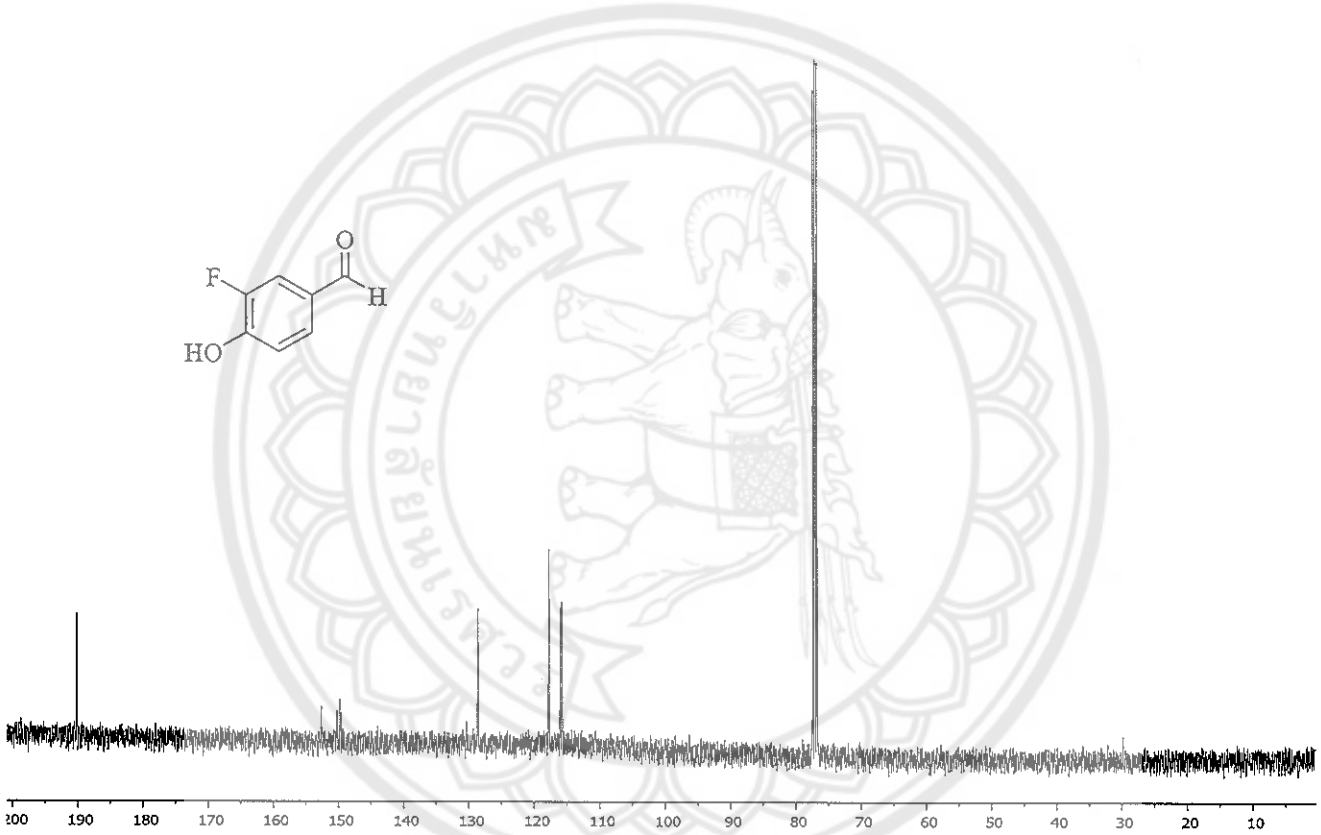

Figure 45 ^{13}C-NMR spectrum of 3-fluoro-4-hydroxybenzaldehyde (3) ($CDCl_3$-d_1)

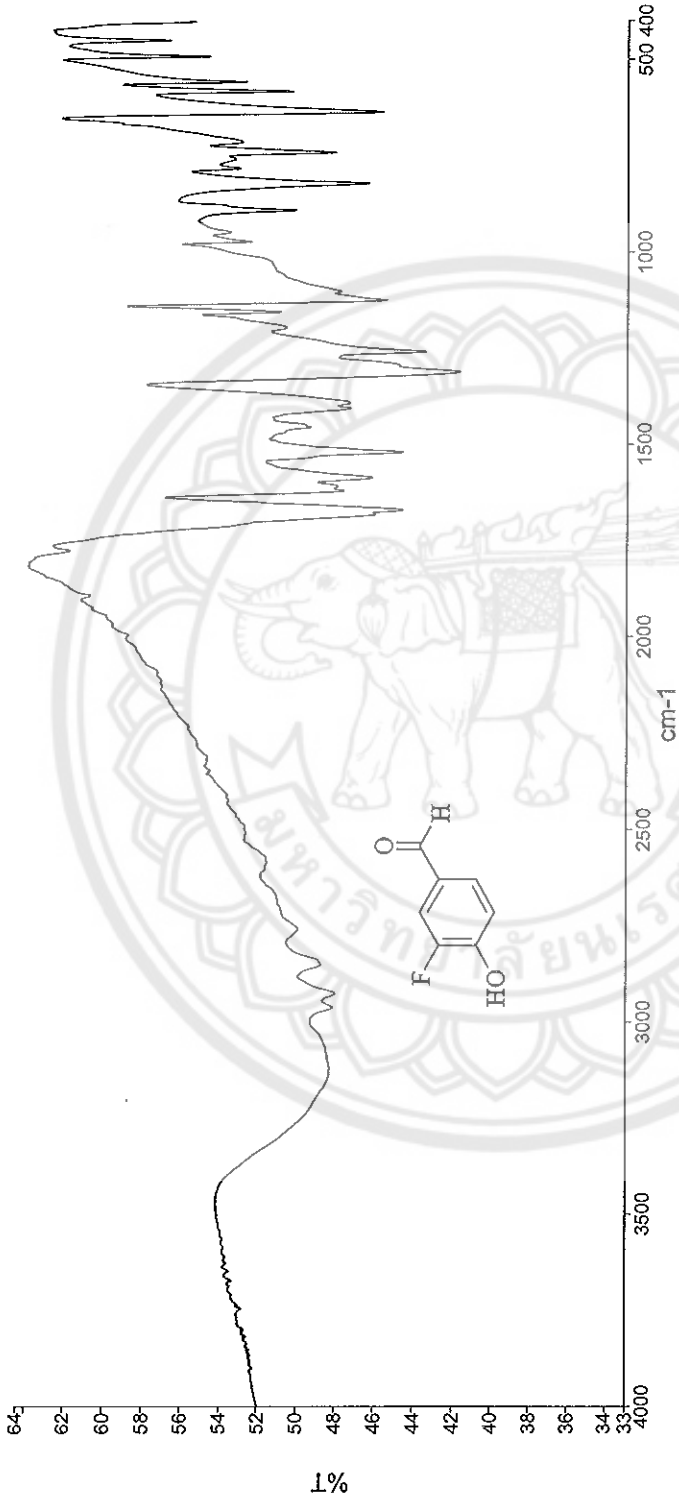

Figure 46 IR spectrum of 3-fluoro-4-hydroxybenzaldehyde (3)

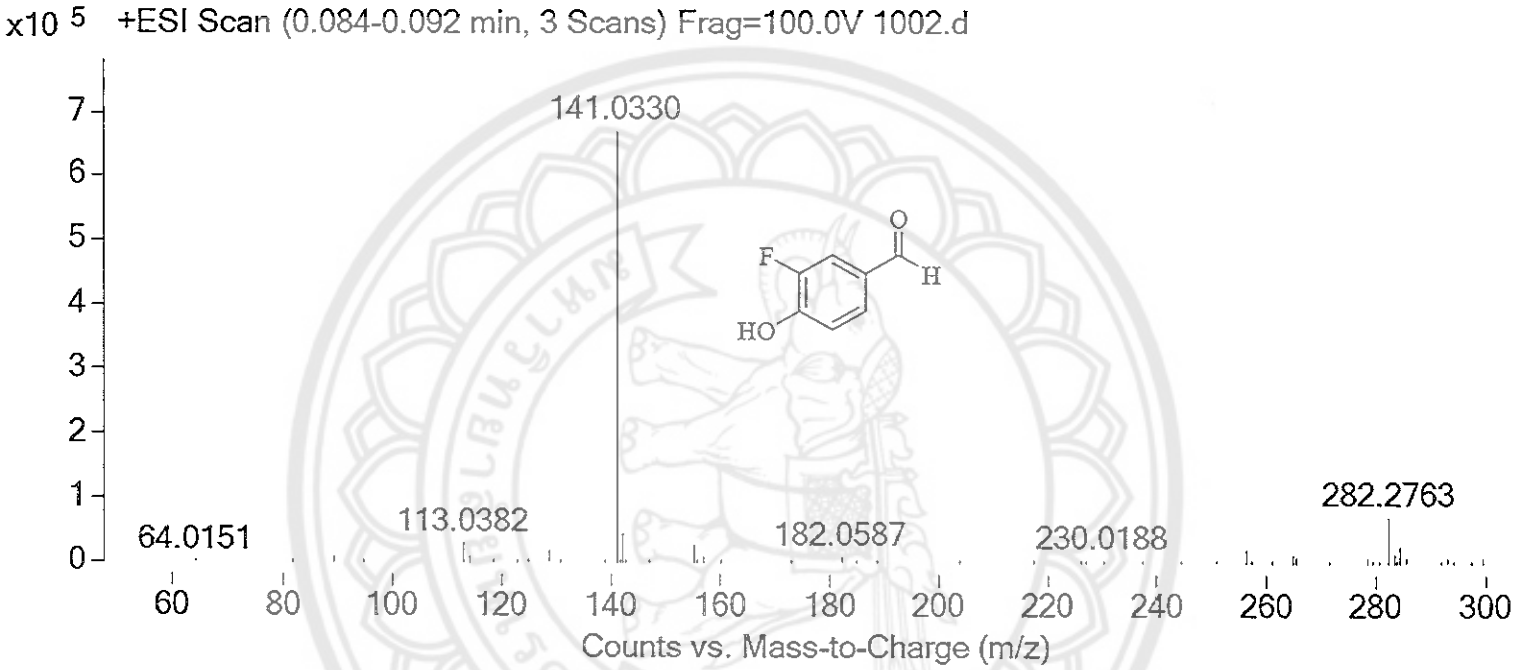

Figure 47 Mass spectrum of 3-fluoro-4-hydroxybenzaldehyde (3)

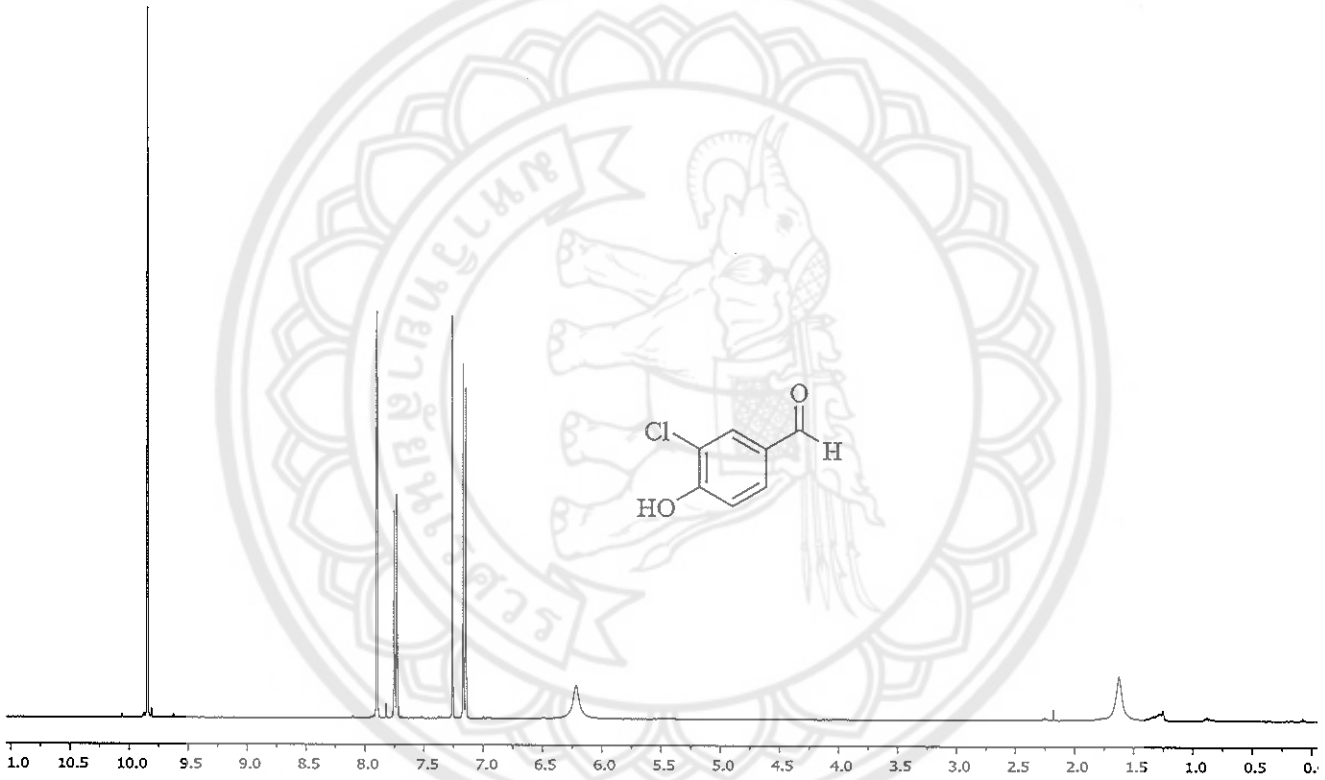

Figure 48 ^{1}H-NMR spectrum of 3-chloro-4-hydroxybenzaldehyde (4) ($CDCl_3$-d_1)

Figure 49 ^{13}**C-NMR spectrum of 3-chloro-4-hydroxybenzaldehyde (4) (CDCl$_3$-d_1)**

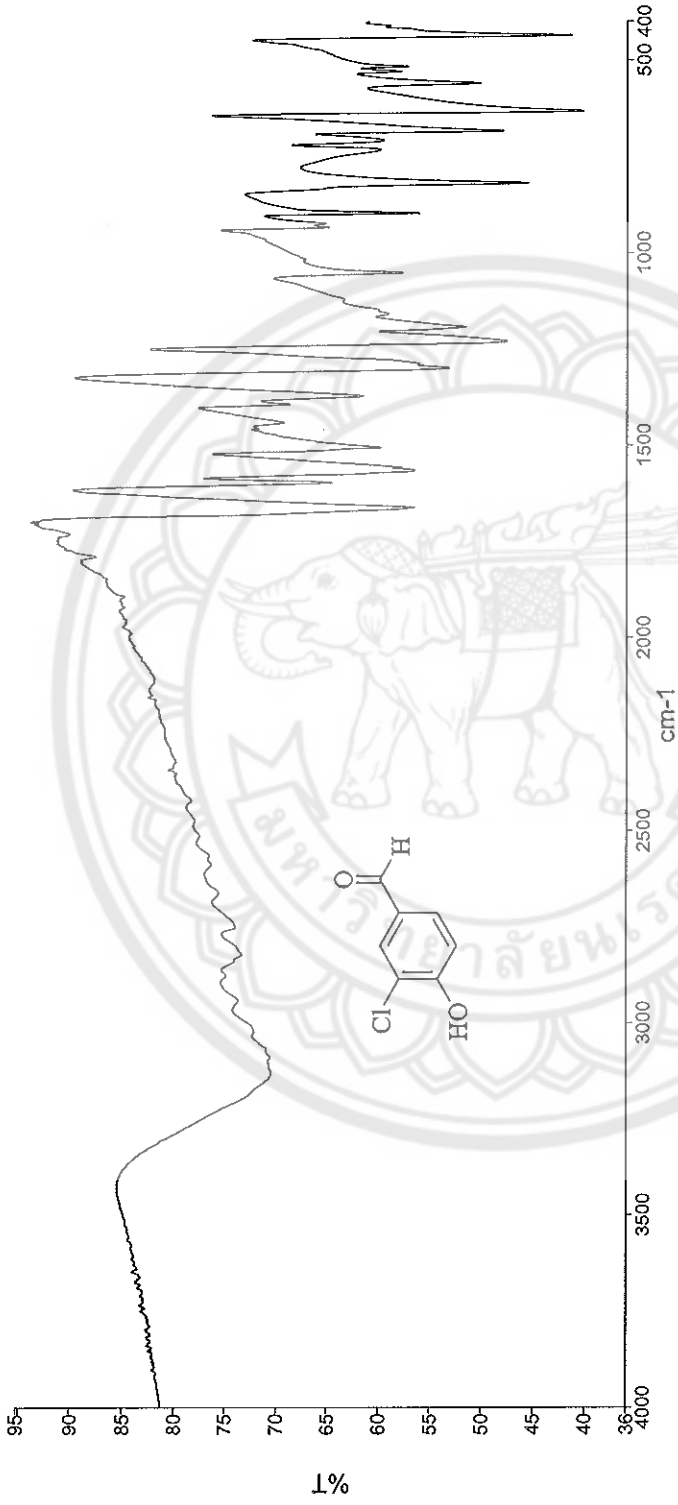

Figure 50 IR spectrum of 3-chloro-4-hydroxybenzaldehyde (4)

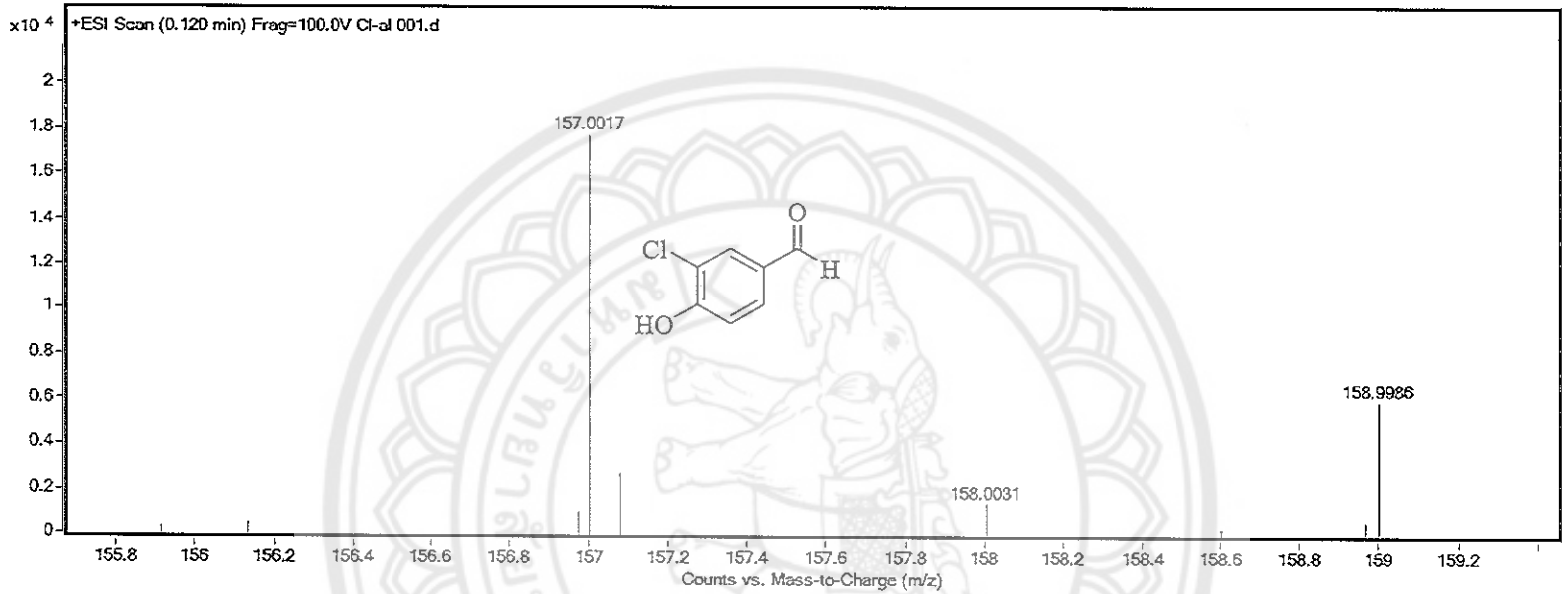

Figure 51 Mass spectrum of 3-chloro-4-hydroxybenzaldehyde (4)

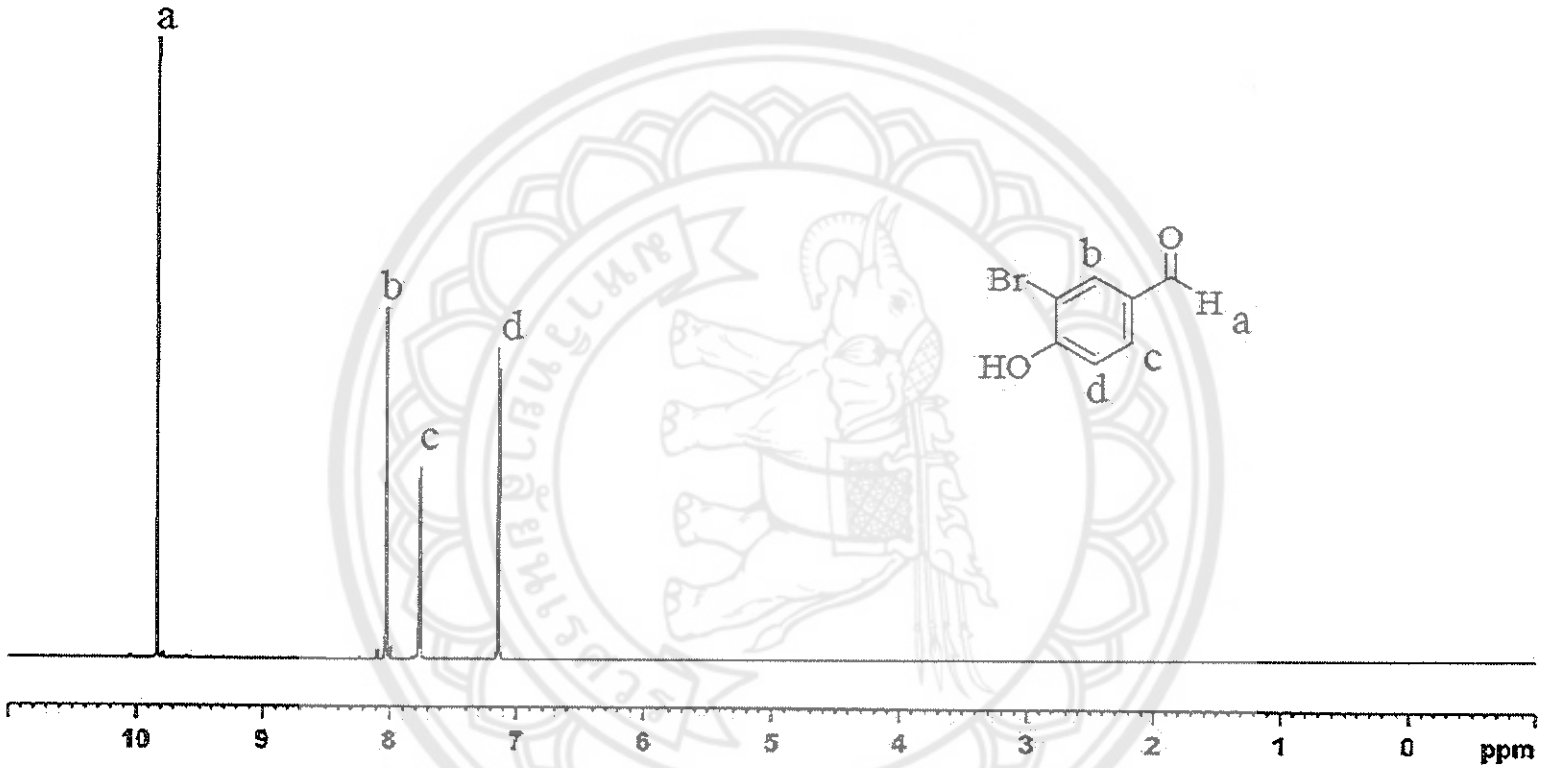

Figure 52 ^{1}H-NMR spectrum of 3-bromo-4-hydroxybenzyaldehyde (5) ($CDCl_3$-d_1)

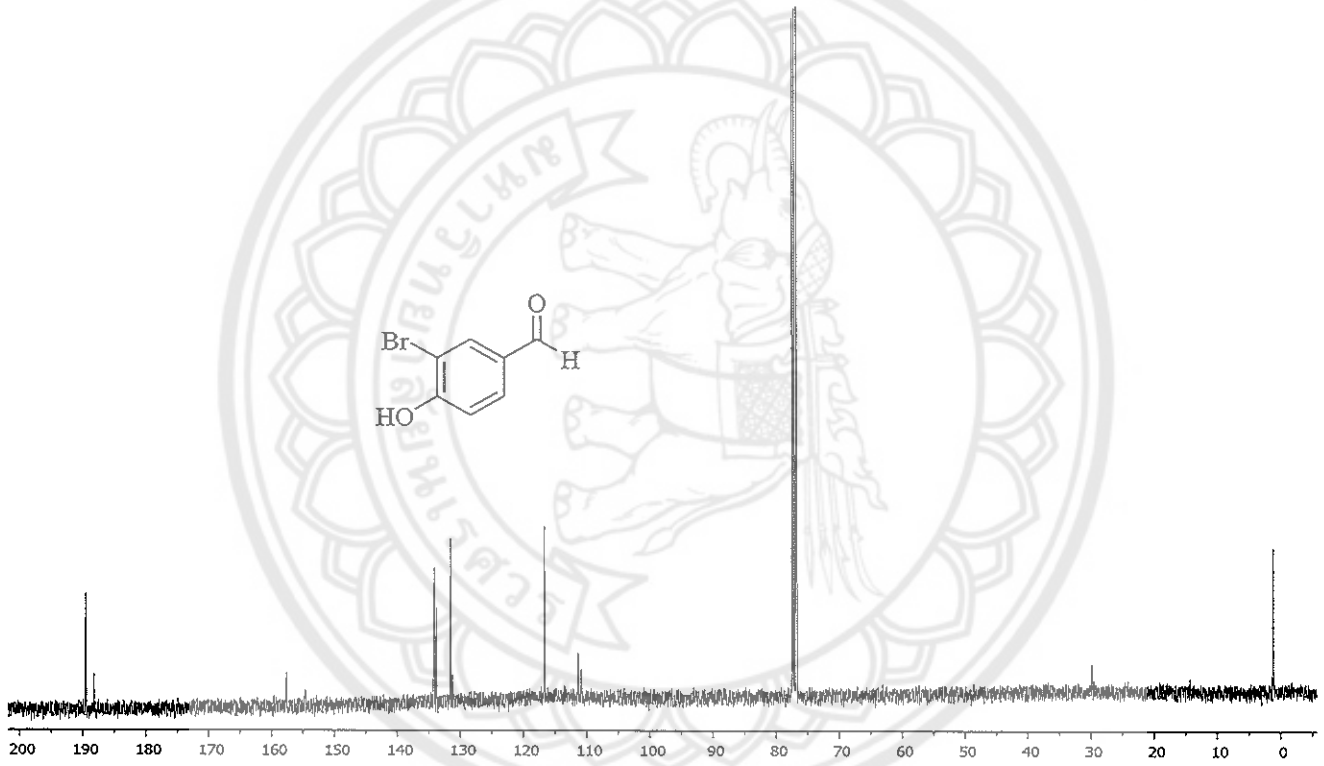

Figure 53 ^{13}C-NMR spectrum of 3-bromo-4-hydroxybenzyaldehyde (5) ($CDCl_3$-d_1)

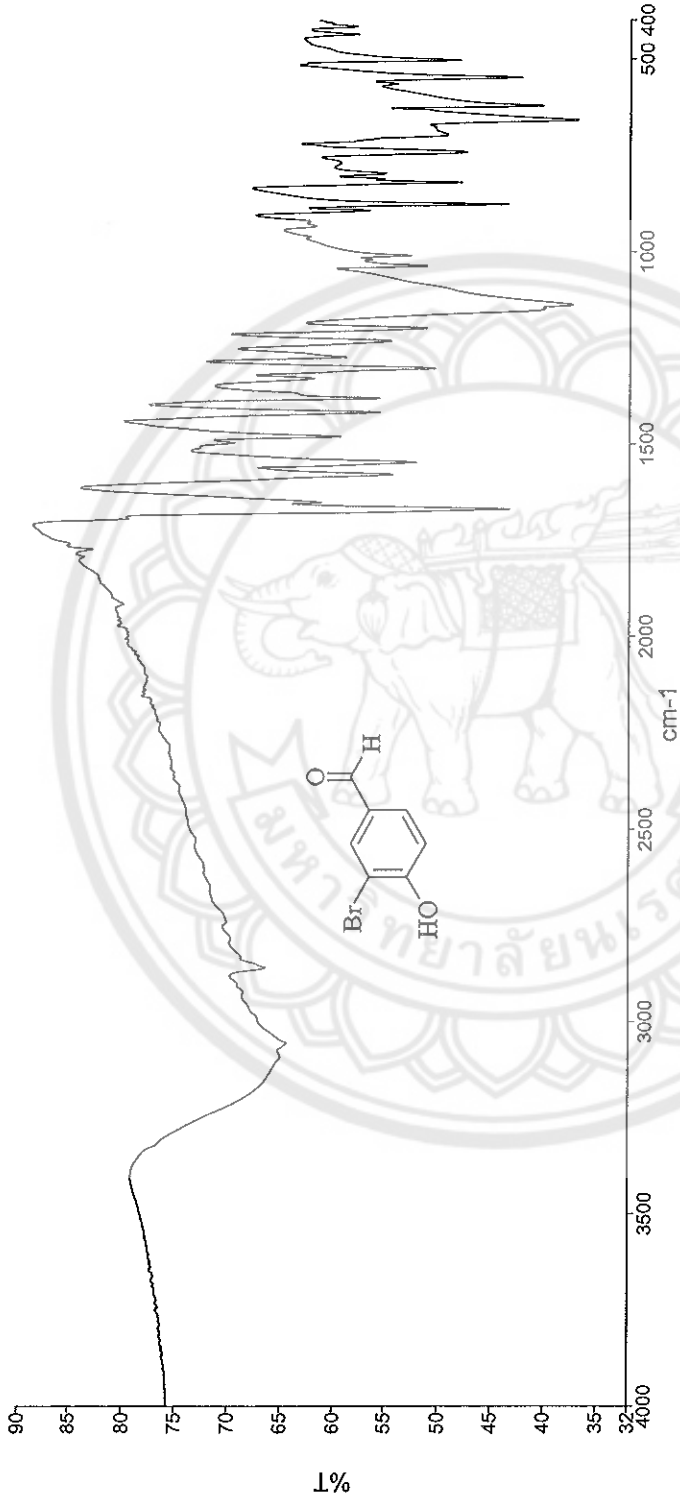

Figure 54 IR spectrum of 3-bromo-4-hydroxybenzyaldehyde (5)

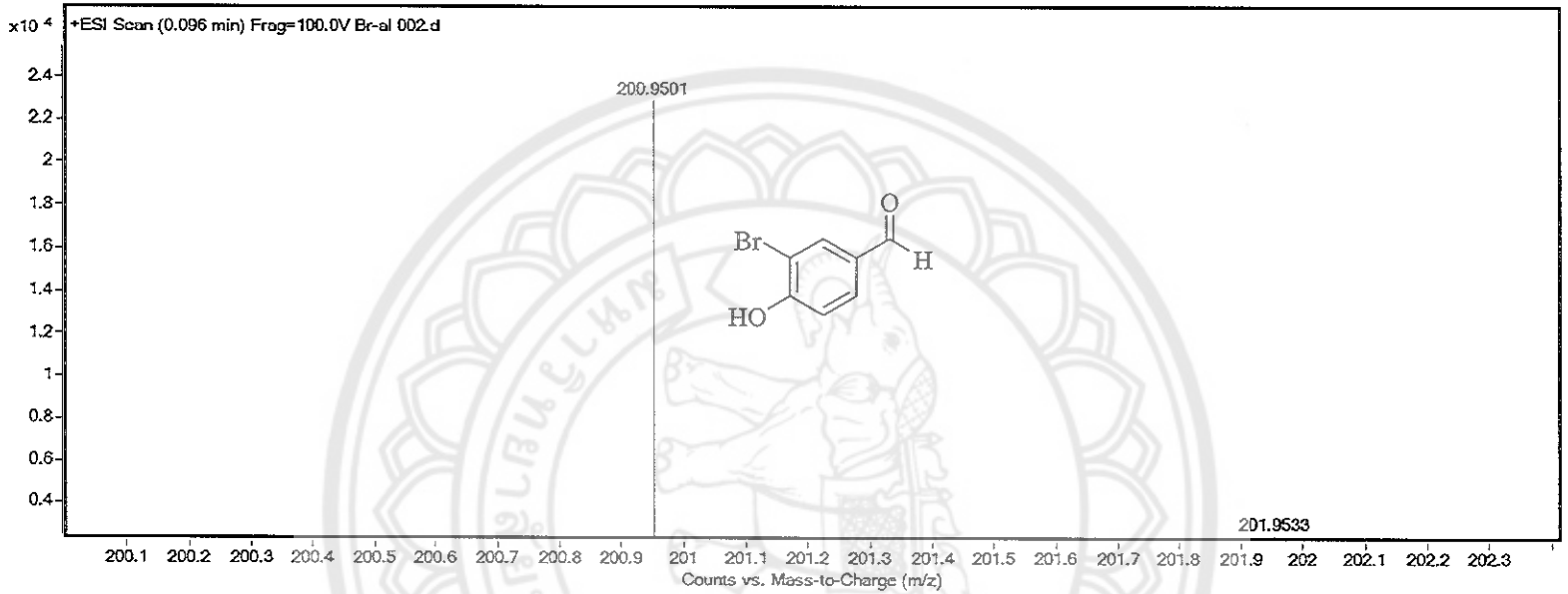

Figure 55 Mass spectrum of 3-bromo-4-hydroxybenzyaldehyde (5)

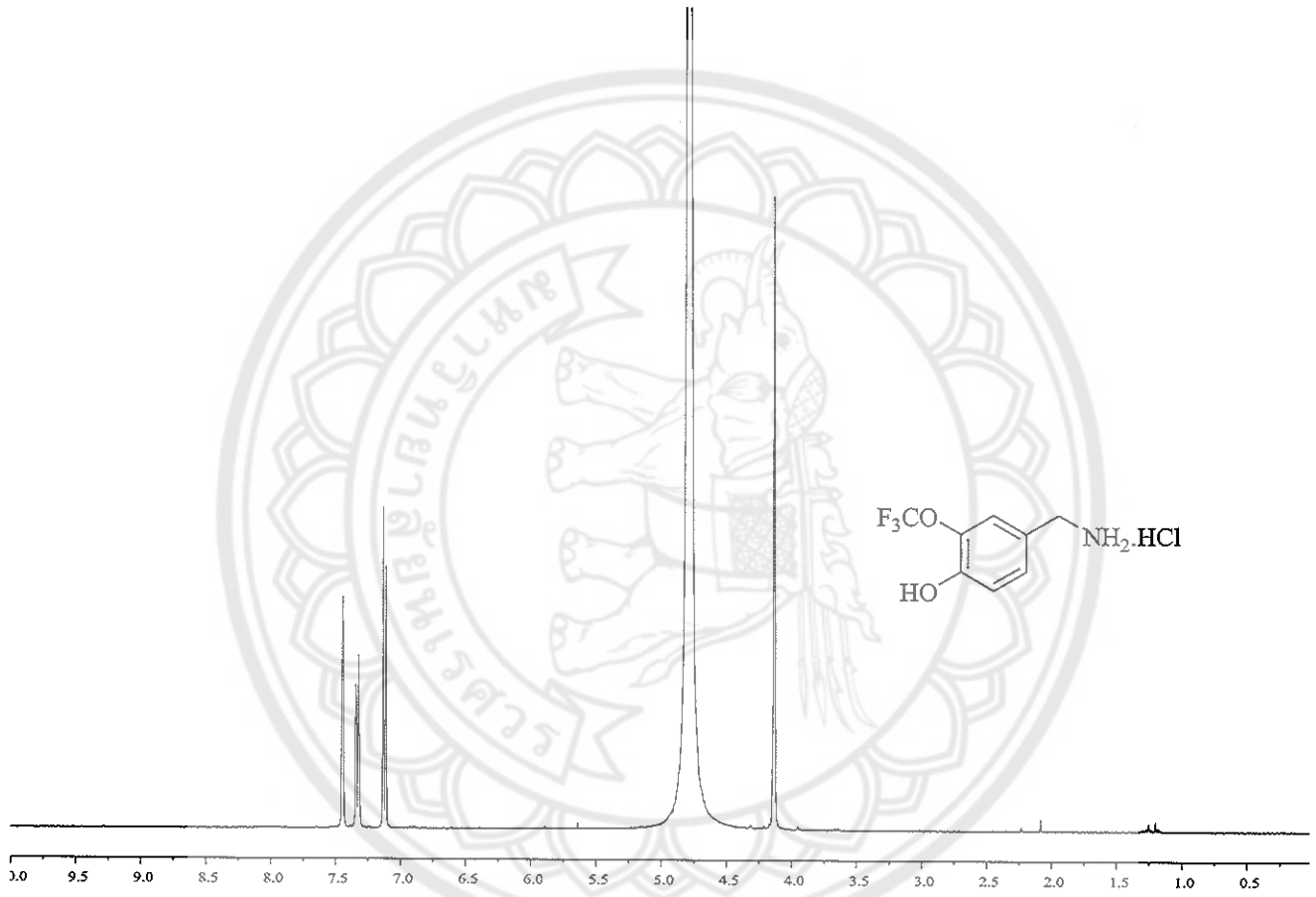

Figure 56 ^{1}H-NMR spectrum of 3-trifluoromethoxy-4-hydroxybenzylamine hydrochloride (14) (D_2O-d_2)

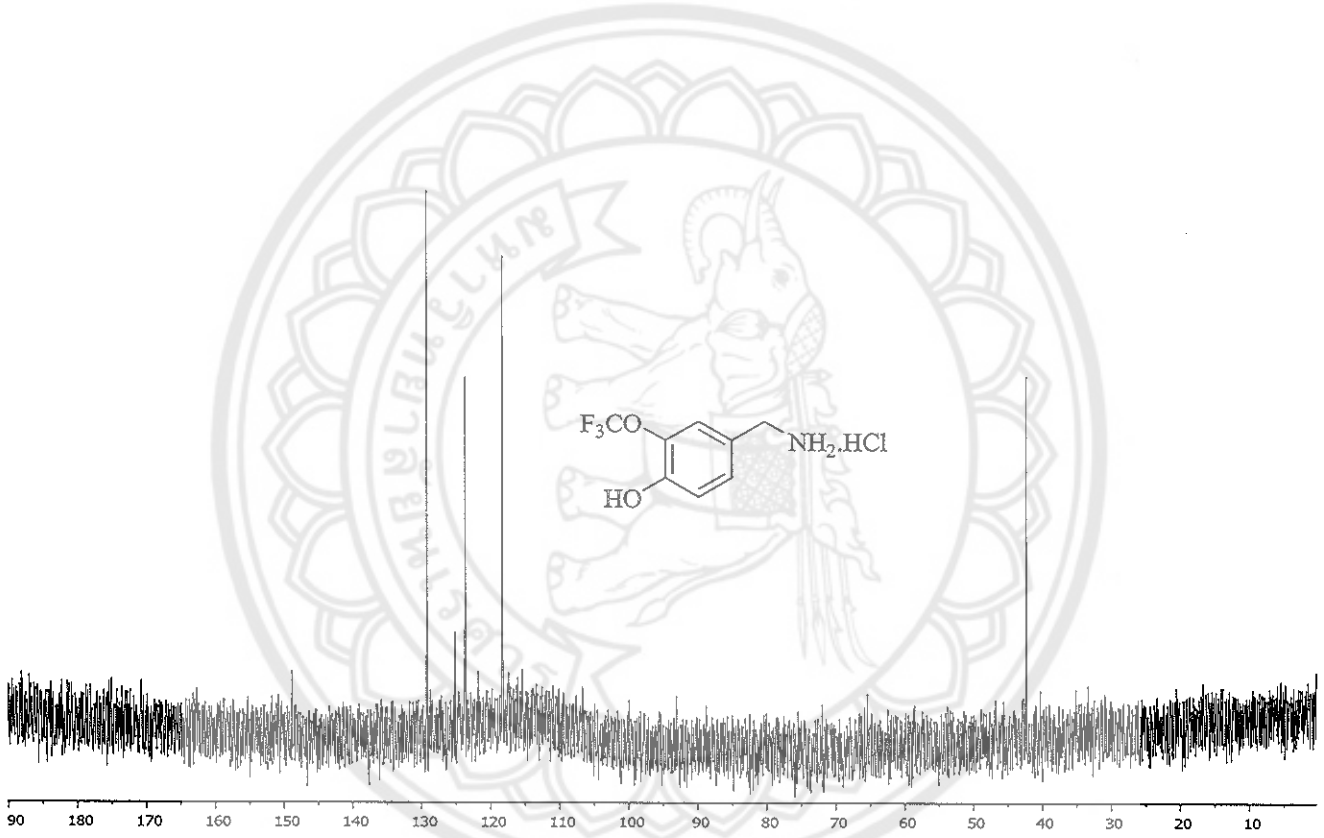

Figure 57 ^{13}C-NMR spectrum of 3-trifluoromethoxy-4-hydroxybenzylamine hydrochloride (14) (D_2O-d_2)

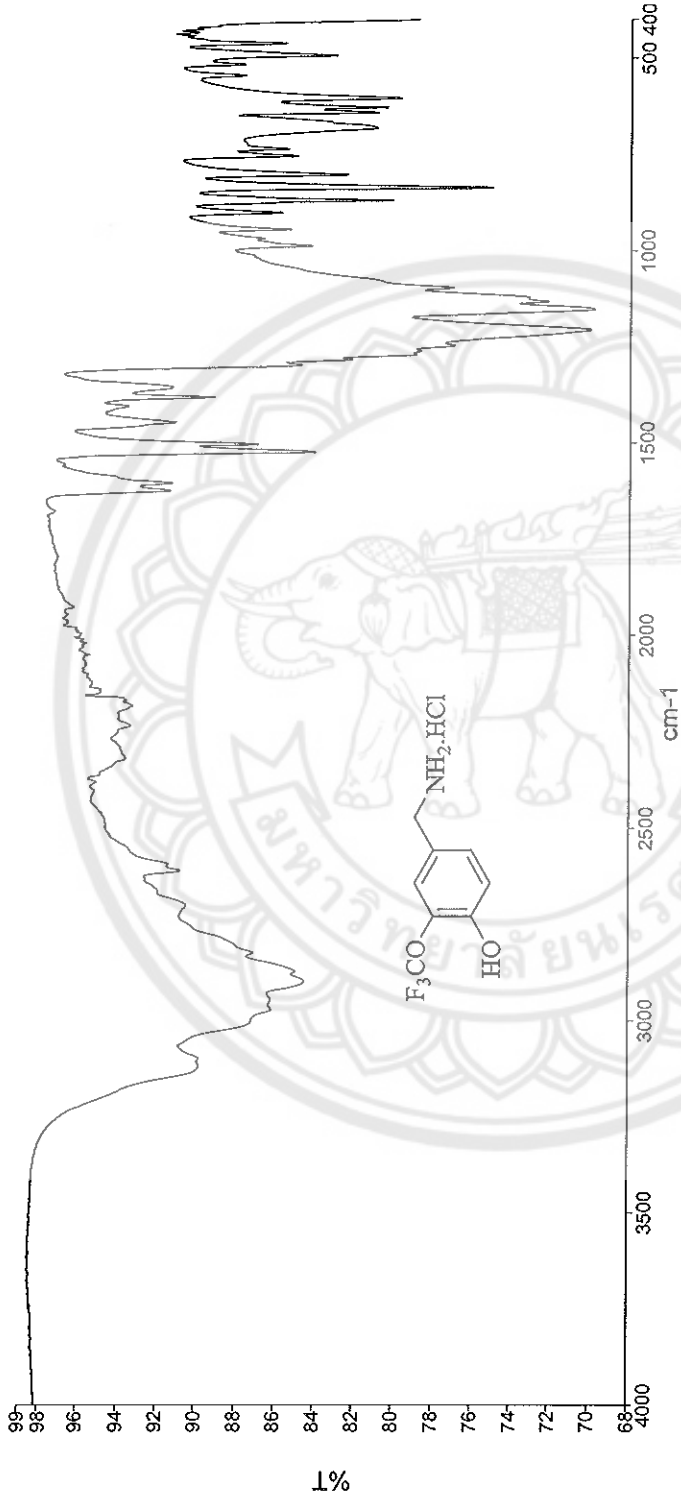

Figure 58 IR spectrum of 3-trifluoromethoxy-4-hydroxybenzylamine hydrochloride (14)

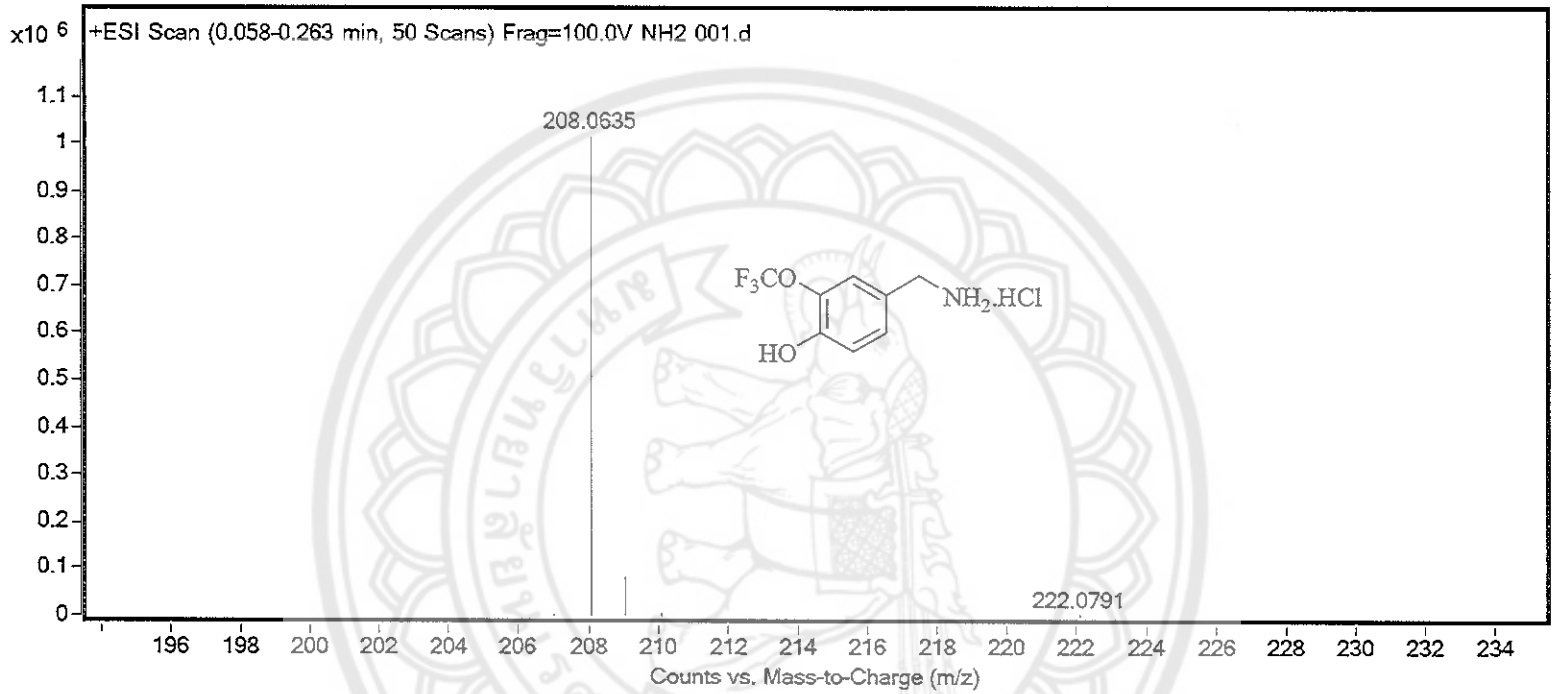

Figure 59 Mass spectrum of 3-trifluoromethoxy-4-hydroxybenzylamine hydrochloride (14)

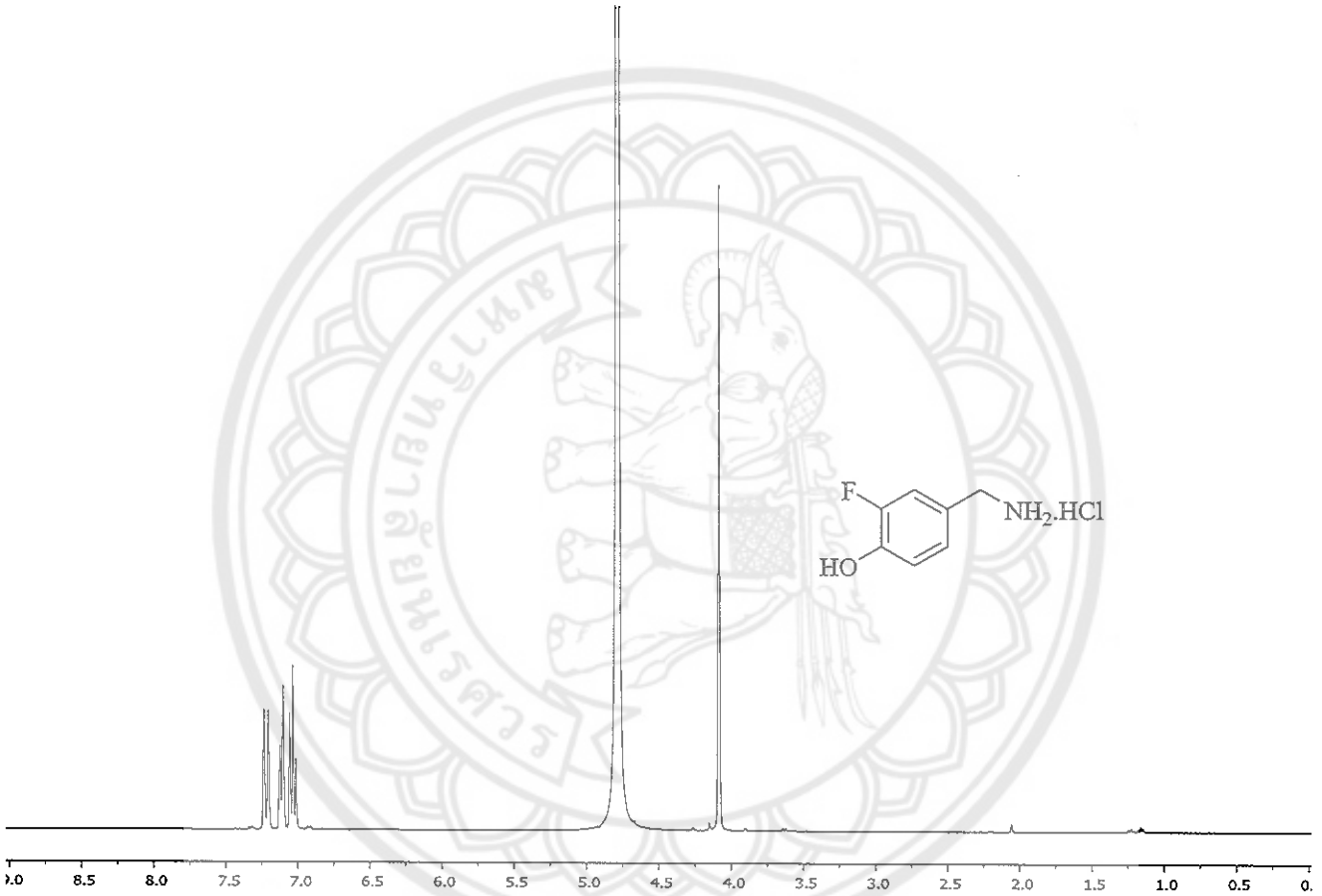

Figure 60 ^{1}H-NMR spectrum of 3-fluoro-4-hydroxybenzylamine hydrochloride (**15**) (D_2O-d_2)

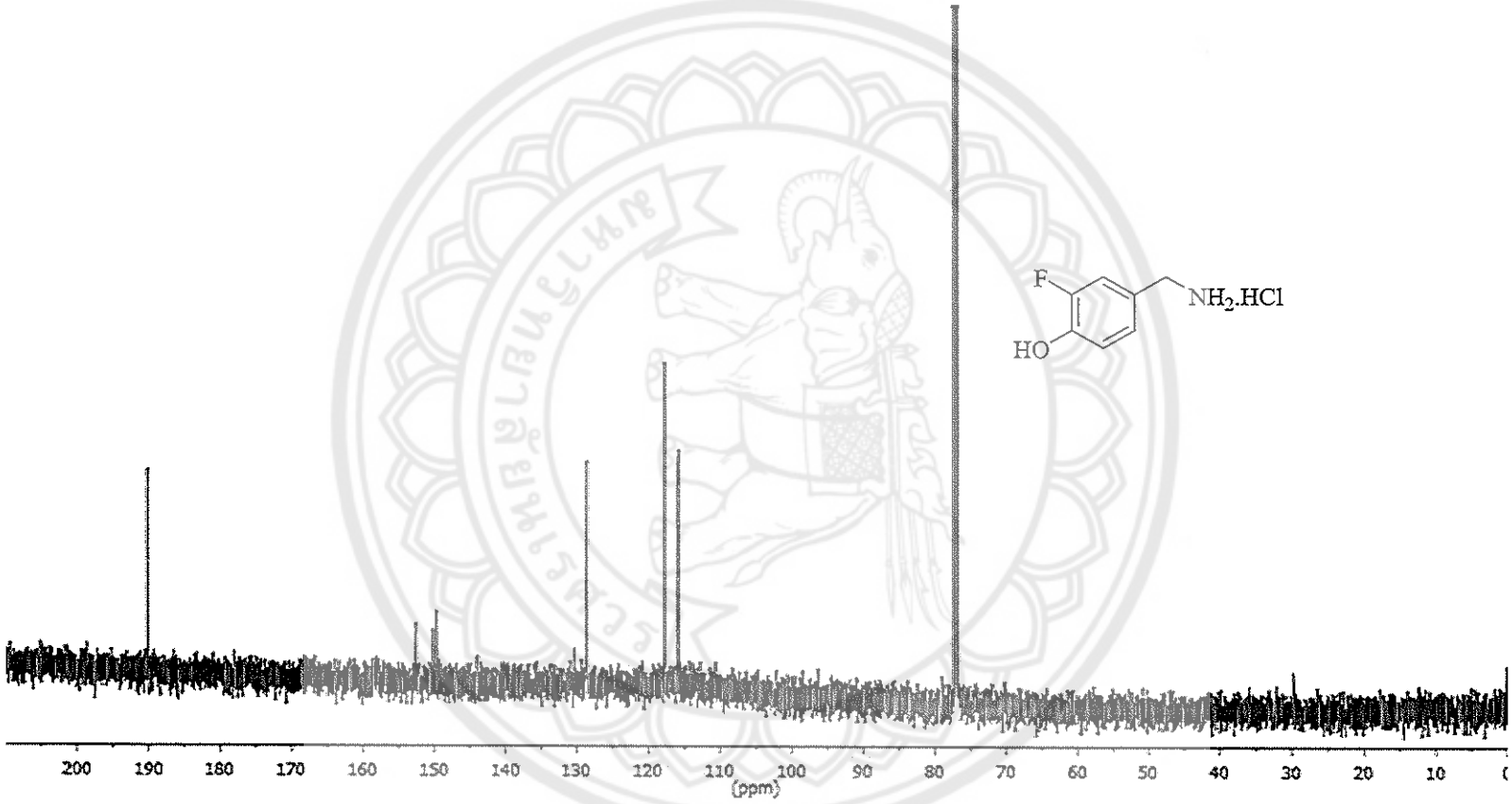

Figure 61 ^{13}C-NMR spectrum of 3-fluoro-4-hydroxybenzylamine hydrochloride (**15**) (D_2O-d_2)

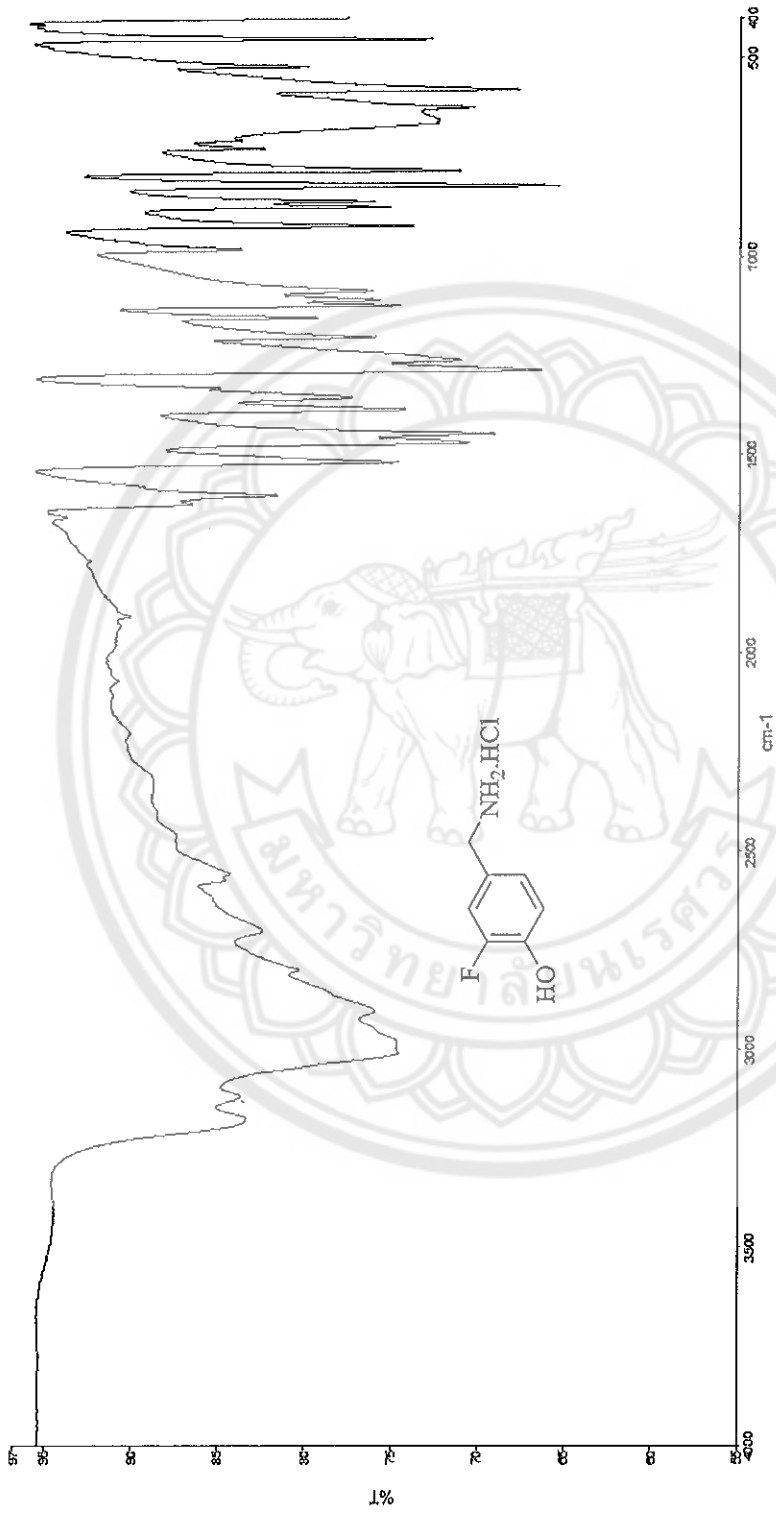

Figure 62 IR spectrum of 3-fluoro-4-hydroxybenzylamine hydrochloride (15)

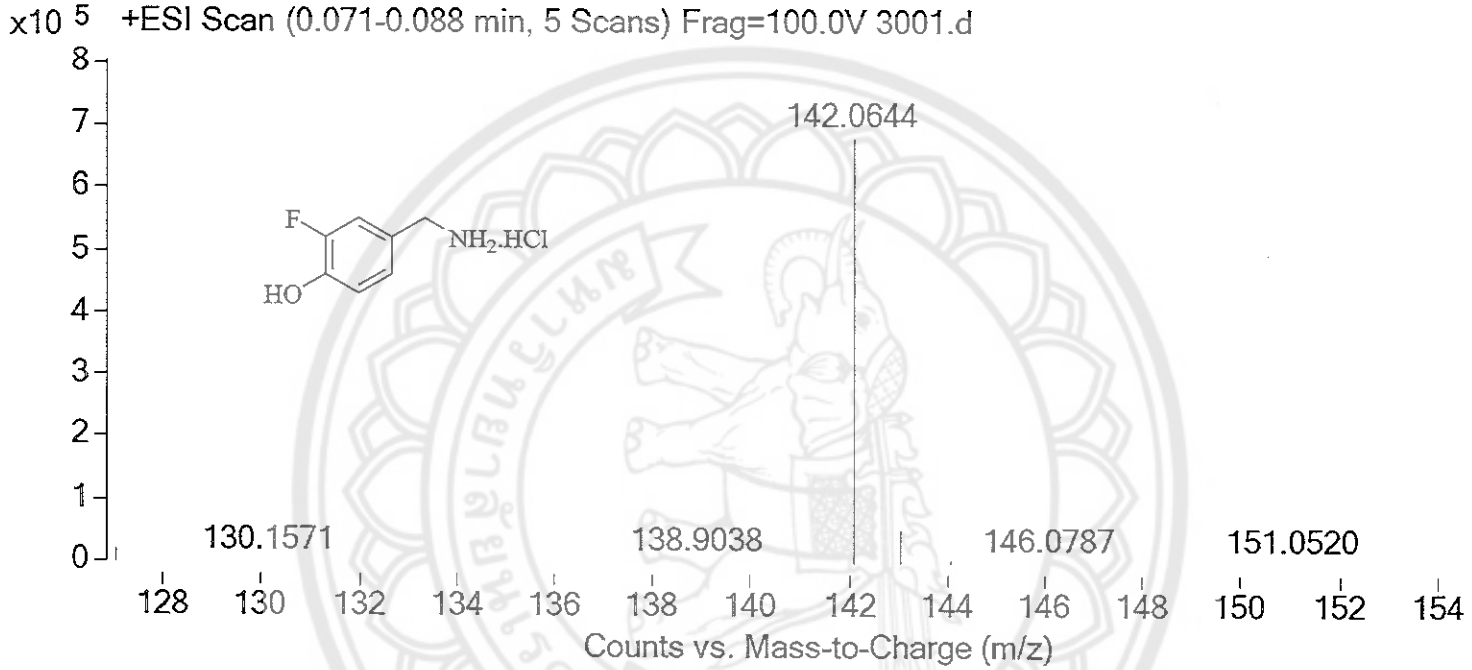

Figure 63 Mass spectrum of 3-fluoro-4-hydroxybenzylamine hydrochloride (15)

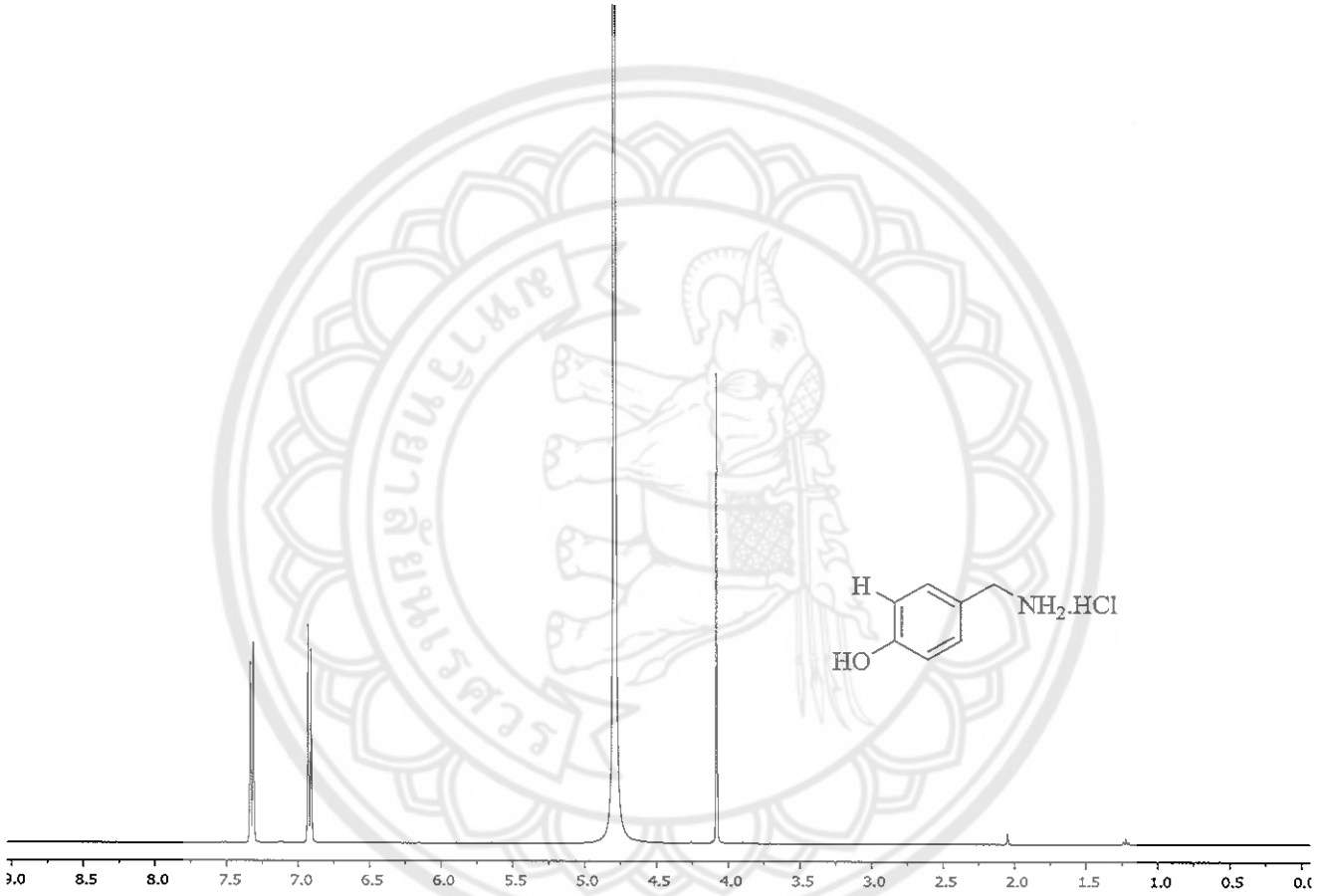

Figure 64 ^{1}H-NMR spectrum of 4-hydroxybenzylamine hydrochloride (18) (D_2O-d_2)

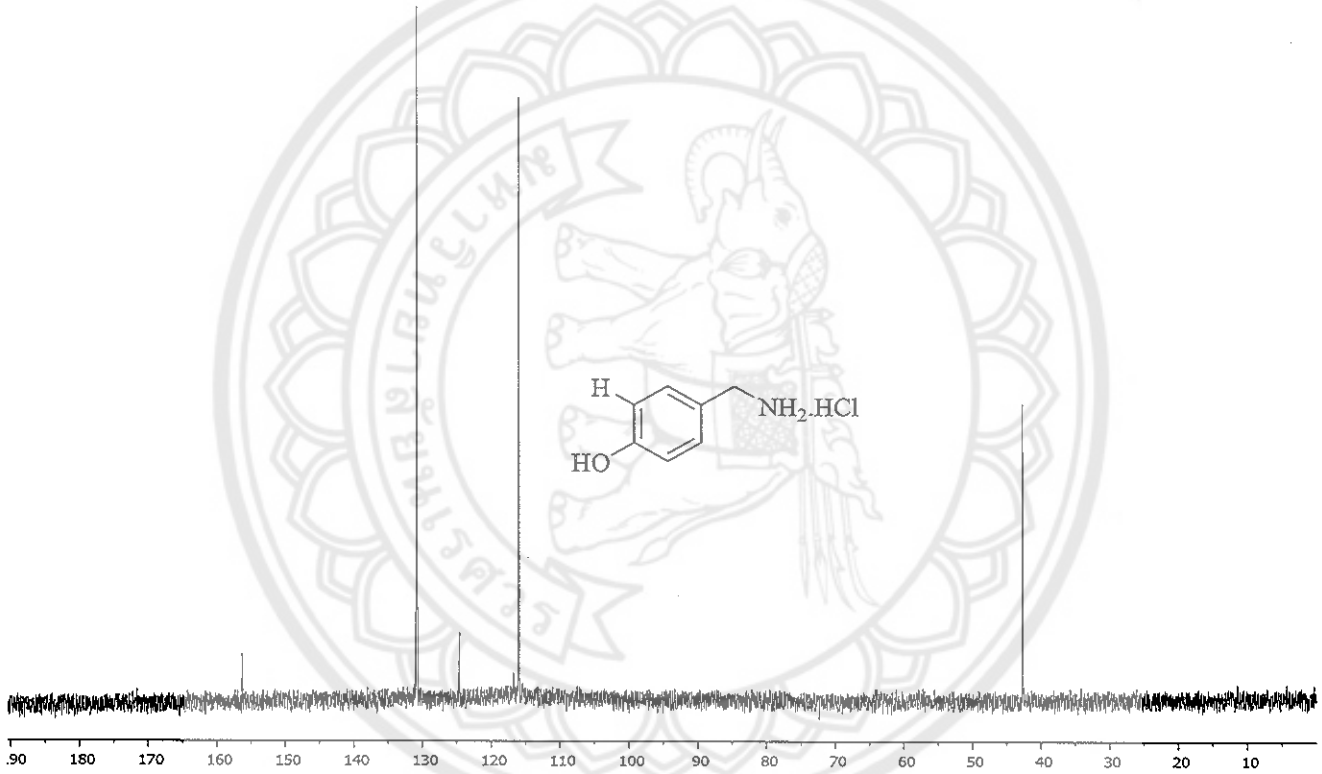

Figure 65 ^{13}**C-NMR spectrum of 4-hydroxybenzylamine hydrochloride (18) (D_2O-d_2)**

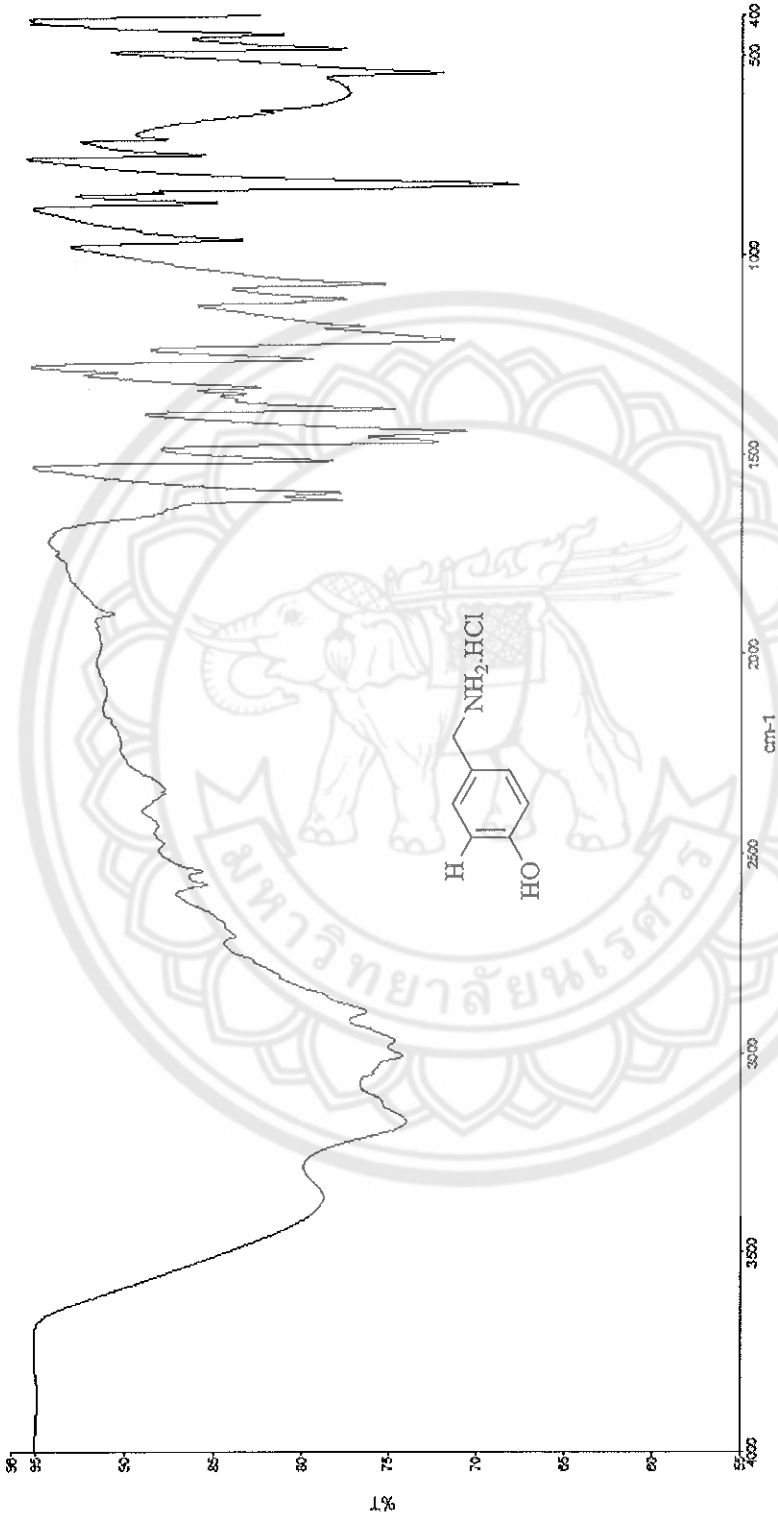

Figure 66 IR spectrum of 4-hydroxybenzylamine hydrochloride (18)

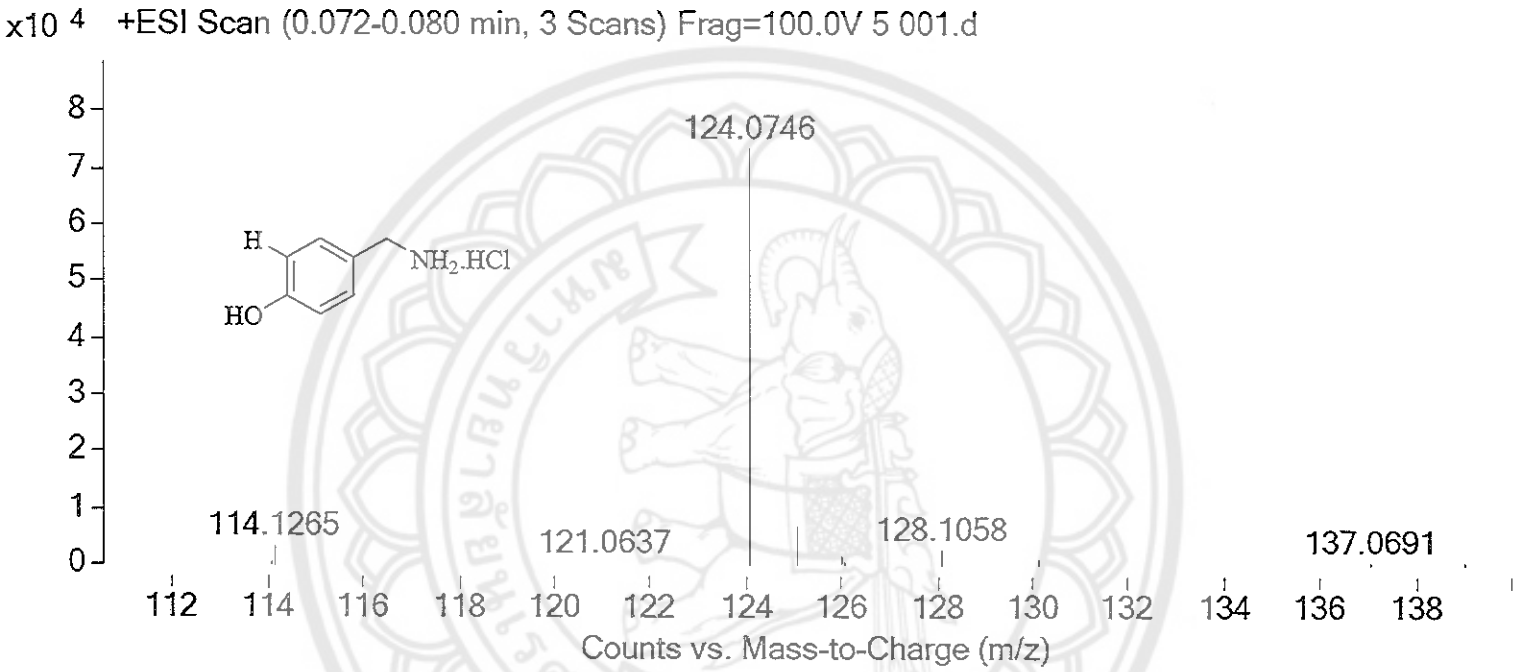

Figure 67 Mass spectrum of 4-hydroxybenzylamine hydrochloride (18)

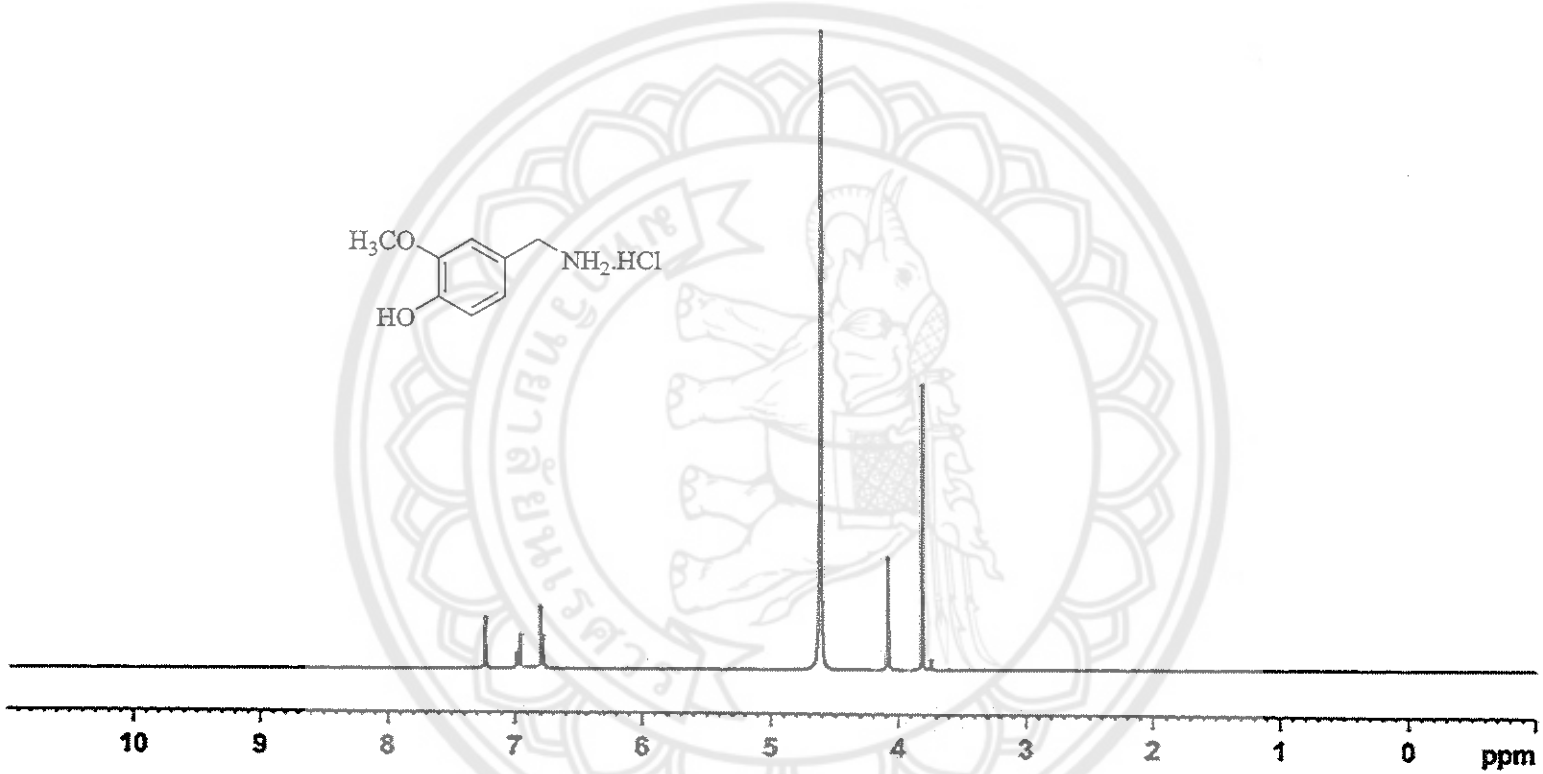

Figure 68 ^{1}**H-NMR spectrum of 4-hydroxy-3-methoxybezylamine hydrochloride (19) (D_2O-d_2)**

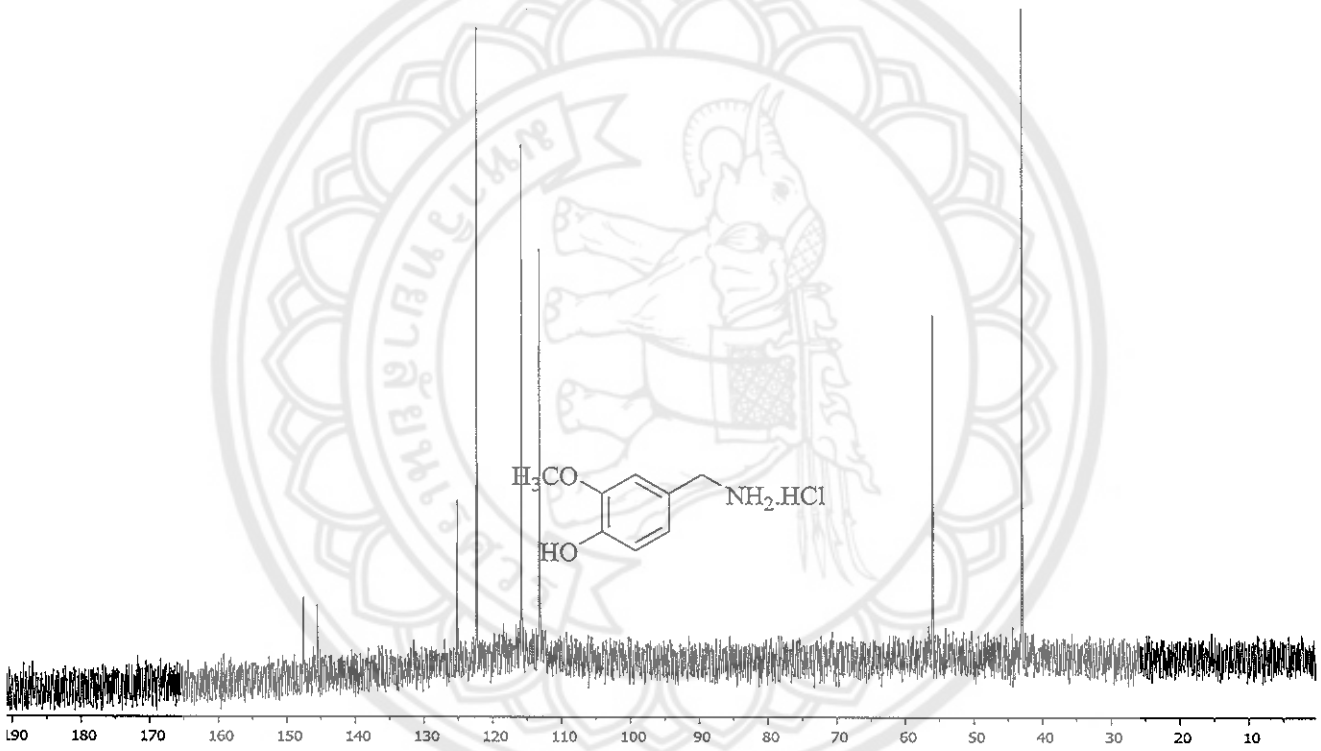

Figure 69 ^{13}**C-NMR spectrum of 4-hydroxy-3-methoxybezylamine hydrochloride (19) (D_2O-d_2)**

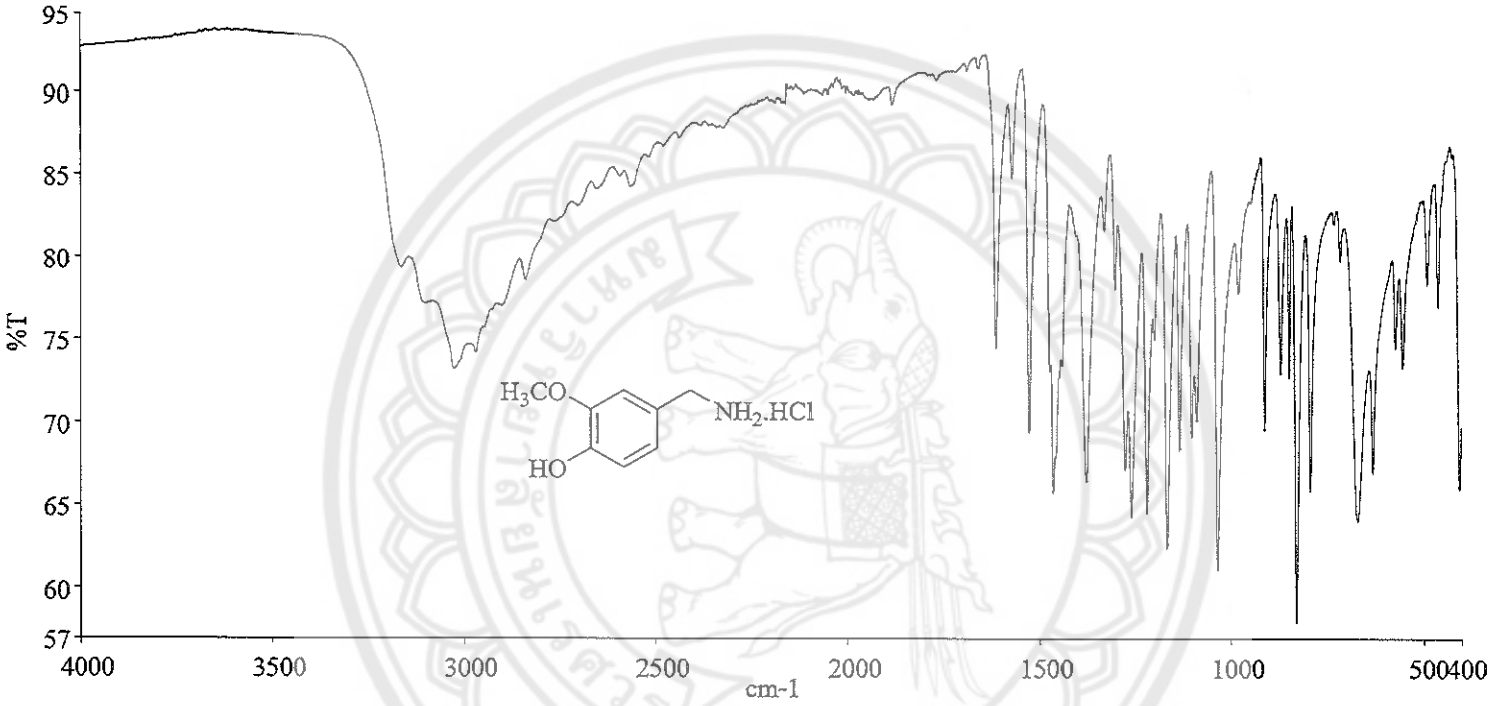

Figure 70 IR spectrum of 4-hydroxy-3-methoxybezylamine hydrochloride (19)

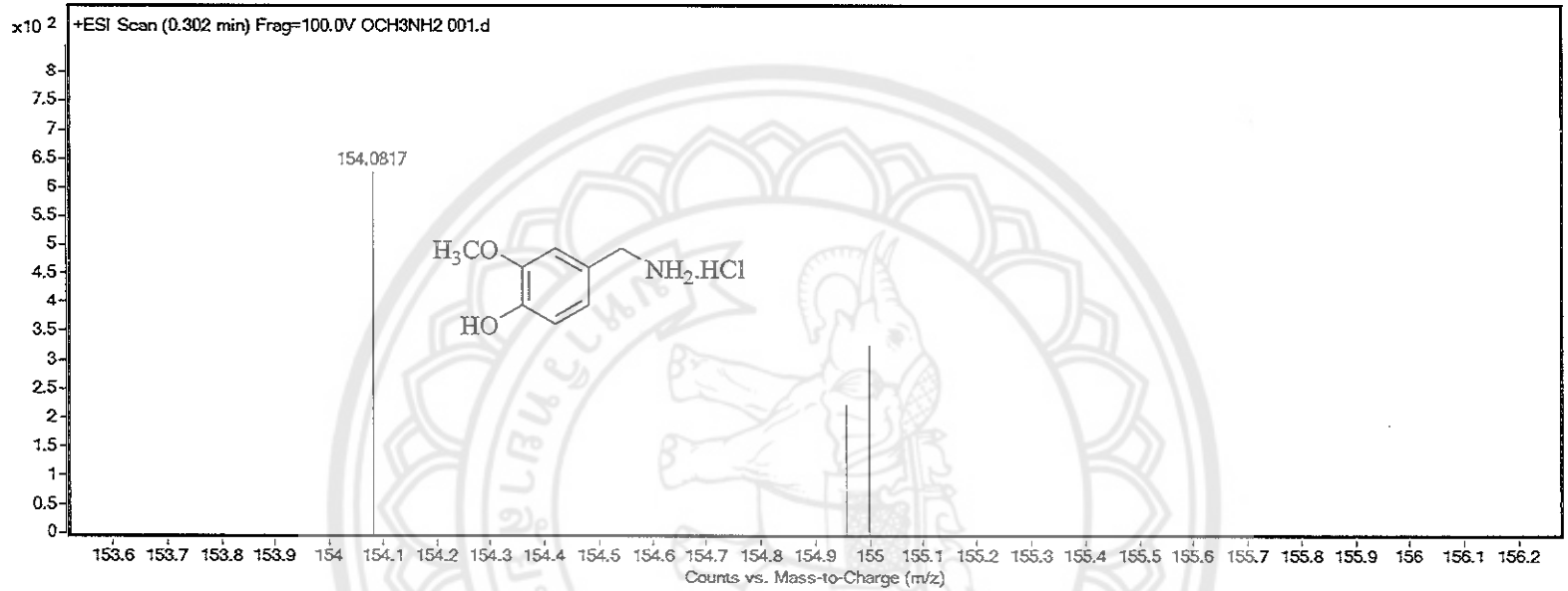

Figure 71 Mass spectrum of 4-hydroxy-3-methoxybezylamine hydrochloride (19)

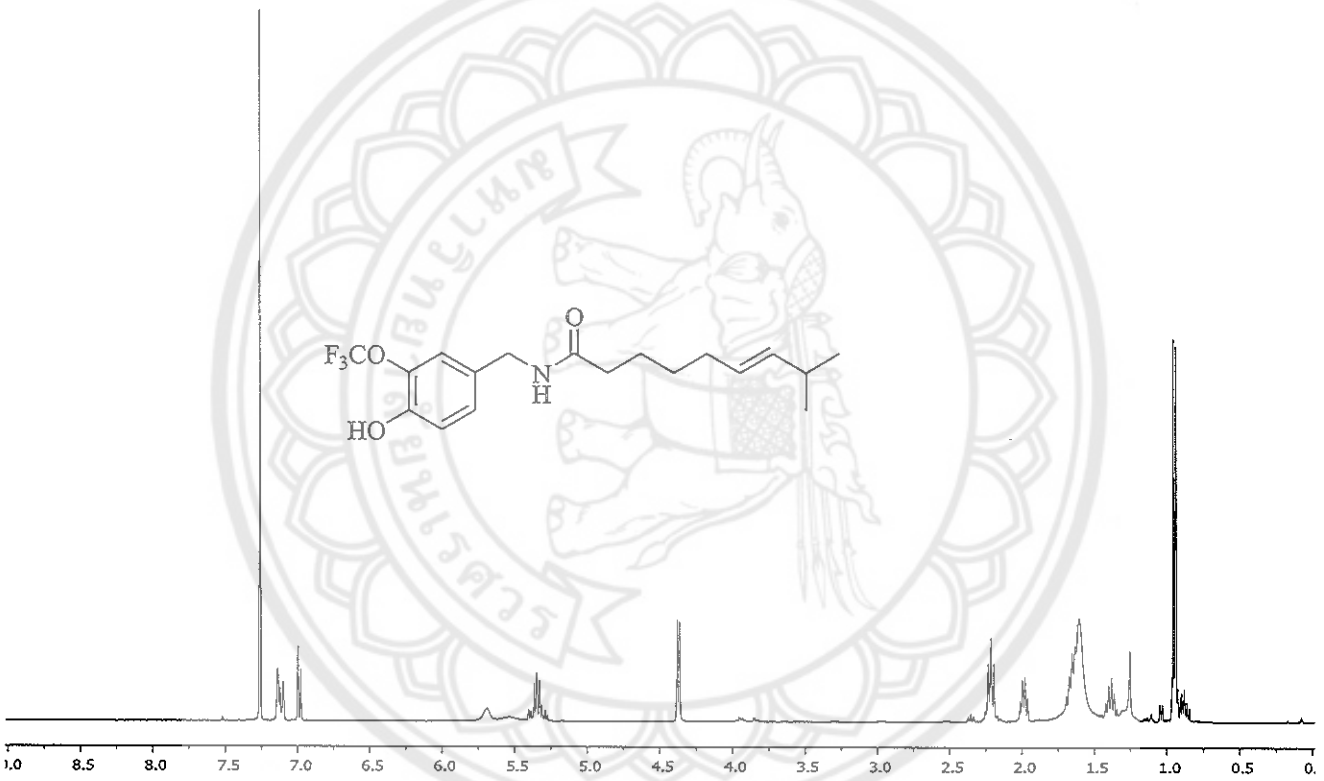

Figure 72 ^{1}H-NMR spectrum of Isostere Capsaicin (21) before purified by HPLC ($CDCl_3$-d_1)

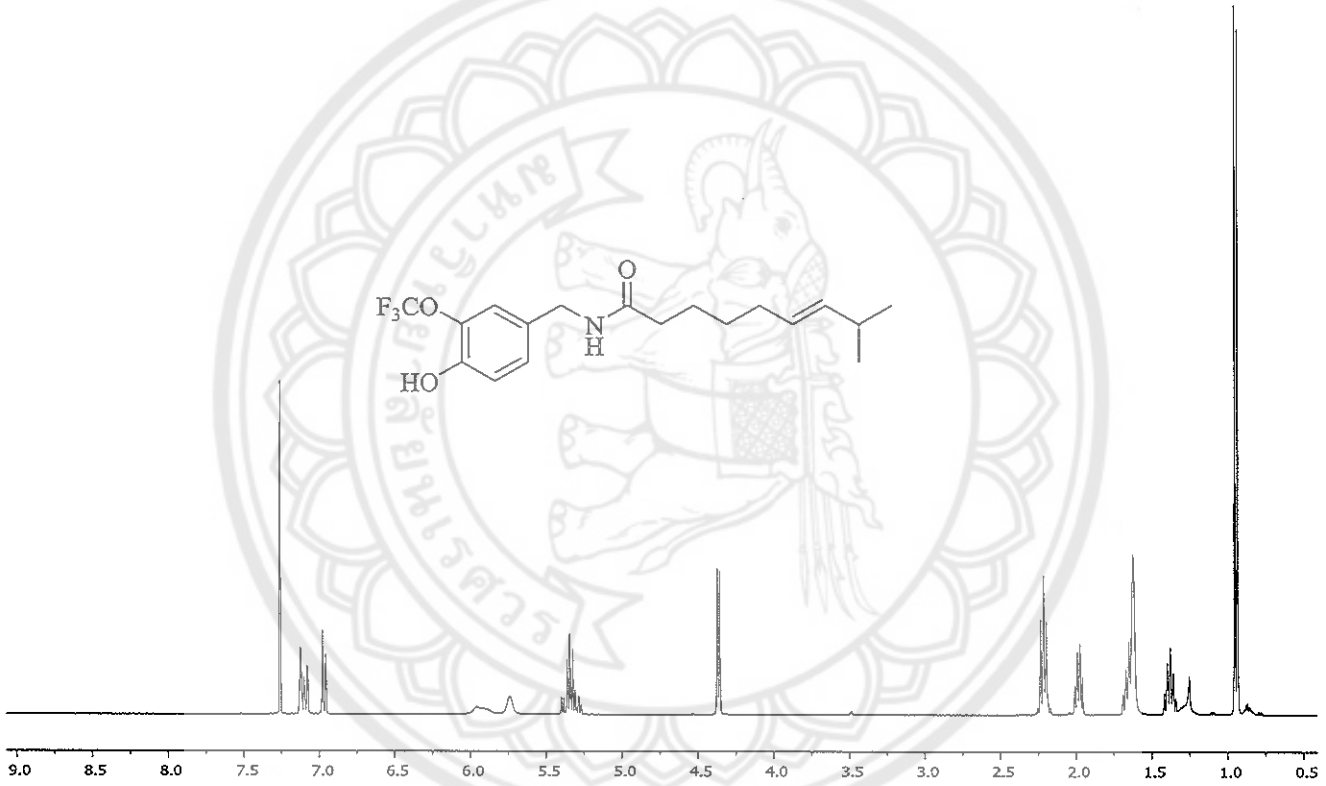

Figure 73 ^{1}H-NMR spectrum of Isostere Capsaicin (21) after purified by HPLC (**$CDCl_3$-d_1**)

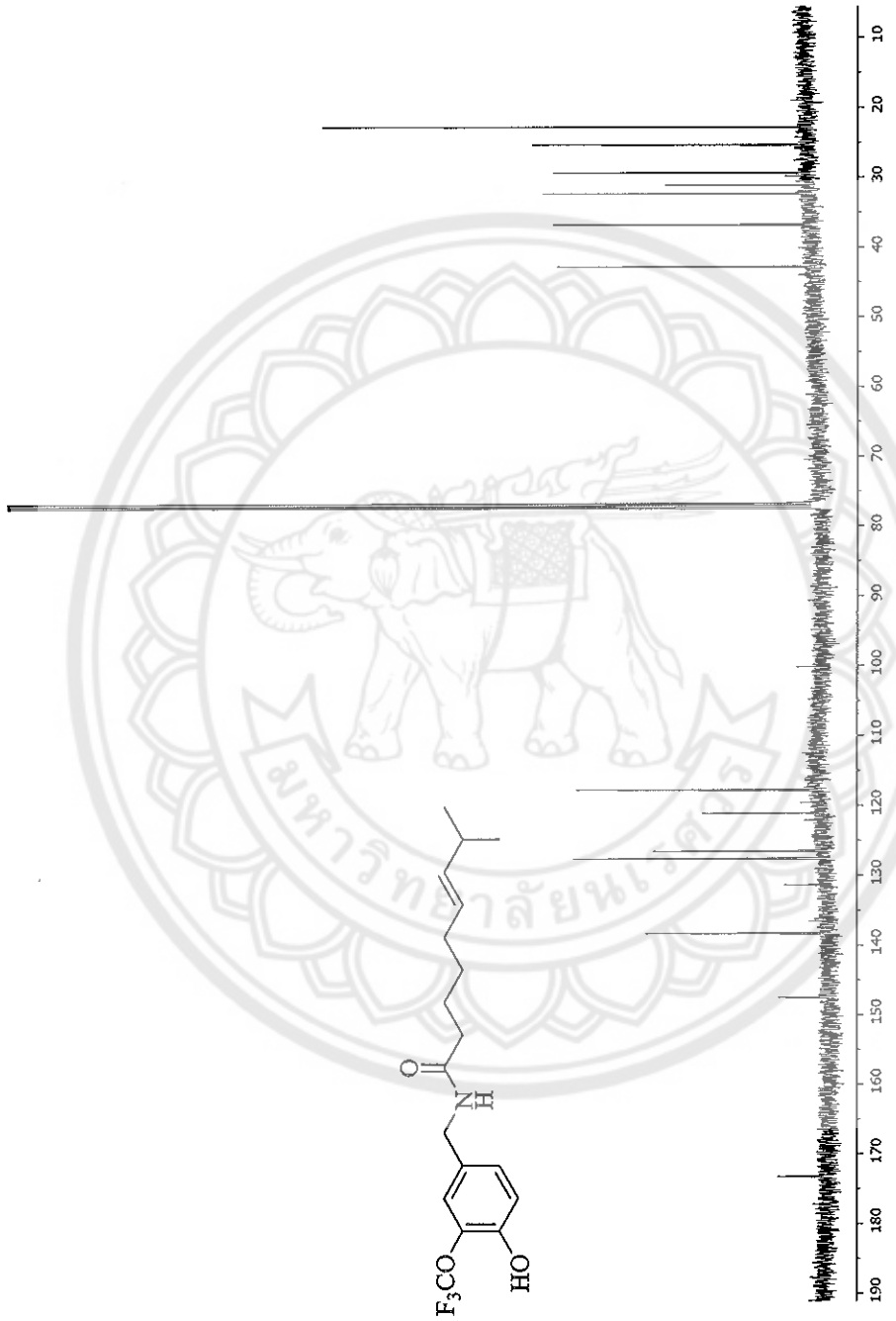

Figure 74 ^{13}C-NMR spectrum of Isostere Capsaicin (21) ($CDCl_3$-d_1)

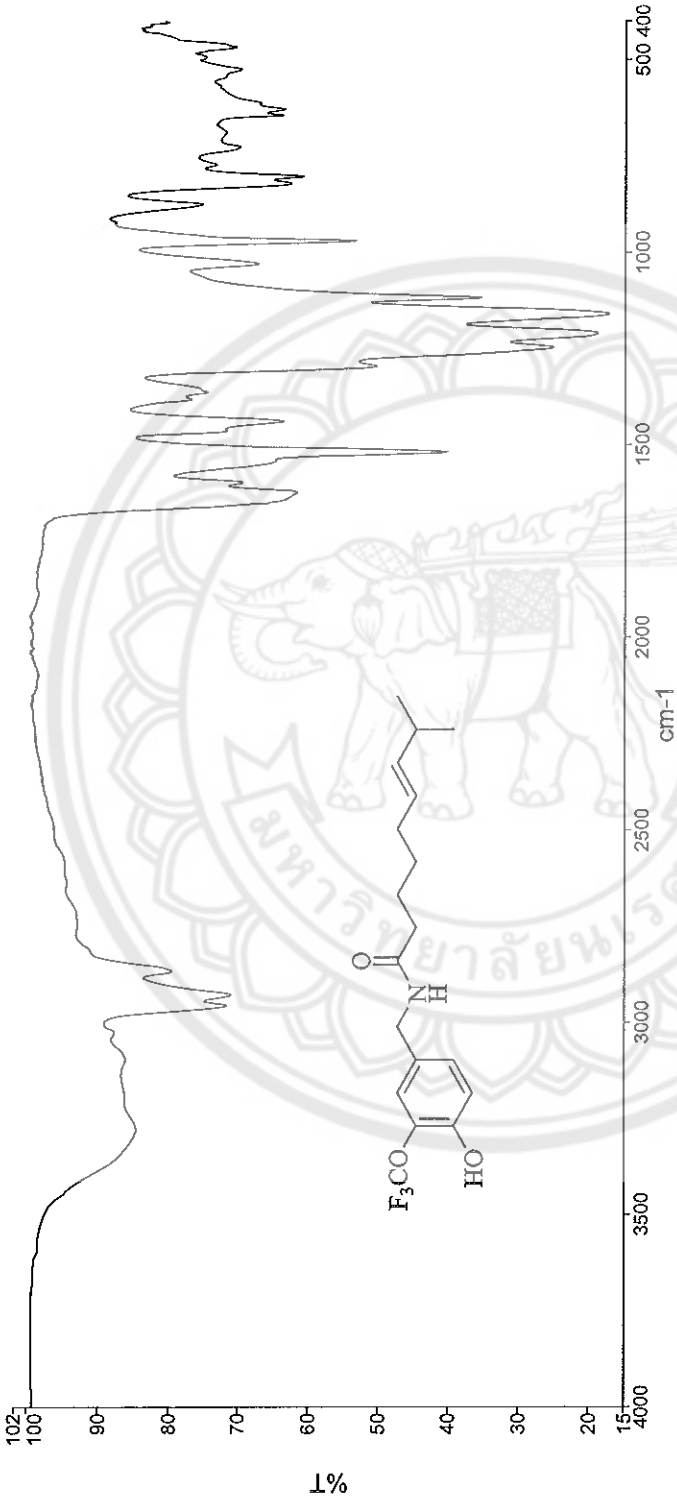

Figure 75 IR spectrum of Isostere Capsaicin (21)

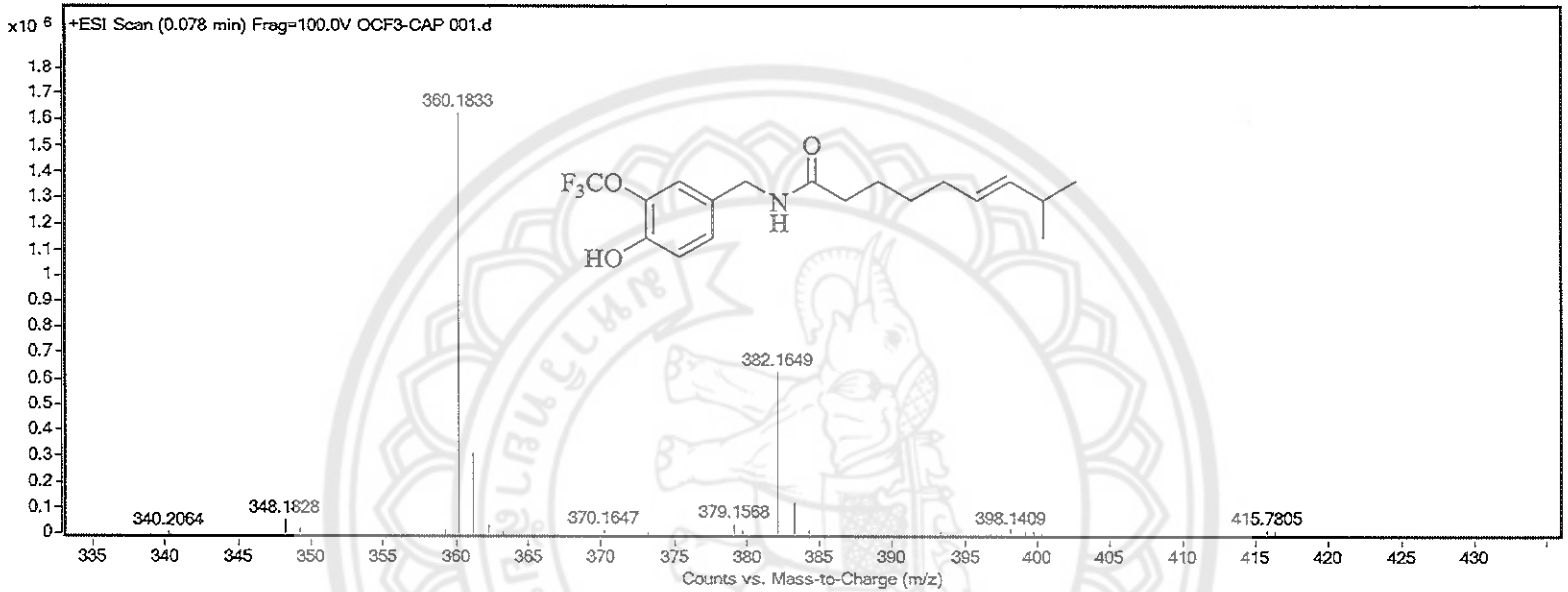

Figure 76 Mass spectrum of Isostere Capsaicin (21)

APPENDIX B Cell Viability Assay

Table 5 Cell viability of isostere capsaicin (21) in 1% of PEG after 24 hours

No.	Sample	%PBMC availability			Average	%RSD
		1	2	3		
1	RPMI	100.00	98.32	99.11	99.14 ± 0.84	0.85
2	200 μM OCF_3	95.29	94.29	95.86	95.15 ± 0.80	0.84
3	100 μM OCF_3	98.26	97.65	97.59	97.83 ± 0.37	0.38
4	50 μM OCF_3	96.67	97.73	97.08	97.16 ± 0.53	0.55
5	5 μM OCF3	99.38	98.93	95.77	98.03 ± 1.97	2.01
6	1 μM OCF_3	99.34	98.73	98.03	98.70 ± 0.66	0.67

APPENDIX C TNF-α assay

Table 6 Absorption of TNF-α standard at 1,000, 500, 250, 125, 62.5, 31.2, 15.6 and 0 pg/mL

Concentration of TNF-α production (pg/mL)	Absorption (nm)		Average	%RSD
1,000	2.894	2.819	2.857 ± 0.053	1.857
500	1.678	1.647	1.663 ± 0.022	1.319
250	0.847	0.943	0.895 ± 0.068	7.585
125	0.466	0.474	0.470 ± 0.006	1.204
62.5	0.258	0.246	0.252 ± 0.008	3.367
31.2	0.153	0.147	0.150 ± 0.004	2.828
15.6	0.097	0.099	0.098 ±0.001	1.443
0	0.051	0.049	0.050 ± 0.001	2.828

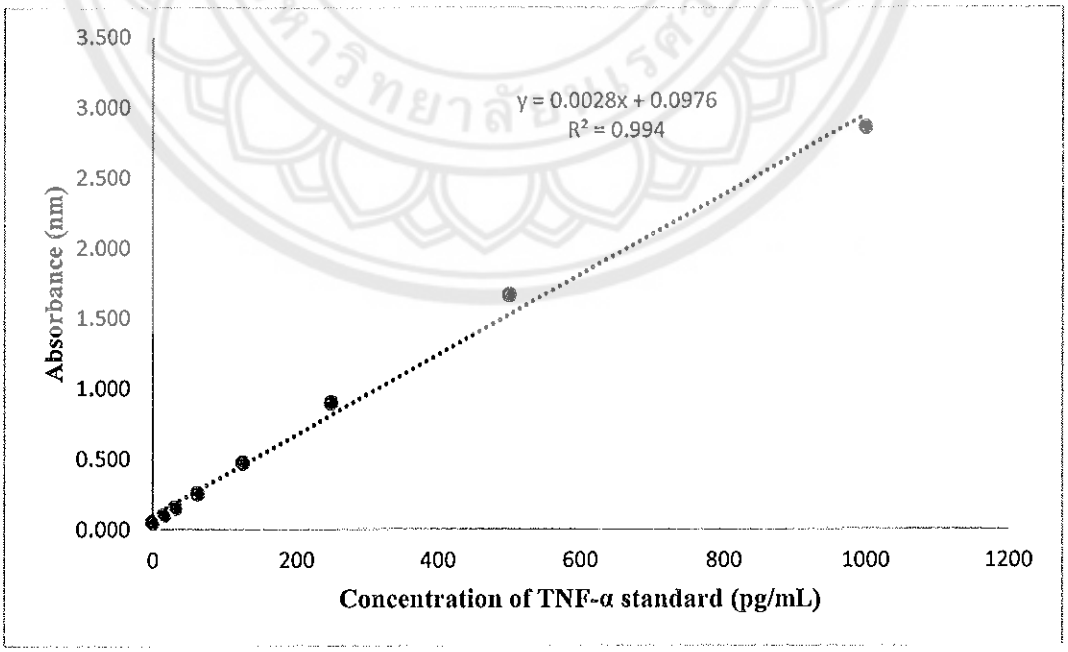

Figure 77 Calibration curve of TNF-α production at 1,000, 500, 250, 125, 62.5, 31.2, 15.6 and 0 pg/mL

Table 7 Absorption of screening assay of TNF-α production after dose 5.00 μM of capsaicin and isostere capsaicin (21) using LPS-stimulated (n=1)

Sample	Absorption		Average	%RSD	Conc. of TNF-α production (pg/mL)	Effect of sample to TNF-α production	% inhibition of TNF-α production
	1	2					
PBMC	0.279	0.287	0.283 ± 0.006	1.999	66.21	0.00	-
PBMC+LPS	2.184	2.315	2.250 ± 0.093	4.118	768.54	702.80	0.00
PBMC+LPS +capsaicin	1.722	1.462	1.592 ± 0.184	11.548	533.71	467.97	33.41
PBMC+LPS+**21**	1.016	1.210	1.113 ± 0.137	12.325	362.64	296.90	57.75

APPENDIX D 3D structure

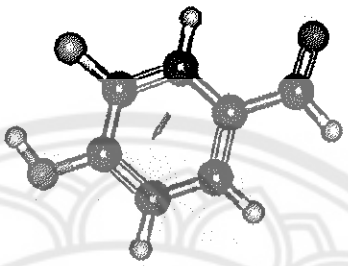

Figure 78 3D structure of 3-fluoro-4-hydroxybenzaldehyde (3)

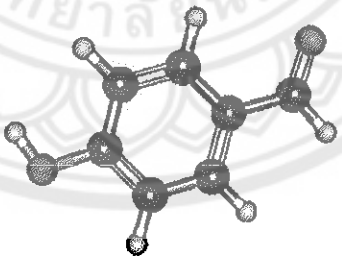

Figure 79 3D structure of 4-hydroxybenzaldehyde (6)

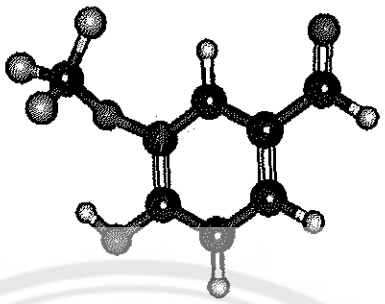

Figure 80 3D structure of 3-trifluoromethoxy-4-hydroxybenzaldehyde (2)

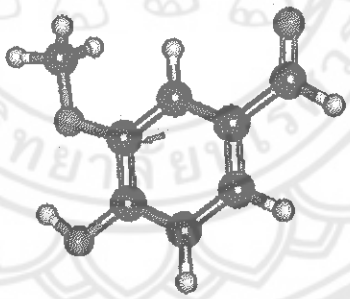

Figure 81 3D structure of 3-methoxy-4-hydroxybenzaldehyde (7)

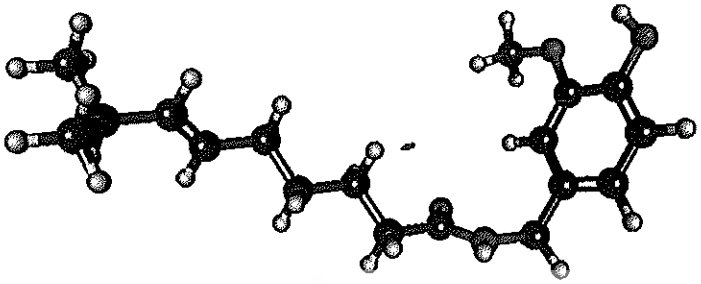

Figure 82 3D structure of capsaicin

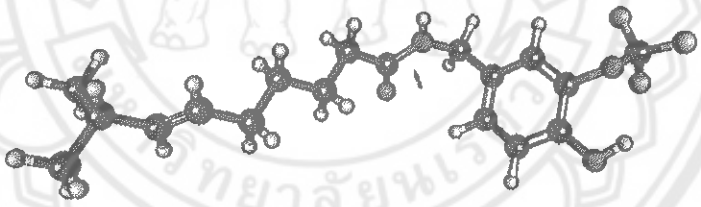

Figure 83 3D structure of isostere capsaicin (21)

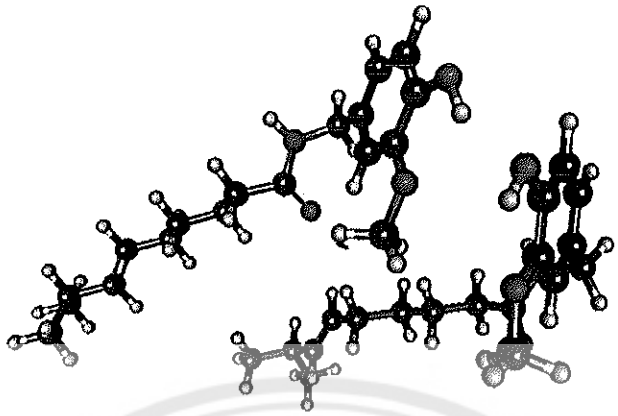

Figure 84 3D structure of interaction of capsaicin and capsaicin *via* H-bond

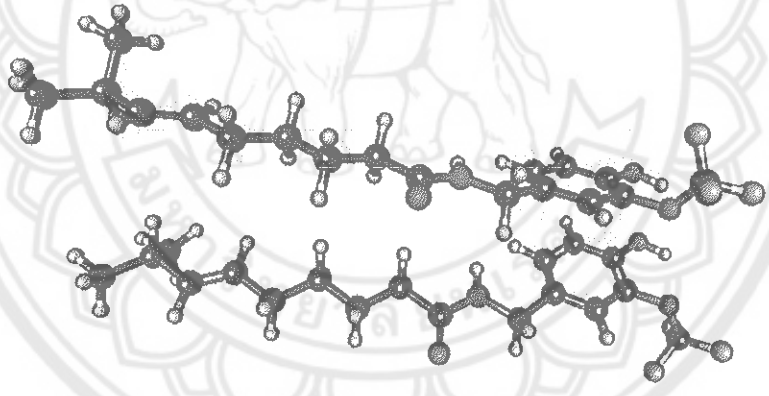

Figure 85 3D structure of interaction of isostere capsaicin and isostere capsaicin *via* π-π stacking

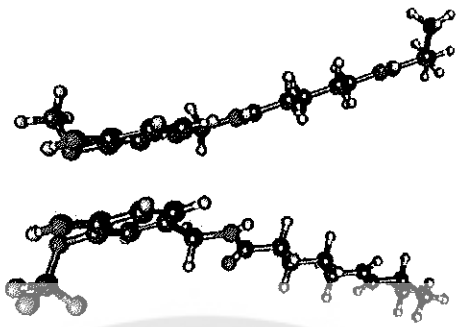

Figure 86 3D structure of interaction of capsaicin and isostere capsaicin *via* π-π stacking